View metadata, citation and similar papers at core.ac.uk

brought to you by CORE

provided by University of Tennessee, Knoxville: Trace

University of Tennessee, Knoxville

TRACE: Tennessee Research and Creative Exchange

Masters Theses

Graduate School

12-1980

Petrologic, Mineralogic, and Ion Exchange Characteristics of the Rome Formation and Pumpkin Valley Shale on the Oak Ridge National Laboratory Reservation, Oak Ridge, Tennessee

Janine Gajda Sledz
University of Tennessee - Knoxville

Follow this and additional works at: https://trace.tennessee.edu/utk_gradthes

 Part of the Geology Commons

Recommended Citation

Sledz, Janine Gajda, "Petrologic, Mineralogic, and Ion Exchange Characteristics of the Rome Formation and Pumpkin Valley Shale on the Oak Ridge National Laboratory Reservation, Oak Ridge, Tennessee. " Master's Thesis, University of Tennessee, 1980.
https://trace.tennessee.edu/utk_gradthes/2659

This Thesis is brought to you for free and open access by the Graduate School at TRACE: Tennessee Research and Creative Exchange. It has been accepted for inclusion in Masters Theses by an authorized administrator of TRACE: Tennessee Research and Creative Exchange. For more information, please contact trace@utk.edu.

To the Graduate Council:

I am submitting herewith a thesis written by Janine Gajda Sledz entitled "Petrologic, Mineralogic, and Ion Exchange Characteristics of the Rome Formation and Pumpkin Valley Shale on the Oak Ridge National Laboratory Reservation, Oak Ridge, Tennessee." I have examined the final electronic copy of this thesis for form and content and recommend that it be accepted in partial fulfillment of the requirements for the degree of Master of Science, with a major in Geology.

O. C. Kopp, Major Professor

We have read this thesis and recommend its acceptance:

Fred B. Keller, T. Tamura, Russell Lewis

Accepted for the Council:
Carolyn R. Hodges

Vice Provost and Dean of the Graduate School

(Original signatures are on file with official student records.)

To the Graduate Council:

I am submitting herewith a thesis written by Janine Gajda Sledz entitled "Petrologic, Mineralogic, and Ion Exchange Characteristics of the Rome Formation and Pumpkin Valley Shale on the Oak Ridge National Laboratory Reservation, Oak Ridge, Tennessee." I recommend that it be accepted in partial fulfillment of the requirements for the degree of Master of Science, with a major in Geology.

Otto C. Kopp

O. C. Kopp, Major Professor

We have read this thesis and recommend its acceptance:

Fred G. Keller

[illegible]

Russell J. Lewis

Accepted for the Council:

L. Evans Roth

Vice Chancellor
Graduate Studies and Research

PETROLOGIC, MINERALOGIC, AND ION EXCHANGE CHARACTERISTICS OF THE ROME FORMATION AND PUMPKIN VALLEY SHALE ON THE OAK RIDGE NATIONAL LABORATORY RESERVATION, OAK RIDGE, TENNESSEE

A Thesis

Presented for the

Master of Science

Degree

The University of Tennessee, Knoxville

Janine Gajda Sledz

December 1980

3046911

ACKNOWLEDGEMENTS

The author wishes to express her thanks to Dr. O. C. Kopp for all his time and energies devoted to this project. The suggestions and criticisms of committee members Dr. F. B. Keller and Dr. T. Tamura were also appreciated. Two ORNL staff members are acknowledged for their contributions to this study: Dr. S. Haase, whose advice was especially helpful since he is presently involved in related studies, and to Dr. R. Floran for the use of his microscope and photographic equipment. Finally, the author would like to acknowledge ORNL, operated by the Union Carbide Nuclear Corporation for their support of this study.

ABSTRACT

Two outcrops of the Rome Formation and lower Conasauga Group, located on the Oak Ridge National Laboratory Reservation were studied with respect to their petrologic, mineralogic, and ion exchange characteristics. Twenty-eight sample pairs (a pair consisted of a fresh and weathered segment) were taken from each outcrop.

The argillaceous samples were analyzed by x-ray diffraction and the remaining samples by thin section analysis. Using an ammonia electrode, CEC values were determined for all argillaceous samples and selected non-argillaceous samples. Porosity determinations of the fresh segments of the sandstones and siltstones were made, using 10 to 12 micron thick petrographic sections.

X-ray analysis established the presence of illite, glauconite, kaolinite, chlorite, biotite, muscovite, quartz, hematite, calcite, dolomite, Kspar, and plagioclase. Quantification of shales is complicated by the clay minerals, therefore the data is strictly qualitative. The presence of randomly interstratified clays, discrete crystallites, or a combination was suggested by a few broad peaks on the diffractograms. The exact nature of these peaks was undeterminable in this study.

For the argillaceous samples, CEC's ranged from 5.52 to 33.61 meq/100 g. A few sandstones analyzed generally had values at or below the lowest value of the siltstones. Clay mineral content (by visual estimates) appeared to be directly proportional to CEC values.

Quartz, Kspar, matrix, cement (quartz overgrowths, hematite, calcite), glauconite, plagioclase, muscovite, and biotite were the

mineral components of the sandstones and siltstones. Based on modal analysis, the following "average" composition for all non-argillaceous samples was calculated: quartz-58%, Kspar-20%, matrix-10%, cement-4%, glauconite-3%, plagioclase-2%, muscovite-1%, miscellany-1%, and biotite-trace.

The "typical" Rome sandstone is mature, well-sorted, subarkosic, and a very fine sandstone to silty sandstone. Sandy siltstones to silty sandstones, which were moderately sorted and immature, are the "average" non-argillaceous units of the Conasauga.

The porosity of the samples examined can be attributed to four factors: deterioration of glauconitic and micaceous grains, microscopic voids, discontinuous microscopic cracks, and macroscopic fractures. Values ranged from 0-10%. A notable difference was observed in the average porosities between samples from the two outcrops: 0.7% at the Comparative Animal Research Lab and 3.7% at the Fuel Reprocessing Road outcrop. The slightly higher degree of weathering at the FR location is believed responsible for the sizeable variations.

Samples from the fresh and weathered segments of all lithologies exhibited little or no mineralogical variation.

The data gathered in this investigation provide information concerning the lithologies directly at or adjacent to waste burial sites. From this data, it is possible to assess the potential for the development of an aquifer, should any material seep from the Pumpkin Valley Shale (where some waste is buried) into the Rome Formation. The uppermost portion of the Rome (thick layers of sandstones) is bound above and below by shale layers. In the event of seepage of waste fluid, shales are significantly more effective in removing cations

than sandstones, and are fairly impervious. If any fluid does reach the Rome sandstones, it is unlikely that an aquifer would develop, since the sandstones have low absolute porosities, thus suggesting low permeabilities.

TABLE OF CONTENTS

LIST OF TABLES

LIST OF FIGURES

CHAPTER I

INTRODUCTION

Introduction

In recent years there has been growing concern over the methods employed for the disposal of radioactive waste materials. One currently used method is burial in selected geological formations which possess characteristics that retain and immobilize radioactive wastes for long periods of time. It must be realized that there are a limited number of geologically suitable sites for burial and that other factors involved may impose yet further restrictions on their use.

Radioactive waste disposal sites on the Oak Ridge National Lab reservation are located in the Conasauga Group which is composed principally of shales, interbedded with claystones, siltstones, and limestones. Directly below lies the Rome Formation which includes sandstones, siltstones, shales, and localized occurrences of dolostone and/or limestone. Previous investigations have shown the Rome on the reservation to be dominantly shale and sandstone (Carroll, 1961). Under certain conditions this combination of lithologies may act as an aquifer system (permeable unit between impermeable layers). Since radioactive waste products are presently being buried in the overlying Conasauga shales, the potential exists for some of this material to move downward into the potentially more porous and permeable beds in the Rome Formation.

The principal goals of this study are to determine the mineralogic, petrologic, and ion exchange characteristics of the typical lithologic

types found in the Rome Formation and the lower Conasauga Group (Pumpkin Valley Shale Member). If these analyses reveal a potential hazard or hazards, then they can be taken into account in the daily operations and in planning for future disposal sites.

Outcrops chosen for study are located approximately 6.5 km (4.2 mi) apart, just south of Bethel Valley Road (refer to Fig. 1). One outcrop is located along the Fuel Reprocessing Plant Road (FR), which is about 4.8 km (3 mi) east of X-10 (a major group of buildings at ORNL), while the other is just within the boundary of the Comparative Animal Research Lab facility (CARL). The FR outcrop consists almost entirely of Rome, while at CARL there are nearly equivalent thicknesses of Rome and Conasauga exposed. See Table 1 for list of abbreviations.

Location

Located in the eastern sector of the state, Oak Ridge is approximately 48 km (30 mi) northwest of Knoxville, Tennessee. The Oak Ridge National Laboratory facilities, adjacent to the southwestern limits of the city, extend about 21 km (13 mi) in an east-west direction, and 10 km (6 mi) in a north-south direction (McMaster, 1963). On the reservation there are four principal units present: the Rome Formation, the Conasauga Group, the Knox Group, and the Chickamauga Group. Only the Rome and Conasauga were studied in this project.

The Rome, of early Cambrian age, is the oldest formation exposed and consists primarily of sandstones, siltstones, and shales on the reservation. The sandstone beds are more prevalent toward the upper segment of the formation, whereas the more argillaceous units dominate the lower half. Shales of the Rome characteristically exhibit banded

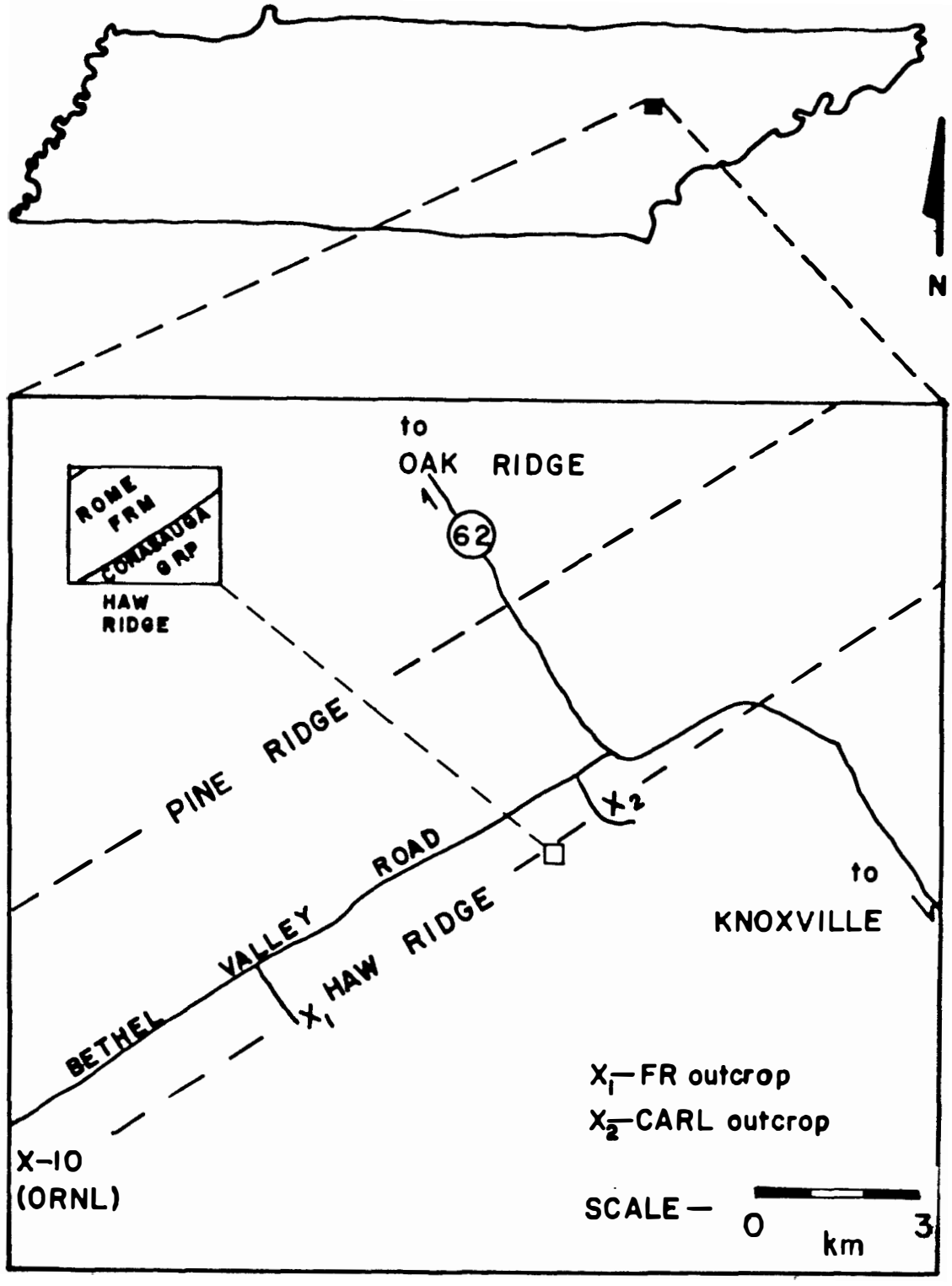

Figure 1. Location map.

TABLE 1

LIST OF TERMS

The following legend applies to all tables and figures in this report, but all terms do not occur in each figure or table.

Q	quartz
ILL	illite
MUS	muscovite
CHL	chlorite
GLAU	glauconite
BIO, BIOT	biotite
KAO	kaolinite
HEM	hematite
CAL	calcite
DOL	dolomite
KSP, KSPAR	alkali feldspar
PLAG	plagioclase
MAT	matrix
CEM	cement
MISC	miscellany
PORO	porosity
C, Clst	claystone
H, sh	shale
L, slt	siltstone
R	Rome Formation

TABLE 1 (continued)

C	Conasauga Group
FR	FR outcrop location
CARL	CARL outcrop location
FRM	formation
LITH	lithology
LOCA	location (see p. 7)
SAM	sample number
WX	fresh (f) or weathered (w) segment of sample
N	number of samples

coloration ranging from maroon, purple, and green, to various shades of brown. It is believed that only the uppermost few hundred meters of the formation are exposed in the area, having left 300 to 600 meters behind during the thrust sheet formation (McMaster, 1963). In all known exposures, thrust faults mark the lower contact, while there is a gradational contact between the Rome and lower Conasauga. The precise upper boundary of the Rome is arbitrary (McMaster, 1963; Harris and Milici, 1977). In this study, the upper limit is drawn 0.5 m above the last thick (30-35 cm) sandstone unit. This investigation involves only the Pumpkin Valley Shale; it comprises the lower 90 meters (300 ft) of the Conasauga Group. This shale-rich member is intercalated with very thin beds of siltstones. Although not as vibrant, the colors are similar to those of the Rome shales with shades of maroon, green, and brown dominating.

Within the bounds of the ORNL reservation, the Rome and lower Conasauga are located along two major parallel ridges trending approximately east-west (refer to Fig. 1): Pine Ridge, which is in the northern portion, and Haw Ridge to the southeast. The two factors bearing the greatest influence on site selection were:

a) the maximum exposure of beds (only outcrops essentially perpendicular to bedding were considered), and

b) the quality of the outcrops (i.e., freshness, minimal covered interval).

A thorough search for suitable outcrops was made over the entire reservation, and two sites were selected on Haw Ridge (see Fig. 1). No outcrops of sufficient size and quality were found along Pine Ridge. An additional incentive to investigate the more southerly ridge results

from the fact radioactive waste burial sites are presently located in the Conasauga Group adjacent (south) to Haw Ridge. The information obtained in this study involving Haw Ridge may not be directly applicable to the Rome and lower Conasauga on Pine Ridge since it is part of a different thrust sheet. Hence, a separate investigation would be in order if burial sites were to be developed in the Conasauga Group adjacent to Pine Ridge.

Previous Studies

There have been numerous studies involving the Rome Formation and the Conasauga Group. Some of these investigations have a fairly broad scope (Safford, 1869; Resser, 1938; Rodgers, 1953, 1956; Pettijohn, 1970; Palmer, 1971; Harris and Milici, 1977), while others have examined more narrowly defined aspects (Spigai, 1963; McMaster, 1963; Harris, 1964; Samman, 1975; Siribhakdi, 1976; Krumhansl, 1979). However, no previous study has characterized in detail the petrology and mineralogy of both the argillaceous and coarser-grained constituents of the Rome and/or Conasauga, nor determined their ion exchange characteristics.

Geologic History

The currently accepted interpretation of the geologic history of the southern Valley and Ridge is based on "thin-skinned" tectonics in which deformation is confined to sedimentary layers above the basement (Rodgers, 1956). Utilizing this concept, Harris and Milici (1977) prepared a generalized basin model to represent the original sedimentary basin in which the sediments that are now preserved in the present day Valley and Ridge were deposited. According to their reconstruction, there was a thick clastic sequence in the eastern portion, rimmed by a

narrow shelf sequence to the west. Rock units ranging from Cambrian to Pennsylvanian form a wedge-shaped sequence which thins from east to west in the southern part of the province. Three depositional episodes, each divided by regional unconformities are represented by the following intervals:

a) Cambrian-lower Ordovician

b) middle Ordovician-lower Devonian

c) upper Devonian-Pennsylvanian

The Rome Formation and Conasauga Group were deposited during the earliest of these three episodes.

Sequence "a" represents a westward transgression with diminishing clastics and increasing carbonates. The first deposits (Chilhowee Group) of shallow marine sandstones, intercalated with deeper water siltstones and shales, were succeeded by a shallow carbonate bank (Shady Dolomite). The shales, sandstones, and siltstones of the Rome Formation were deposited in shallow subtidal and intertidal environments directly west of the carbonate banks throughout the early and middle Cambrian. A deeper marine setting evolved after the deposition of the Rome by gradual subsidence of the basin. With a source to the northwest, a deep water lagoonal sequence of shale, thinly bedded limestone, and siltstone formed in the basin's western region; carbonates increased in abundance in the eastern segment where shallow marine conditions prevailed. These interfingering clastic and carbonate deposits constitute the Conasauga Group. During the late Cambrian, carbonate facies expanded westward from their eastern domain to cover the entire basin, resulting in the deposition of the Knox Group. Uplift, affecting much of the eastern and southern United States, terminated sedimentation

in Early Ordovician time. Later deposits were mainly derived from easterly sources uplifted during orogenic episodes during the remainder of the Paleozoic.

Field Work

Major divisions were made at each outcrop based on lithologic ratios and assigned a letter. In a few instances color played an important role particularly when subdividing the shales. At the CARL outcrop, 131 meters (430 ft) of measured section were split into nine major groups (A-I), while at the FR site the 197 meters (645 ft) were divided into seven groups (L-R). Although both outcrops exhibit faulting and folding, beds can generally be traced and fairly complete stratigraphic columns were prepared (see Figs. 2 and 3).

A minimum of two sample pairs were collected from every lettered group. The following is an example of the sample designations used:

FQ 3 F SS

F - sample from FR outcrop

Q - group in FR outcrop

3 - sample number taken from group

SS - sandstone lithology

When necessary, additional samples were taken to provide a complete representation of significant lithologies in each group. Each sample pair consisted of a relatively "fresh" and a relatively "weathered" portion. The weathered portion of the sample was taken directly from the surficial exposure, whereas the fresh segment was removed from a location parallel to the bedding plane, anywhere from 10 cm (4 in) to 30 cm (14 in) from the surface, depending on the difficulty in securing

I. Total thickness 131 meters
Scale
0 ———— 4 m

Groups A-I
A-G Rome Formation
H-I Conasauga Group (Pumpkin Valley Shale)

II. Symbols

Fault ------ F
Ripples ∿∿∿
Missing interval =/=
Continued -----

III. Abbreviations

Ss sandstone
Slt siltstone
Sh shale
Cl/Clst claystone
alt alternate sample
W weathered
F fresh

IV. Bed thicknesses (cm)

thick 30-100
medium 10-30
thin 3-10
very thinly 1-3
thickly laminated 0.3-1
thinly laminated < 0.3

V. Areas showing a marked increase in weathering effects (i.e., change in coloration, extent of weathered rind) are noted as such, on a comparative basis with the overall weathering conditions of the outcrop as a standard.
highly - greatest weathering effects noted
significantly - notable increase in weathering effects

Figure 2. Stratigraphic column for the CARL outcrop.

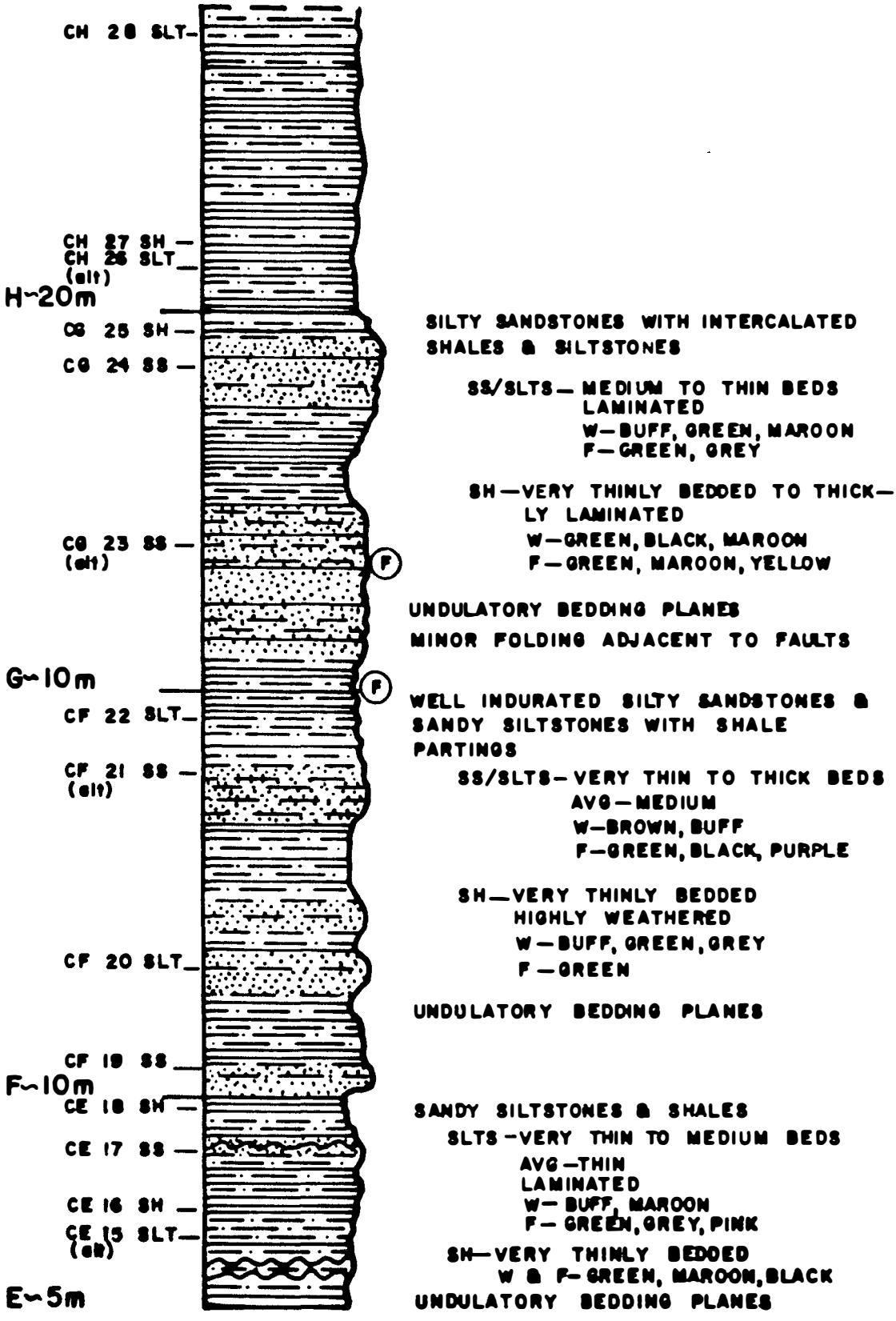

Figure 2 (continued)

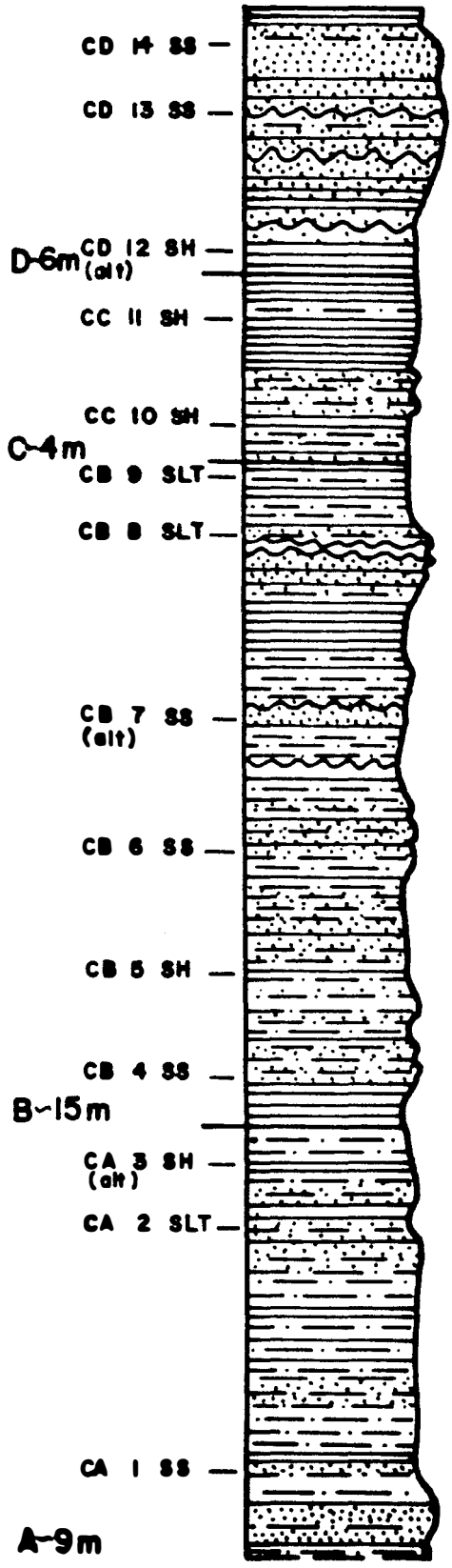

FINE-GRAINED SANDSTONES WITH INTER-BEDDED SHALES & SILTSTONES

SS — THIN TO THICK BEDS AVG-MEDIUM
W — BUFF, PINK
F — GREEN, GREY, MAROON
LAMINATED, SYMMETRICAL RIPPLES

SH — VERY THINLY BEDDED
THIN TO THICK LAMINATIONS
W & F — GREEN, MAROON

FINE-GRAINED SANDSTONES & SILTSTONES WITH INTERSEDDED SHALES

SS — VERY THINLY BEDDED
LAMINATED, FRIABLE
W & F - MAROON, GREEN

SH — VERY THINLY BEDDED
LAMINATED W & F GREEN, MAROON

SANDY SILTSTONES TO SILTY SANDSTONES INTERCALATED WITH SHALES

SS/SLTS — VERY THIN TO MEDIUM BEDDED
AVG — THIN
MASSIVE TO LAMINATED
MINOR STARVED RIPPLES
W — BUFF, MAROON, GREEN
F — MAROON, GREEN

SH — VERY THINLY BEDDED TO THINLY LAMINATED
W — MAROON, GREEN, GREY
F — MAROON, GREEN

MINOR TO MODERATE FOLDING
MINOR FAULTING
UNDULATORY BEDDING PLANES

SILTY SANDSTONES TO SANDY SILTSTONES INTERBEDDED WITH SHALES

SLTS/SS — THIN TO THICK BEDS
AVG — THIN
MASSIVE TO LAMINATED
W — PINK, BUFF
F — TAN, BROWN, GREY

SH — VERY THINLY BEDDED TO VERY THINLY LAMINATED
W — ORANGE, TAN, GREY
F — GREEN, GREY, BROWN

MINOR FOLDING
MINOR FAULTING

Figure 2 (continued)

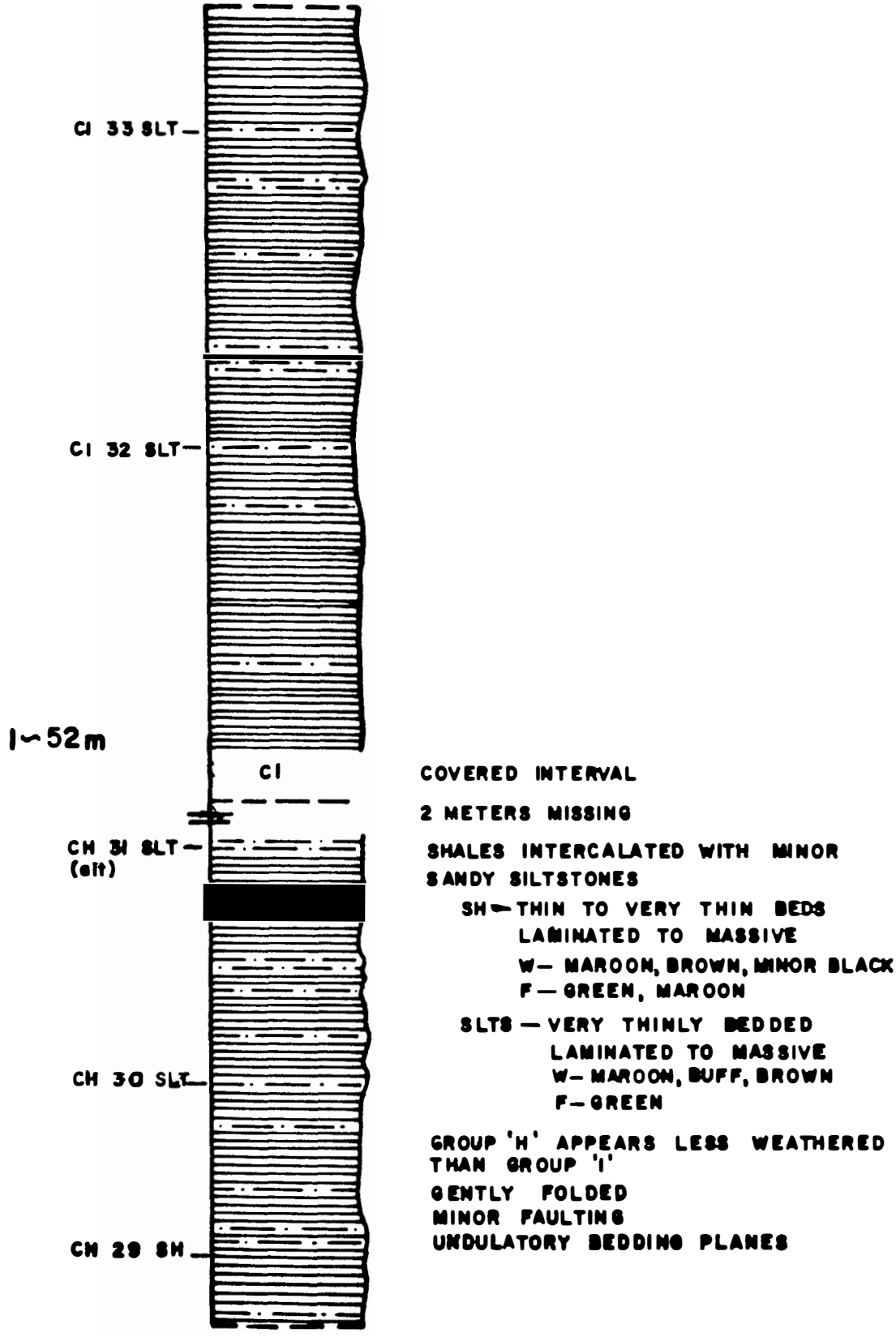

Figure 2 (continued)

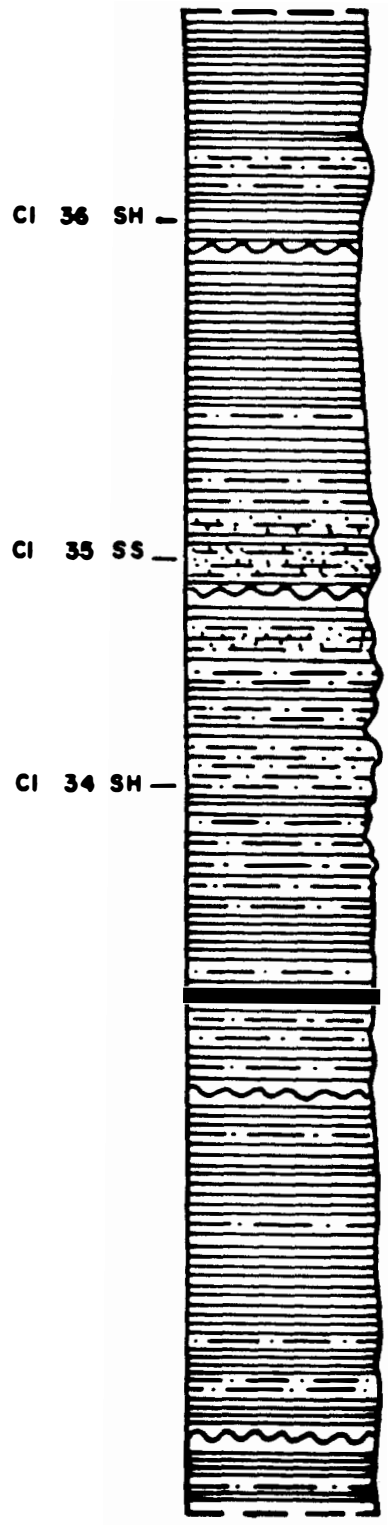

SHALES INTERCALATED WITH SILTSTONES & SANDY SILTSTONES

SH THINLY BEDDED TO THICKLY LAMINATED

W—MAROON, PURPLE, BROWN, GREEN YELLOW, BLACK

F—GREEN

SLTS —VERY THINLY TO THINLY BEDDED
LAMINATED TO MASSIVE
W—BUFF, GREEN
F—GREEN

GENTLY TO SEVERELY FOLDED
SYMMETRICAL RIPPLES
HIGHLY WEATHERED

Figure 2 (continued)

I. Total thickness 197 meters
Scale
0 4 m

Groups L-R
L-Q Rome Formation
R Conasauga Group (Pumpkin Valley Shale)

II. Symbols

Fault ------ F
Ripples ∿∿∿
Missing interval ≠
Continued ---

III. Abbreviations

Ss sandstone.
Slt siltstone
Sh shale
Cl/Clst claystone
alt alternate
W weathered
F fresh

IV. Bed thicknesses (cm)

thick 30-100
medium 10-30
thin 3-10
very thinly 1-3
thickly laminated 0.3-1
thinly laminated < 0.3

V. Areas showing a marked increase in weathering effects (i.e., change in coloration, extent of weathering rind) are noted as such, on a comparative basis with the overall weathering conditions of the outcrop as a standard.
highly - greatest weathering effects noted
significantly - notable increase in weathering effects

Figure 3. Stratigraphic column for the FR outcrop.

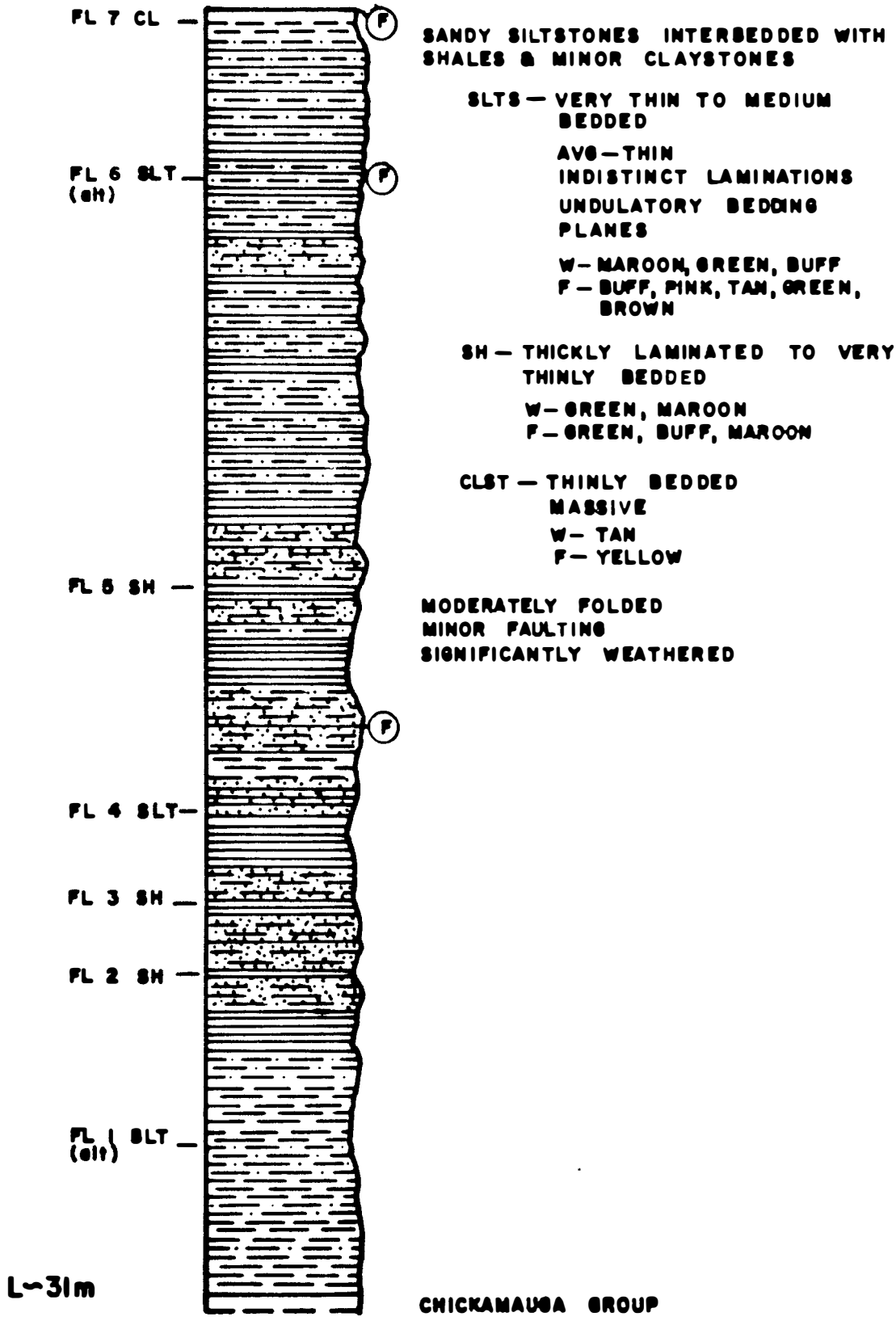

Figure 3 (continued)

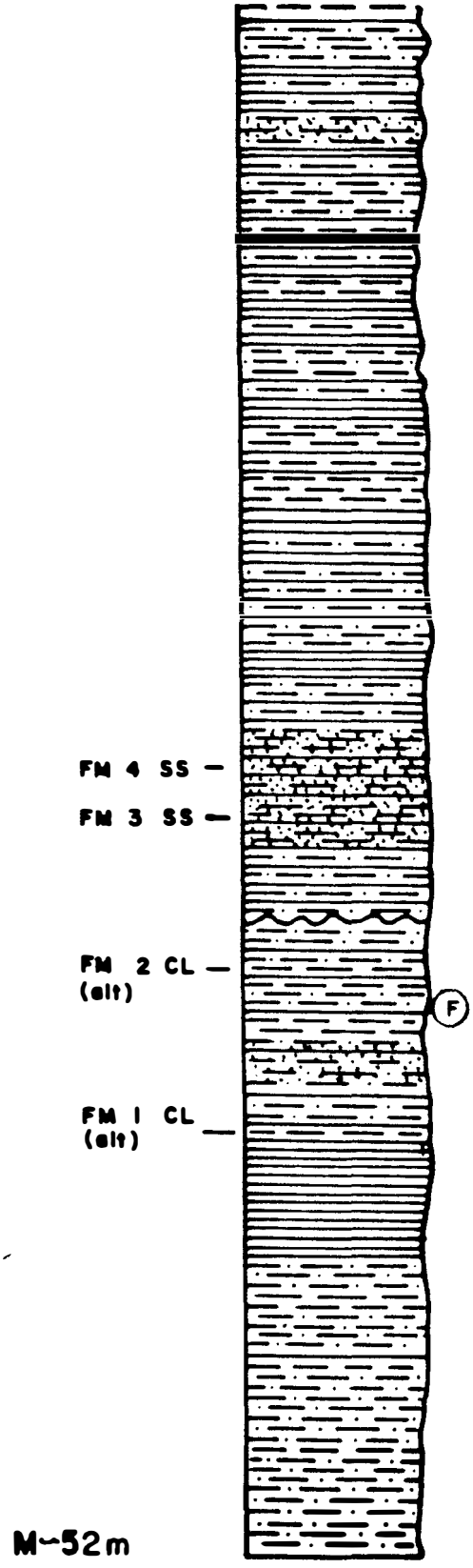

Figure 3 (continued)

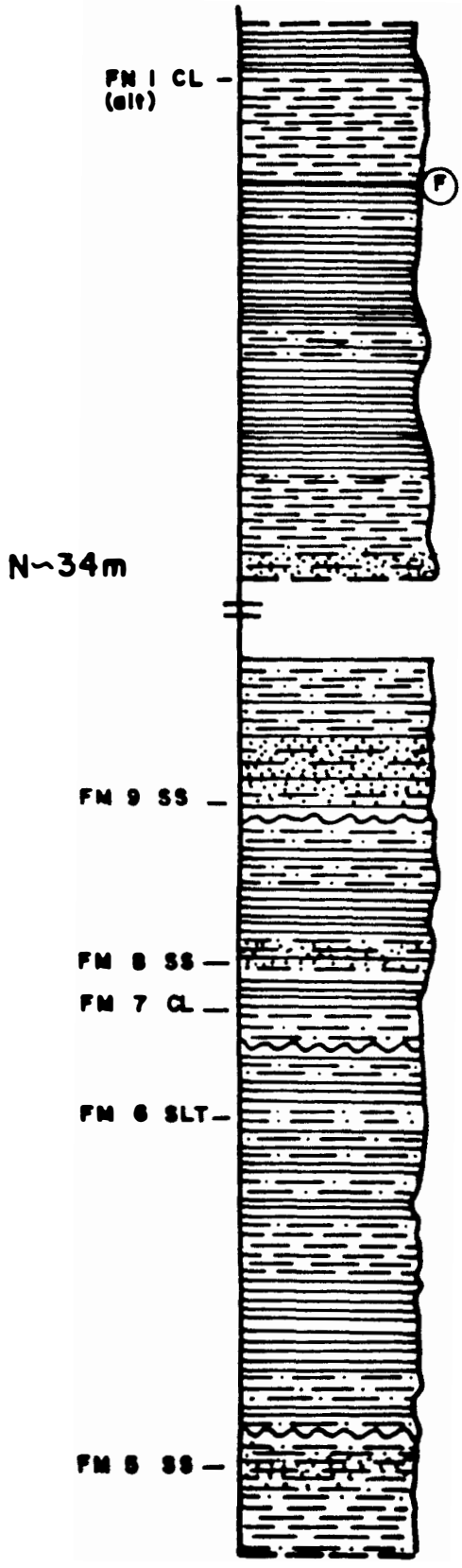

8 METERS MISSING

SILTSTONES & SHALES WITH MINOR CLAYSTONES & SANDSTONES

SH— THINLY LAMINATED TO THINLY BEDDED

W & F—GREEN, GREY, MAROON

SLTS—THIN TO THICK BEDS
AVG—THIN
LAMINATED
UNDULATORY BEDDING PLANES
SYMMETRICAL RIPPLES
W—MAROON, BUFF, BLACK
F—MAROON, GREY, GREEN, BUFF, YELLOW

CLST—THINLY BEDDED
MASSIVE
W—BUFF, MAROON, GREEN
F—YELLOW, BUFF, MAROON, GREEN

SS—VERY THINLY TO THINLY BEDDED
LAMINATED TO MASSIVE

W & F—BUFF

MINOR FAULTING
GENTLY FOLDED
SIGNIFICANTLY WEATHERED

Figure 3 (continued)

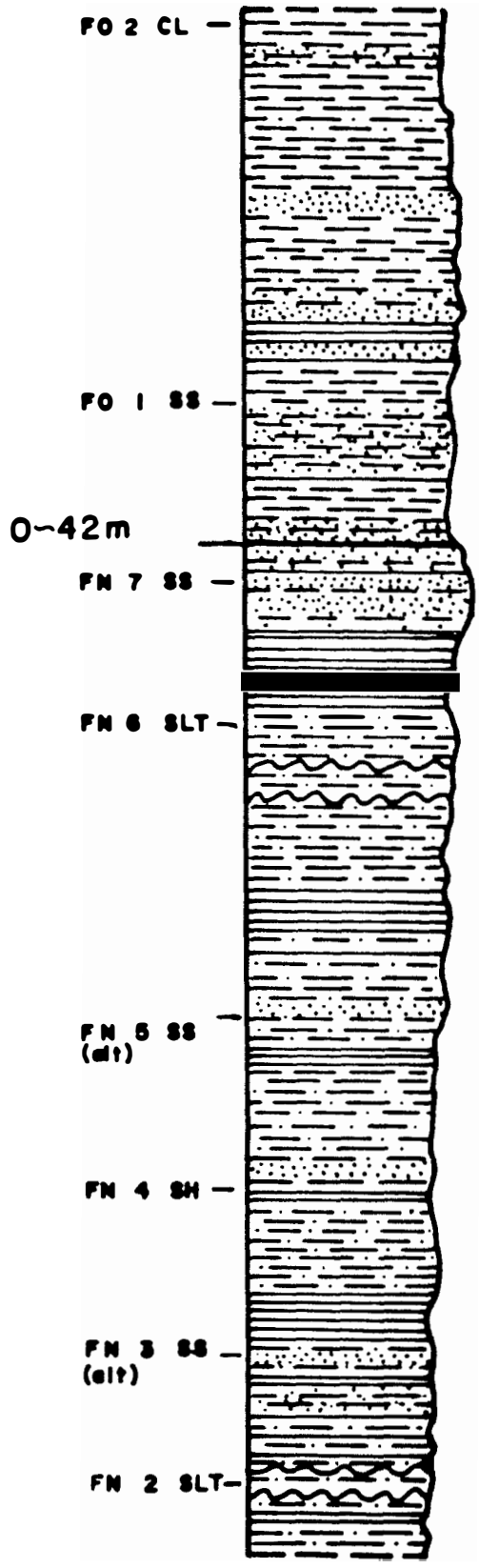

SILTSTONES & SHALES INTERBEDDED WITH MINOR CLAYSTONES & SAND STONES

SH—THICKLY LAMINATED TO THINLY BEDDED

W—MAROON, GREEN, BROWN, BUFF
F—GREEN, MAROON, BROWN

SLTS—VERY THIN TO THIN BEDS
LAMINATED TO MASSIVE
UNDULATORY BEDDING PLANES
SYMMETRICAL RIPPLES

W—BUFF, BROWN, MAROON, BLACK
F—GREEN, BROWN, YELLOW, MAROON, BLACK

SS—VERY THIN TO THICK BEDS
AVS—THIN
WELL INDURATED
MASSIVE TO LAMINATED
W—BUFF, BLACK
F—CREAM, GREEN

CLST—THINLY BEDDED
MASSIVE

W & F—YELLOW, MAROON, BUFF, GREEN

SIGNIFICANTLY WEATHERED
GENTLY FOLDED
FAULTED

Figure 3 (continued)

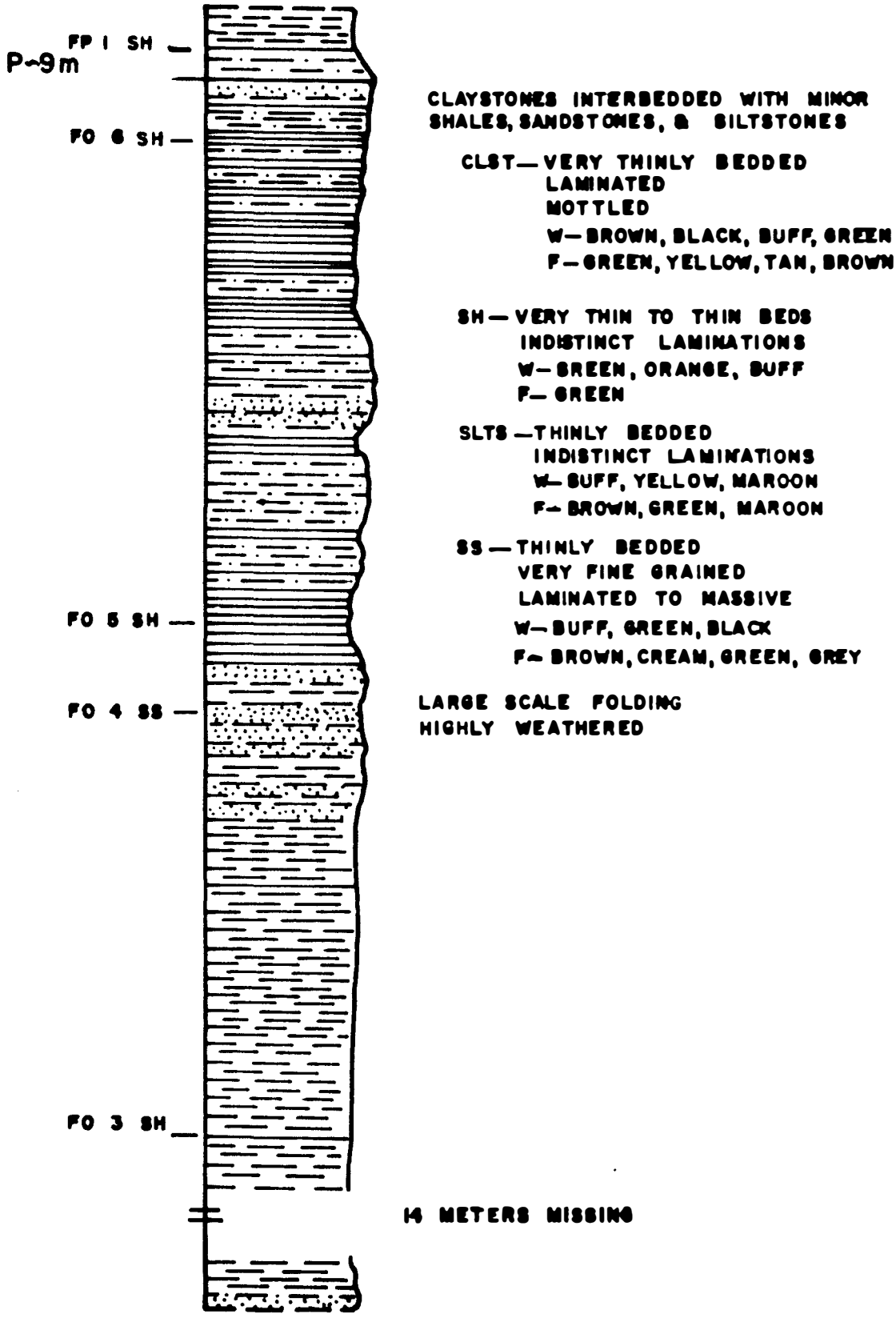

Figure 3 (continued)

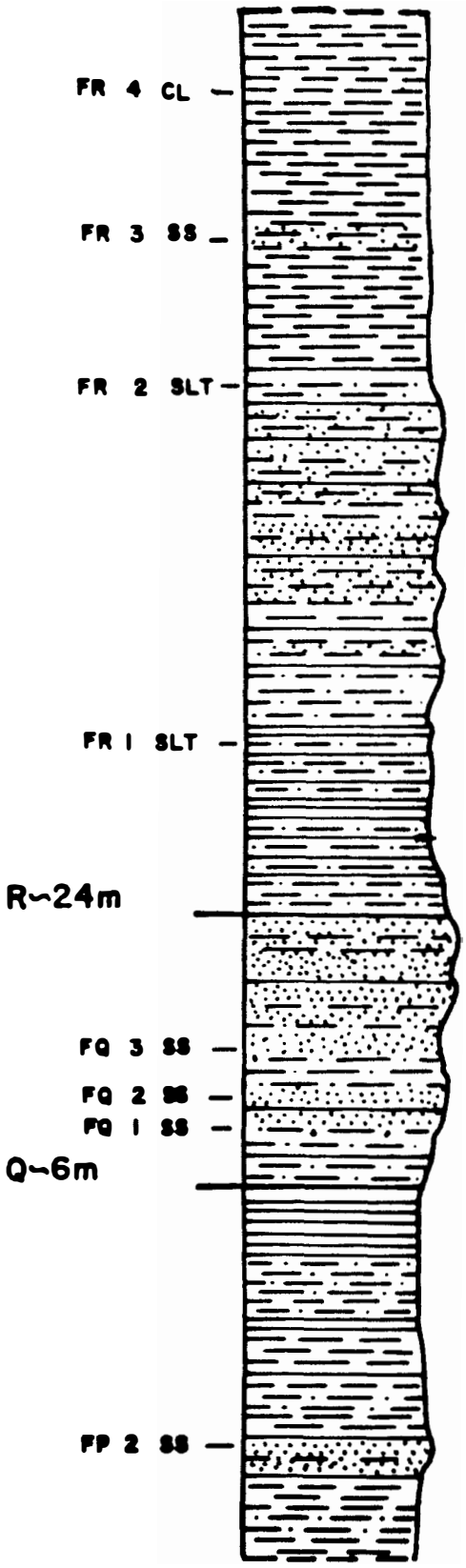

SS — THIN TO MEDIUM BEDDED
AVG — THIN
LAMINATED
UNDULATORY BEDDING PLANES
FAIRLY WELL INDURATED
W — BROWN, BLACK, BUFF, GREEN
F — CREAM, GREEN, BLACK, BROWN, YELLOW

SLTS — VERY THINLY TO THINLY BEDDED
AVG — THIN
MOTTLED
W — BROWN, BLACK, BUFF, GREEN
F — CREAM, GREEN, BLACK, BROWN YELLOW

SIGNIFICANTLY WEATHERED

SANDSTONES & SILTY SANDSTONES WITH MINOR SHALE PARTINGS

SS/SLTS — THIN TO THICK BEDS
AVG - MEDIUM
MASSIVE TO LAMINATED
FAIRLY WELL INDURATED
W — MAROON, BUFF, BROWN
F — BUFF, YELLOW, CREAM

SH — VERY THINLY BEDDED
W & F — GREEN & MAROON

CLAYSTONES & SHALEY CLAYSTONES WITH INTERBEDDED SILTSTONES TO SANDY SILTSTONES

CLST — LAMINATED
MOTTLED
W — GREEN, BROWN, BLACK, YELLOW
F — GREEN, YELLOW, BROWN

SLTS — VERY THIN TO MEDIUM BEDS
AVG — THIN
LAMINATED
FRIABLE
W MAROON, BLACK, BUFF
F MAROON, CREAM, GREEN

Figure 3 (continued)

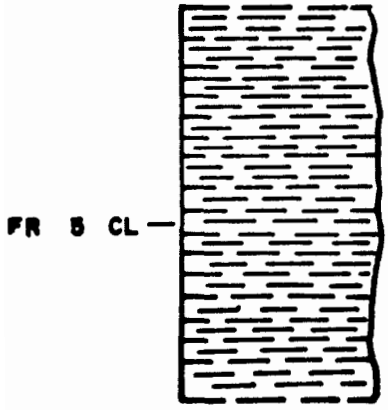

CLAYSTONES & SHALES INTERBEDDED
WITH MINOR SILTSTONES & SANDSTONES

CLST/SH – VERY THINLY TO THINLY BEDDED
MOTTLED TO LAMINATED
W – PINK, GREEN, BLACK, BROWN
F – PINK, GREEN, YELLOW, MAROON, BLACK

Figure 3 (continued)

samples of reasonable size. A total of 56 pairs of samples were taken, 28 from CARL, 28 from FR. Eighteen alternate samples were collected at the same time, to be available if the need arose to examine additional samples of certain lithologies.

CHAPTER II

INVESTIGATION OF THE ARGILLACEOUS COMPONENTS

Introduction

Burial in shallow pits and trenches, dug into completely or partially weathered Conasauga Group, has been conducted for over two decades at ORNL, and a major concern is long term hazards associated with the wastes (Lomenick et al., 1967). A knowledge of the cation exchange capacity (CEC) of shales is important, since it is a mechanism by which ions can be immobilized. CEC is dependent on the mineralogy of the shales, as clays are the principal minerals contributing to CEC. A knowledge of the mineralogy is also vital in understanding and predicting any potential interactions between the waste material, ground or meteoric water, and the enclosing lithologic units.

Previous Studies

Numerous studies of shales have focused specifically on the clay mineral components or a particular clay mineral present. In contrast, there are a fairly limited number of studies of whole rock shales. Investigations by Shaw and Weaver (1965), Schultz (1964), Greensmith (1958), and Grim et al. (1957), provide some of the most complete sources of information because they describe numerous methods of analysis of the bulk rock shales and their mineral constituents. X-ray techniques were exclusively employed by Purton and Youell (1969) and Evans and Adams (1974).

According to Weaver (1957), there is a significant change in clay mineral suite composition of Paleozoic rocks: Pre-Upper Mississippian

rocks contain fairly simple suites, whereas later rocks tend to be more variable and complex in clay mineral composition. This distribution is thought to be primarily a function of tectonics and source rocks, later modified by metamorphism, epigenesis, syngenesis, preferential segregation, and climate.

Previous studies of Cambrian and older shales are scarce. Their focus is on the clay mineral constituents, as illustrated in works by Suchecki et al. (1977), Tank and McNeeley (1970), and Velde and Hower (1963). Although the Rome and Conasauga are of Cambrian age, valuable information regarding the characterization of the argillaceous materials was obtained from the many studies spanning the Paleozoic from the Ordovician to Permian.

Methods of Analysis

In analyzing the argillaceous components of the Rome and Conasauga, two basic methods were employed: x-ray diffraction (XRD) and cation exchange capacity (CEC) determination. The former technique provides valuable information on all the major crystalline constituents of the whole rock samples, while CEC's are largely attributed to the clay minerals present in each sample.

The argillaceous samples, which include all shales and claystones as well as a few siltstones which were unsuitable for thin section preparation, were ground manually with a mortar and pestle to pass through a 2 mm mesh (number 10) sieve. To insure uniform grinding throughout the entire array of samples, equivalent quantities were ground further by a mechanical grinder for one hour. A preliminary test was conducted to determine the optimum length of time for grinding mechanically (see Appendix 1).

X-Ray Diffraction

Preparation and Analysis

From the mechanically ground samples, smear slides were prepared (see Appendix 2). This particular type of mount was selected on the basis of precision and accuracy (Stokke and Carson, 1973; Gibbs, 1965). After air drying, each was run from 5° to 68° 2θ on a Norelco diffractometer at 1/2°/min, with CuKα radiation, at 35 kv, and 17 ma.

Selected samples were x-rayed after glycolation and after heat treatment at 550° for one hour. Based on their responses, it was deemed unnecessary to treat all samples. As a further check, the coarser segment (sand to medium silt) was removed from several samples, and the finer fractions analyzed by x-ray diffraction and subjected to treatments (heat and glycolation). Results indicated separations of the remaining samples were unwarranted.

Interpretation

Broad peaks, specifically in the 8-12 Å and 2.7-2.3 Å ranges, were noted in all patterns. The peak heights varied from sample to sample, but the overall shapes remained fairly constant. The broadened peaks were believed to harbor maximum intensity peaks of illite, muscovite, biotite, and/or glauconite. However, many reflections (aside from those of the broadened peaks) were obscured by peaks of other minerals.

In an attempt to resolve the clay mineralogy, diffractograms of the finer-grained ($<2\mu$) fractions were analyzed. These patterns did show an enhancement of the clay mineral peaks and supression of the peaks of the coarser-grained components (i.e., feldspar, quartz, etc.). The resolution of the broadened peaks did not change. Overlapping

peaks will not be resolved if the spacing between peaks is less than the width at one half the maximum of the individual peaks.

Peak broadening can be the result of mechanical mixing of discrete minerals, interstratification, or various gradational stages between the two (Grim, 1968; Brown, 1961). Interstratified minerals are a special case of intergrowths permitted by genetic similarities, both as regular and random mixed-layer clays.

In regularly interstratified sequences, regular repetition of layers along the c-axis yields a unit cell equal to the sum to the components and regular basal reflections are observed. There was no evidence for regular interstratification in any pattern, since no regular periodicity (integral sequence) was observed.

Random mixed-layers (non-regular intergrowths) do not produce an integral sequence, hence are generally more difficult to establish. There is little deviation from the standard pattern of the major components if one mineral dominates (90%). Changes in diffraction effects will occur if both (considering a two component system) are abundant. Random interstratifications are often characterized by a non-integral series of basal reflections; they are composites of reflections of the pairs (two components). Their exact positions and intensities are dependent on the quantities present.

According to Weaver (1957), randomly interstratified 2:1 layer clays (i.e., illite-montmorillonite, chlorite-montmorillonite, illite-chlorite-montmorillonite) are fairly common in sedimentary rocks (note: smectite is now the accepted group name for clay minerals with a layer charge between 0.2 and 0.6/formula unit, thus antiquating the term montmorillonite; Bailey, 1980). Weaver (1957) examined more than

6,000 sedimentary specimens, ranging in age from Cambrian to Recent, and found that approximately 70% contained some form of mixed layer clays. Most were randomly interstratified. The development of mixed layers is commonly attributed to the aggradation or degradation of pre-existing clays during weathering, ion exchange during transportation, diagenesis, etc.

Since the broadened and overlapping diffraction peaks crucial to the identification of the clay minerals were not resolved (even with treatment), it is not possible to conclusively report the presence of random interstratifications, discrete crystallites, or a combination (Mills and Zwarich, 1972; Heller-Kallai and Kalman, 1972). Further studies involving only the clay fraction might offer more conclusive evidence.

Phyllosilicate constituents identified by XRD are illite, glauconite, kaolinite, chlorite, biotite, and muscovite. The latter two were sufficiently coarse in grain size to be identified in several samples with a binocular microscope. Many biotite reflections, however, are generally obscured by quartz peaks.

In an investigation involving the Conasauga, Rome, and Chickamauga from the Joy test well core, calcite, quartz, illite, kaolinite, chlorite, feldspars, dolomite, montmorillonite, and mixed-layer sequences were identified by R. E. Grim (de Laguna et al., 1968). Most of the constituents of the Rome and Conasauga were recognized in both the present study and that of de Laguna et al. (1968) with the exception of montmorillonite and mixed-layers. The latter has been discussed previously. There was no evidence for the presence of montmorillonite (smectite) in the samples analyzed in this study.

Glycolation of both whole rock and the finer fraction samples did not result in a peak shift (from 14 Å to 17 Å), or even an alteration in peak configuration. Krumhansl (1979) also reported no response of the Conasauga shales to glycolation, although interstratification of illite-smectite was suspected. In this investigation, heat treatment verified the presence of chlorite by a slight increase in peak height at 7 Å.

Non-Clay Minerals

Recognition of non-clay minerals was not complicated by peak broadening, as with the clays. Minor peak overlaps do exist, but do not greatly hamper identification, as other distinguishing reflections are denerally present. Quartz, hematite, calcite, dolomite, Kspar, and plagioclase were identified.

Quantification

The argillaceous samples are complex, multicomponent systems making quantification by x-ray diffraction difficult. In addition, there appears to be a significant amount of clay present, based on visual inspection of the samples themselves. Clays are notorious for their extensive substitution capabilities which further complicate any quantification attempts. Standards are more easily obtained for non-clay minerals, such as quartz and dolomite. In general, the greater the amount of non-clay material, the more easily the shale is quantified (Cubitt, 1975).

The possibility of attempting a quantitative or semi-quantitative analysis was considered in the embryonic stages of this investigation. However, upon examining the resultant patterns and reviewing the most

recent developments in quantification of x-ray diffractograms (Bardossy et al., 1980; Pearson, 1978; Cubitt, 1975; Towe, 1974; Stokke and Carson, 1973; Pierce and Siegel, 1969; Gibbs, 1965), it was not considered feasible in this particular study due to numerous obstacles (i.e., obtaining standards, amount and complexities of the clays present, etc.).

Results

A typical pattern is shown in Fig. 4. The diffraction patterns were analyzed and the peak heights (intensities) of the mineral components believed present were recorded. Intensities for those minerals believed to be included in the broadened peaks are estimates. It should be noted that the maximum possible number of minerals present in a sample were recorded (see Table 2). Due to certain conditions previously discussed it was not always possible to unequivocally identify the presence or absence of a particular mineral solely on the basis of x-ray data. Mineral frequencies for all 48 samples (fresh and weathered) are presented in Figure 5. Since the x-ray diffraction data could not be quantified, discussion is limited. Numerical values (peak intensities) are thought to have significance only when comparing fresh and weathered samples of the same specimen.

Most of the diagnostic peaks for biotite were obscured by other minerals, therefore XRD data for biotite is questionable. Small amounts were noted in about half of hand specimens (using a binocular microscope). Although biotite is by no means a quantitatively significant constituent, it is certainly reasonable to assume small quantities are present in most, if not all samples.

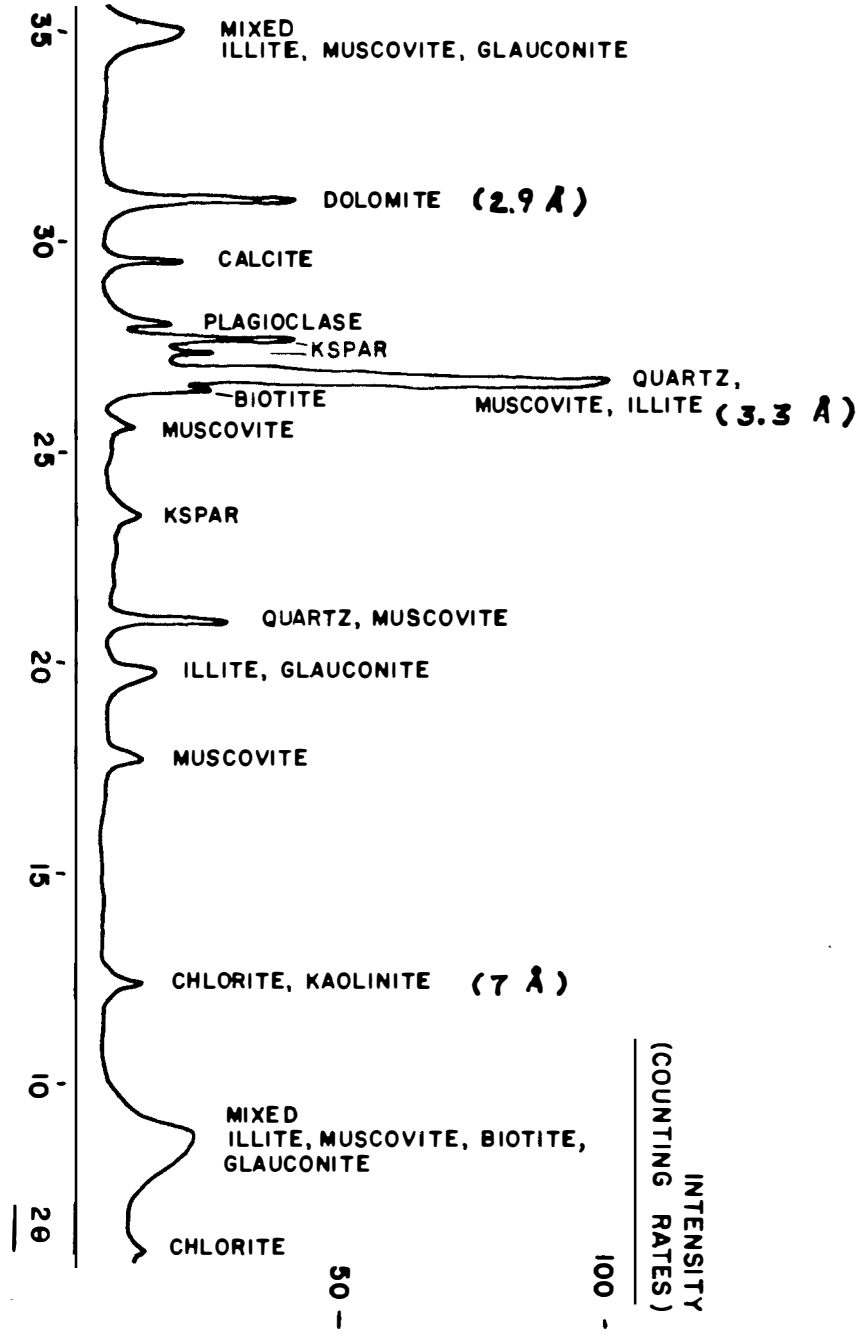

Figure 4. Typical diffraction pattern of an argillaceous sample.

TABLE 2

MINERALS DETECTED IN THE ARGILLACEOUS SAMPLES AND CEC VALUES
(ALL ARGILLACEOUS SAMPLES)

AREA=CARL

OBS	LOCA	SAM	WX	LITH	CEC	Q	ILL	MUS	CHL	GLAU	BIO	KAO	HEM	CAL	DOL	KSPAR	PLAG	N	SPP	FRM
1	CB	5	F	M	14.24	1	1	1	1	1	1	1	0	0	1	1	1	1	1	R
2	CB	5	W	M	9.64	1	1	1	1	1	1	1	0	1	1	1	1	2	2	R
3	CC	10	F	M	14.29	1	1	1	1	1	1	1	0	1	1	1	1	3	3	R
4	CC	10	W	M	13.57	1	1	1	1	1	1	1	0	1	1	1	1	4	4	R
5	CC	11	F	M	13.82	1	1	1	1	1	1	0	1	0	0	1	1	5	5	R
6	CC	11	W	M	14.47	1	1	1	1	1	1	1	1	0	0	1	1	6	6	R
7	CE	16	B	M	10.48	1	1	1	0	0	1	1	0	1	1	1	1	7	7	R
8	CE	16	*	M	19.71	1	1	1	0	0	0	1	0	0	0	1	0	8	8	R
9	CE	18	F	M	15.84	1	1	1	1	1	1	1	0	1	1	1	0	9	9	R
10	CE	18	W	M	12.35	1	1	1	1	1	1	0	0	1	1	1	0	10	10	R
11	CG	25	F	M	16.71	1	1	1	0	1	1	1	0	1	1	1	1	11	11	R
12	CG	25	W	M	13.68	1	1	1	0	1	1	1	0	1	1	1	1	12	12	R
13	CH	27	F	M	12.67	1	1	1	1	1	1	0	1	1	0	1	0	13	13	C
14	CH	27	W	M	14.43	1	1	1	1	1	1	1	1	1	0	0	0	14	14	C
15	CH	29	F	M	12.67	1	1	1	1	1	1	1	0	1	0	1	0	15	15	C
16	CH	29	W	M	11.81	1	1	1	1	1	1	1	0	1	0	1	0	16	16	C
17	CH	30	F	L	14.59	1	1	1	1	1	1	0	0	1	0	1	1	17	17	C
18	CH	30	W	L	12.22	1	1	1	1	1	1	1	0	0	0	1	1	18	18	C
19	CI	34	F	M	28.72	1	1	1	1	1	1	1	0	0	0	1	1	19	19	C
20	CI	34	W	M	19.60	1	1	1	1	1	1	1	0	0	0	1	1	20	20	C
21	CI	36	F	M	22.23	1	1	1	1	1	1	0	1	0	0	1	1	21	21	C
22	CI	36	W	M	19.37	1	1	1	1	1	1	0	1	0	0	0	0	22	22	C

AREA=FR

OBS	LOCA	SAM	WX	LITH	CEC	Q	ILL	MUS	CHL	GLAU	BIO	KAO	HEM	CAL	DOL	KSPAR	PLAG	N	SPP	FRM
23	FL	2	F	M	12.03	1	1	1	0	1	1	1	0	0	1	1	0	23	23	R
24	FL	2	W	M	13.38	1	1	1	0	1	0	1	0	0	1	1	0	24	24	R
25	FL	3	F	M	15.47	1	1	1	0	1	1	1	1	1	1	1	0	25	25	R
26	FL	3	W	M	13.10	1	1	1	0	1	1	1	1	0	1	1	1	26	26	R
27	FL	5	F	M	11.95	1	1	1	0	1	1	1	0	1	1	1	0	27	27	R
28	FL	5	W	M	11.43	1	1	1	0	1	1	1	0	0	1	1	0	28	28	R
29	FL	7	F	C	18.90	1	1	1	0	1	1	1	0	0	1	1	0	29	29	R
30	FL	7	W	C	17.12	1	1	1	0	1	1	1	0	0	1	1	0	30	30	R
31	FM	6	F	L	18.26	1	1	1	0	1	1	0	0	0	1	1	0	31	31	R
32	FM	6	W	L	15.38	1	1	1	0	1	1	0	0	0	1	1	0	32	32	R
33	FM	7	F	C	18.31	1	1	1	0	1	1	0	0	0	1	1	0	33	33	R
34	FM	7	W	C	26.78	1	1	1	0	1	1	0	0	0	1	1	0	34	34	R
35	FN	4	F	M	13.60	1	1	1	0	1	1	1	0	0	1	1	1	35	35	R
36	FN	4	W	M	16.80	1	1	1	0	1	1	1	0	0	0	1	1	36	36	R
37	FO	2	F	C	15.40	1	1	1	0	0	1	0	1	0	0	1	0	37	37	R
38	FO	2	W	C	15.22	1	1	1	0	0	1	0	1	0	1	1	0	38	38	R
39	FO	5	F	M	15.63	1	1	1	1	1	1	1	0	1	1	1	0	39	39	R
40	FO	5	W	M	12.34	1	1	1	0	1	1	1	0	0	1	1	0	40	40	R
41	FO	6	F	C	27.97	1	1	1	0	1	1	0	1	0	1	1	0	41	41	R
42	FO	6	W	C	33.61	1	1	1	0	1	1	0	1	1	1	1	0	42	42	R
43	FR	1	F	L	5.52	1	1	1	0	0	1	0	0	1	0	1	0	43	43	C
44	FR	1	W	L	6.02	1	1	1	0	0	1	0	0	0	1	1	0	44	44	C
45	FR	4	F	C	17.33	1	1	1	0	1	1	0	0	0	0	1	0	45	45	C
46	FR	4	W	C	17.27	1	1	1	0	1	1	0	0	1	0	1	0	46	46	C
47	FR	5	F	C	13.67	1	1	1	0	1	1	0	0	0	0	1	0	47	47	C
48	FR	5	W	C	12.70	1	1	1	1	1	1	0	0	0	0	1	0	48	48	C

1 = minerals detected; 2 = minerals not detected.

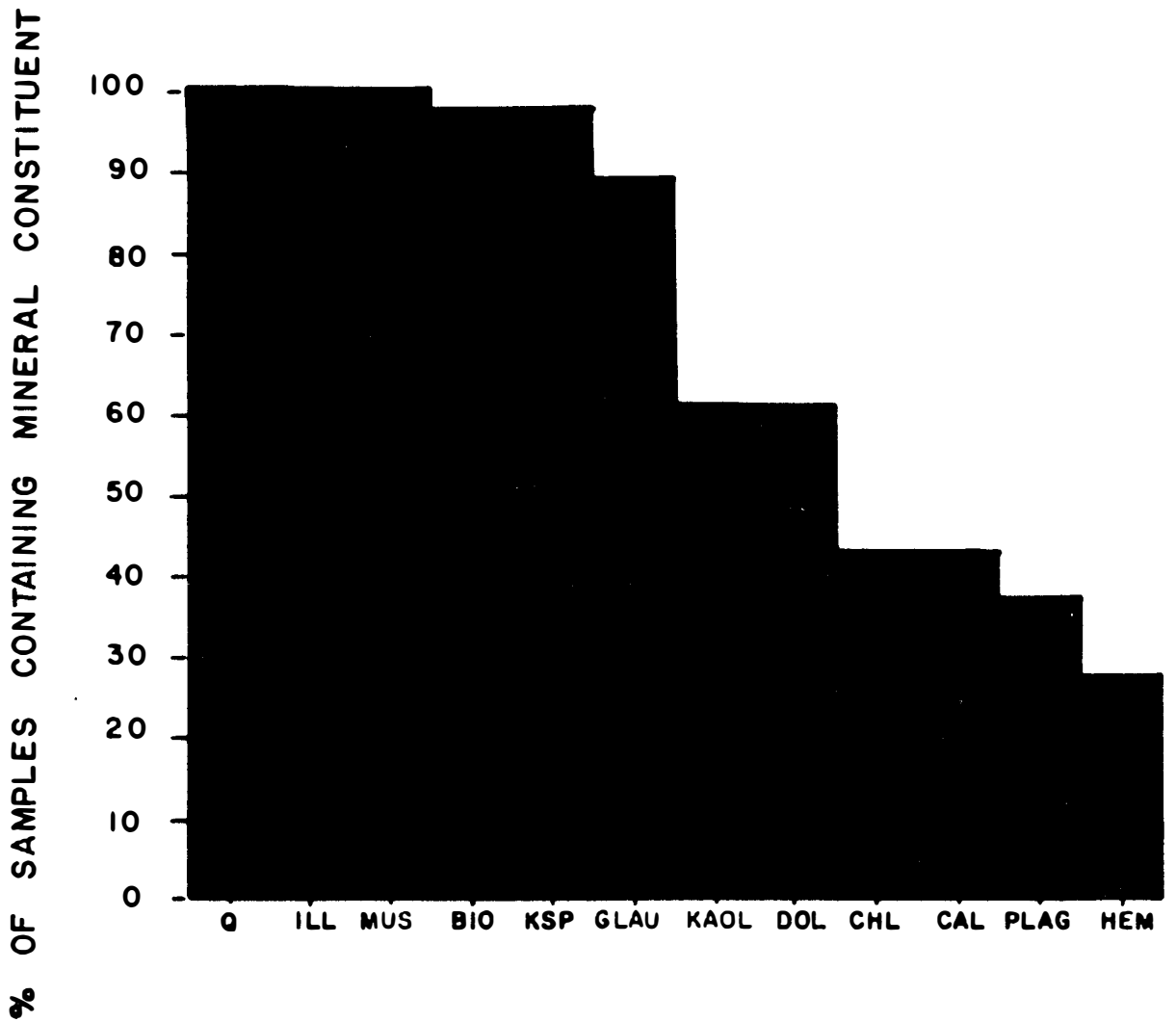

Figure 5. Mineral distribution for the argillaceous samples.

Fresh and Weathered. Although the majority of constituents maintained fairly equivalent intensities in the comparison of their fresh (f) and weathered (w) segments, there were notable exceptions with certain minerals: quartz, calcite, dolomite, and/or Kspar exhibit an intensity difference of more than ten in some sample pairs (Table 3). Neither the cause nor significance is known. No obvious trend for intensities (ex. f > w, f < w) of any mineral was noted.

Every sample appears to contain quartz, illite, and muscovite in both fresh and weathered segments. When present, hematite and glauconite are the only other minerals that consistently appear in both fresh and weathered segments (refer to Tables 2 and 3).

CARL and FR. There was considerable decrease in occurrence of chlorite and plagioclase in the FR outcrop (Table 2) compared to the CARL outcrop. The significance of this difference is uncertain, but may be attributable to depositional environment, diagenesis, or weathering.

Rome and Conasauga. In the CARL data, the only apparent significant mineralogical difference between the argillaceous samples of the Rome (CB 5-CG 25) and Conasauga (CH 27-CI 36; see Table 2), is the lack of dolomite in the Conasauga samples. At the FR location, there is an apparent scarcity of kaolinite and hematite in the Conasauga (FR 1,4,5). It should be noted that very little of the Pumpkin Valley Shale (lowest member of the Conasauga Group) is exposed at FR, hence no significant comparative statement can be made.

Cation Exchange Capacity

CEC Defined

Cation exchange capacity (CEC) refers to the number of cation exchange sites per unit weight; CEC values are commonly reported in

TABLE 3

PEAK INTENSITIES OF THE ARGILLACEOUS SAMPLES (ALL 48)

AREA=CARL

OBS	LOCA	SAM	WX	LITH	CEC	Q	ILL	MUS	CHL	GLAU	BIO	KAO	HEM	CAL	DOL	KSPAR	PLAG	N	SMP	FRM
1	CB	5	F	M	14.24	126	18	21	7	21	22	7	0	0	9	27	59	1	1	A
2	CB	5	W	M	9.64	184	15	19	9	19	15	7	0	16	10	44	74	2	2	A
3	CC	10	F	M	14.29	63	15	16	8	17	14	6	0	12	9	18	19	3	3	A
4	CC	10	W	M	13.57	124	13	16	9	18	16	7	0	12	9	23	18	4	4	A
5	CC	11	F	M	13.82	120	21	26	9	26	26	0	8	0	0	29	24	5	5	A
6	CC	11	W	M	14.67	81	15	17	7	17	17	6	7	0	0	18	14	6	6	A
7	CE	16	B	M	10.48	143	11	10	0	0	10	5	0	10	13	56	25	7	7	A
8	CE	16	*	M	19.71	45	12	16	0	0	0	6	0	0	0	26	0	8	8	A
9	CE	18	F	M	15.84	69	13	13	8	14	12	4	0	13	45	35	0	9	9	A
10	CE	18	W	M	12.35	166	14	21	10	11	12	0	0	16	47	12	0	10	10	A
11	CG	25	F	M	16.71	95	15	15	0	15	14	6	0	9	9	40	20	11	11	A
12	CG	25	W	M	13.68	100	12	13	0	12	12	5	0	9	8	54	24	12	12	A
13	CH	27	F	M	12.67	60	13	14	15	14	15	0	10	9	0	5	0	13	13	C
14	CH	27	W	M	14.43	63	16	17	8	18	18	8	9	10	0	0	0	14	14	C
15	CH	29	F	M	12.67	260	13	11	8	12	12	7	0	9	0	12	0	15	15	C
16	CH	29	W	M	11.81	268	13	13	8	13	13	7	0	6	0	11	0	16	16	C
17	CH	30	F	L	14.59	150	12	12	5	12	12	0	0	7	0	11	15	17	17	C
18	CH	30	W	L	12.22	2100	12	12	7	5	12	8	0	0	0	18	24	18	18	C
19	CI	34	F	M	28.72	188	17	18	16	17	17	8	0	0	0	11	31	19	19	C
20	CI	34	W	M	19.60	253	14	15	13	15	15	12	0	0	0	8	32	20	20	C
21	CI	36	F	M	22.23	178	12	15	9	12	14	0	7	0	0	9	10	21	21	C
22	CI	36	W	M	19.37	136	14	14	10	10	11	0	8	0	0	0	0	22	22	C

AREA=FR

OBS	LOCA	SAM	WX	LITH	CEC	Q	ILL	MUS	CHL	GLAU	BIO	KAO	HEM	CAL	DOL	KSPAR	PLAG	N	SMP	FRM
23	FL	2	F	M	12.03	116	12	12	0	9	10	7	0	0	14	44	0	23	23	A
24	FL	2	W	M	13.38	47	14	10	0	8	0	7	0	0	11	30	0	24	24	A
25	FL	3	F	M	15.47	43	18	13	0	14	14	6	9	11	14	19	0	25	25	A
26	FL	3	W	M	13.10	40	11	12	0	5	5	6	8	0	16	15	20	26	26	A
27	FL	5	F	M	11.95	59	8	10	0	10	10	6	0	52	51	32	0	27	27	A
28	FL	5	W	M	11.43	82	10	11	0	11	8	8	0	0	16	38	0	28	28	A
29	FL	7	F	C	18.90	60	10	10	0	9	10	6	0	0	13	35	0	29	29	A
30	FL	7	W	C	17.12	55	13	14	0	13	12	7	0	0	11	52	0	30	30	A
31	FN	6	F	L	18.26	144	13	11	0	12	11	0	0	0	10	37	0	31	31	A
32	FN	6	W	L	15.38	158	8	12	0	12	12	0	0	0	11	35	0	32	32	A
33	FN	7	F	C	18.31	146	10	10	0	10	10	0	0	0	7	24	0	33	33	A
34	FN	7	W	C	26.78	4250	9	10	0	9	9	0	0	0	8	27	0	34	34	A
35	FN	4	F	M	13.60	175	14	15	0	14	15	5	0	0	8	70	8	35	35	A
36	FN	4	W	M	16.80	52	17	18	0	17	14	5	0	0	0	25	13	36	36	A
37	FO	2	F	C	15.40	31	6	16	0	0	12	0	5	0	0	5	0	37	37	A
38	FO	2	W	C	15.22	55	7	8	0	0	8	0	10	0	5	22	0	38	38	A
39	FO	5	F	M	15.63	126	14	14	5	14	14	8	0	8	9	36	0	39	39	A
40	FO	5	W	M	12.34	169	13	11	0	12	12	8	0	0	12	48	0	40	40	A
41	FO	6	F	C	27.97	122	14	14	0	12	12	0	9	0	9	42	0	41	41	A
42	FO	6	W	C	33.61	150	12	12	0	8	12	0	10	5	8	54	0	42	42	A
43	FR	1	F	L	5.52	9999	9	7	0	0	7	0	0	7	0	15	0	43	43	C
44	FR	1	W	L	6.02	9999	8	8	0	0	7	0	0	0	5	35	0	44	44	C
45	FR	4	F	C	17.33	285	9	8	0	8	8	0	0	0	0	25	0	45	45	C
46	FR	4	W	C	17.27	395	12	9	0	8	8	0	0	8	0	11	0	46	46	C
47	FR	5	F	C	13.67	270	8	8	0	8	8	0	0	0	0	16	0	47	47	C
48	FR	5	W	C	12.70	340	8	8	8	8	8	0	0	0	0	27	0	48	48	C

milliequivalents (meq)/100 grams (g). For example, if a substance has a CEC of 1 meq/100 g, then there are 6.02×10^{20} negatively charged adsorption sites present (Foth and Turk, 1972).

According to Grim (1968), there are three major causes of CEC in clay minerals:

1) Broken bonds around the peripheries of the silica-alumina units result in unbalanced charges which would be satisfied by adsorbed cations. Lattice distortions tend to increase broken bonds, hence CEC would increase with a decreasing degree of crystallinity. For illites and chlorites broken bonds are a major cause of CEC.

2) Within the lattice structures, there can be substitution of lower valence ions for Al^{+3} in the octahedral sheet, and Al^{+3} for Si^{+4} in the tetrahedral sheet. Aside from adsorbed cations, other lattice changes such as OH^{-1} replacing O^{-2} can occasionally rectify the imbalance. In this situation exchangeable cations are normally located on cleavage planes. Charges resulting from substitution in the tetrahedral sheet have a stronger bond due to the shorter distance as opposed to the longer bond for substitutions in the octahedral sheet. Replacements can occur in either or both the ocatahedral or tetrahedral layers. Substitutions contribute to a limited degree to the CEC of illites and chlorites.

3) The hydrogen of exposed hydroxyls (which is in the structure rather than the result of bond breakage) can be replaced by an exchangeable cation. This is not a particularly common cause of CEC since the hydrogen is held tightly when compared with those resulting from broken bonds. This particular cause can be of importance when considering kaolinite, due to the presence of the hydroxyl sheet on one side of the basal cleavage surface.

Significance of CEC

Many ionic species are rapidly tied-up or held by clays in shales. Illite is believed to be the predominant clay mineral in the Conasauga shales (Lomenick et al., 1967; de Laguna, 1968; Carroll, 1961). Radionuclides such as ^{90}Sr and ^{137}Cs are of importance, and to a lesser degree, ^{106}Ru, ^{89}Sr, ^{134}Cs, ^{125}Sb, ^{60}Co, ^{94}Zr-Nb, ^{103}Ru (Lomenick et al., 1967). A significant amount of ^{137}Cs and ^{90}Sr is adsorbed onto the illite along the edges of the crystal lattice (Lomenick et al., 1967). Sawhney (1970) also attributes Cs adsorption (surficial adhesion) in illites to frayed edges created during weathering. According to Tamura and Jacobs (1960), illite's high affinity for Cs is primarily due to its 10Å spacing (c-axis dimension) and abundance of potassium ions which initiate and maintain a collapsed state (not significantly affecting the CEC), allowing for the incorporation of Cs. CEC values alone do not fully explain Cs sorption (absorption and adsorption phenomena).

Quartz and other silt sized (and larger) components are believed to have negligible roles in CEC (Foth and Turk, 1972).

Method

The ammonia electrode technique, as discussed by Busenberg and Clemency (1973), was selected for CEC determinations of bulk shale samples. Aside from the obvious advantages of speed, simplicity, the use of fairly inexpensive equipment, and freedom from interferences by certain ions, this technique is accurate to low values on the order of 0.01 meq/100 g. Such low values may be encountered when dealing with whole rock shales, and other methods of CEC determinations may not be reliable for very low values.

Procedure

Samples manually ground (to pass a 2 mm sieve) were used for two reasons: to insure analysis of the bulk rock sample (as would be encountered at the outcrop) and to avoid creation of exchange sites by excessive grinding which would yield artificially high CEC's. The procedure outlined below adheres closely to that presented by Busenberg and Clemency (1973).

1) Approximately 10 g of each sample was saturated overnight in 100 mls of 1N ammonium acetate.

2) The samples were rinsed with an additional 50 mls of ammonium chloride. Excess ammonium salts were leached with 100 mls of isopropanol.

3) One hundred mls of deionized water were added to 5 g (exact weights were recorded) of thoroughly air dried samples. Stirring was commenced, using a magnetic stirrer; the Orion model Ammonia Electrode was immersed, and 1 ml of 10 M sodium hydroxide was added by volumetric pipette.

4) After delivery of the sodium hydroxide, a reading was taken in millivolts (mv), at 30 second intervals, from an Orion 701/digital pH meter. Electrode readings were recorded until a constant potential was observed for 1.5 minutes (3 readings).

5) CEC values were determined by the method described by Busenberg and Clemency with precision to 0.01 meq/100 g (see Appendix 3).

Results

The CEC values measured for the argillaceous samples ranged from 5.52 to 33.61 meq/100 g. A complete listing is presented in Tables 2 and 3, pages 32 and 35. These values support a previous investigation

of CEC values of some Rome and Conasauga core samples which ranged from 5.76 to 29.40 meq/100 g (de Laguna et al., 1968). The clay minerals in the samples analyzed include illite, muscovite, chlorite, glauconite, biotite, and kaolinite. The following is a list of CEC values for certain clay minerals: kaolinite, 3-15; illite, 10-40; smectite, 80-150 meq/100 g (Grim, 1968).

With reference to all tables and figures it is important to note the two CE 16 SH samples. They are unique in that they are not fresh and weathered segments, as are all the others. In this case, fresh and weathered samples were unobtainable. CE 16 B SH is a very thinly bedded black shale, and CE 16 * SH is a thin, pale green shale immediately below. They are relatively insignificant in the overall view of lithologies as they are atypical samples and constitute a very minor fraction of the shales exposed.

Comparative CEC data. Table 4 is a compilation of the CEC data in terms of means ($\bar{X}$) and standard deviations (σ) for both CARL and FR samples with varying emphasis. In each case the "B" grouping differs from the "A" in that the two highest and the two lowest values from FR and the highest and the lowest values from CARL were not included in the calculations. This was done to moderate the effects the extremely high and low values exercise on the means. In Table 4,

1) Groups 1 A and B compare all the data from each outcrop.
2) Groups 2 A and B compare fresh and weathered segments.
3) Groups 3 A and B compare the individual lithologies present.

In the CARL data, the comparatively high value of 28.72 (6.5 greater than any other CARL value) and the somewhat low value of 9.64 meq/100 g (only 0.5 meq/100 g difference from the fresh value)

TABLE 4

CEC DATA COMPARISONS BASED ON THE OUTCROP LOCATION, DEGREE OF WEATHERING, AND LITHOLOGIC TYPE

Group	Description	N	Min.	Max.	$\bar{X}$*	σ**
1A	CARL	20	9.64	28.72	15.35	4.31
	FR	26	5.52	33.61	15.96	6.02
	CARL + FR	46	5.52	33.61	15.70	5.30
1B	CARL	18	11.81	22.23	14.93	2.85
	FR	22	11.43	26.78	15.54	3.39
	CARL + FR	40	11.43	26.78	15.27	3.13
2A	CARL-f	10	12.67	28.72	16.57	5.08
	CARL-w	10	9.64	19.60	14.13	3.17
	FR-f	13	5.52	27.97	15.69	5.13
	FR-w	13	6.02	33.61	16.24	7.01
2B	CARL-f	9	12.67	22.23	15.22	2.93
	CARL-w	9	11.81	19.60	14.63	2.91
	FR-f	11	11.95	18.90	15.50	2.49
	FR-w	11	11.43	26.78	15.59	4.23
3A	CARL-sh	18	9.64	28.72	15.57	4.48
	CARL-slt	2	12.22	14.59	13.40	1.67
	FR-clst	12	12.70	33.61	19.62	6.44
	FR-sh	10	11.43	16.80	13.57	1.81
	FR-slt	4	5.52	18.26	11.29	6.49
3B	CARL-sh	16	11.81	22.23	15.12	2.95
	CARL-slt	2	12.22	14.59	13.40	1.67
	FR-clst	10	12.70	26.78	17.27	3.88
	FR-sh	10	11.43	16.80	13.57	1.81
	FR-slt	2	15.38	18.26	16.82	2.03

Min. = Minimum

Max. = Maximum

$\bar{X}$* = mean

σ** = one standard deviation

probably reflect the inhomogeneities of the rock units. The lowest number eliminated is not a true extreme; however, to be statistically valid, if the highest value is eliminated, so must the lowest. The other CARL (fresh and weathered) values do not exhibit such extreme differences.

The extremes of the FR data were the two high values of FO 6 (fresh and weathered) and the two lows of FR 1 (fresh and weathered). In this instance the extreme values can be explained as a function of lithology: the claystone with the highest, and the siltstone with the lowest.

Comparison of fresh and weathered samples, and CARL and FR. A comparison of CEC values for the fresh and weathered segments of the same sample is given in Table 5. Fresh and weathered are considered essentially equal, provided the difference is less than 1.00 meq/100 g. In the equation for the determination of CEC (see Appendix 3) the concentration is determined graphically; a difference of only 6% (concentration) can result in a CEC value differential of 1.00. Hence, any differences less than 1.00 are considered negligible. For the CARL data, f > w appears to be significant, with an average difference of 2.44. This was not the case with the FR data. Combining the data for the two outcrops reveals no consistent trend (refer to Figs. 6, 7, 8, and 9). Elimination of the extreme values in both data sets can greatly affect the mean and standard deviation; a few inconsistent or extreme results can obscure a pattern or trend (Table 5). The difference between the fresh and weathered segments, in both CARL and FR, is less than 1.00 meq/100 g, hence is insignificant.

TABLE 5

COMPARISON OF CEC VALUES OF FRESH AND WEATHERED SAMPLES IN THE CARL AND FR OUTCROPS

CARL (all 10 observations)		Mean	
fresh = weathered	30%	fresh	16.57 ± 5.09 meq/100g
fresh > weathered	60	weathered	14.13 ± 3.17
fresh < weathered	10	difference	2.44
FR (all 13 observations)			
fresh = weathered	38%	fresh	15.69 ± 5.14
fresh > weathered	31	weathered	16.24 ± 7.01
fresh < weathered	31	difference	0.55
FR and CARL (all 23 observations)			
fresh = weathered	35%	fresh	16.13
fresh > weathered	43	weathered	15.19
fresh < weathered	22	difference	0.94
CARL (9 observations)			
fresh	15.22 ± 2.94		
weathered	14.63 ± 2.92	difference	0.59
FR (11 observations)			
fresh	15.50 ± 2.49		
weathered	15.59 ± 4.23	difference	0.09

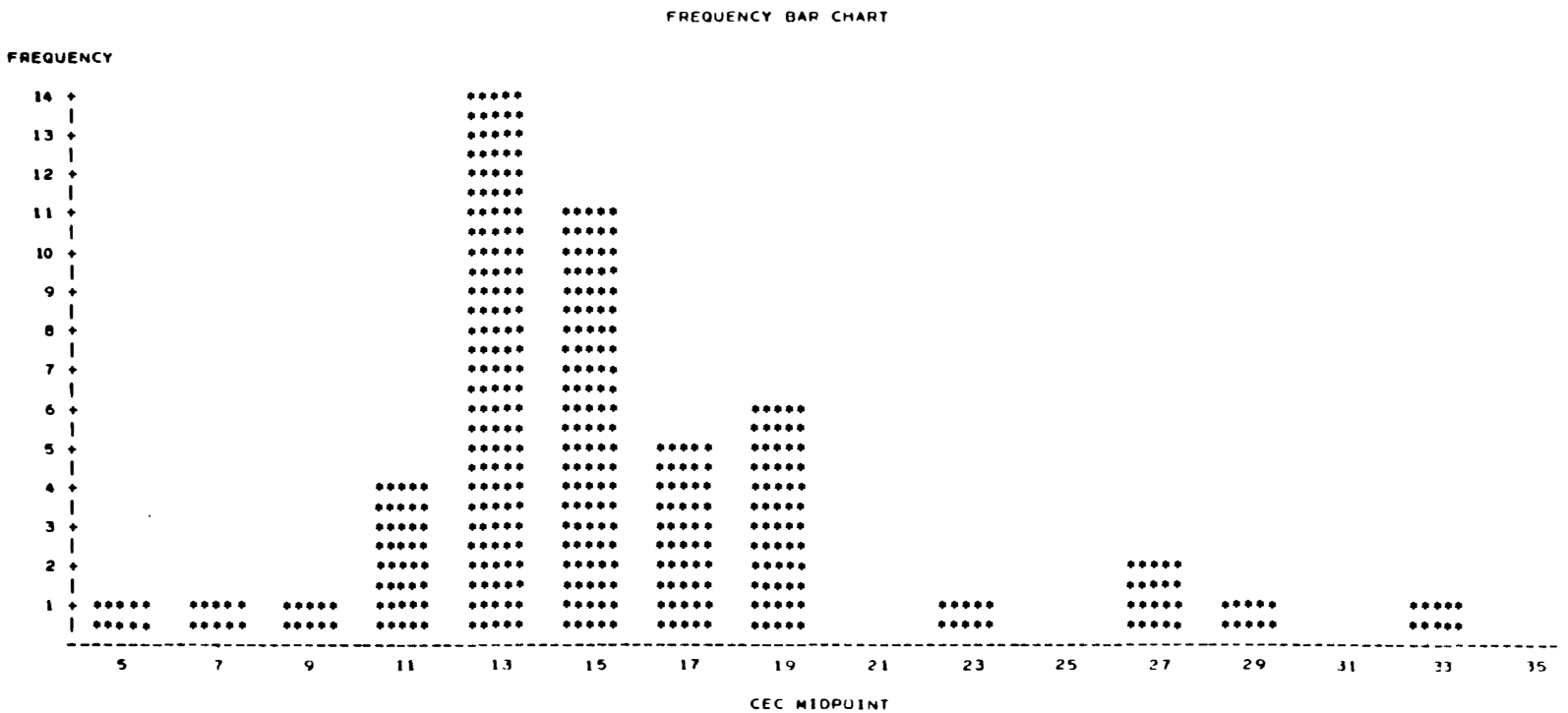

Figure 6. Frequency bar chart for CEC distribution of samples from CARL and FR (all 48 samples).

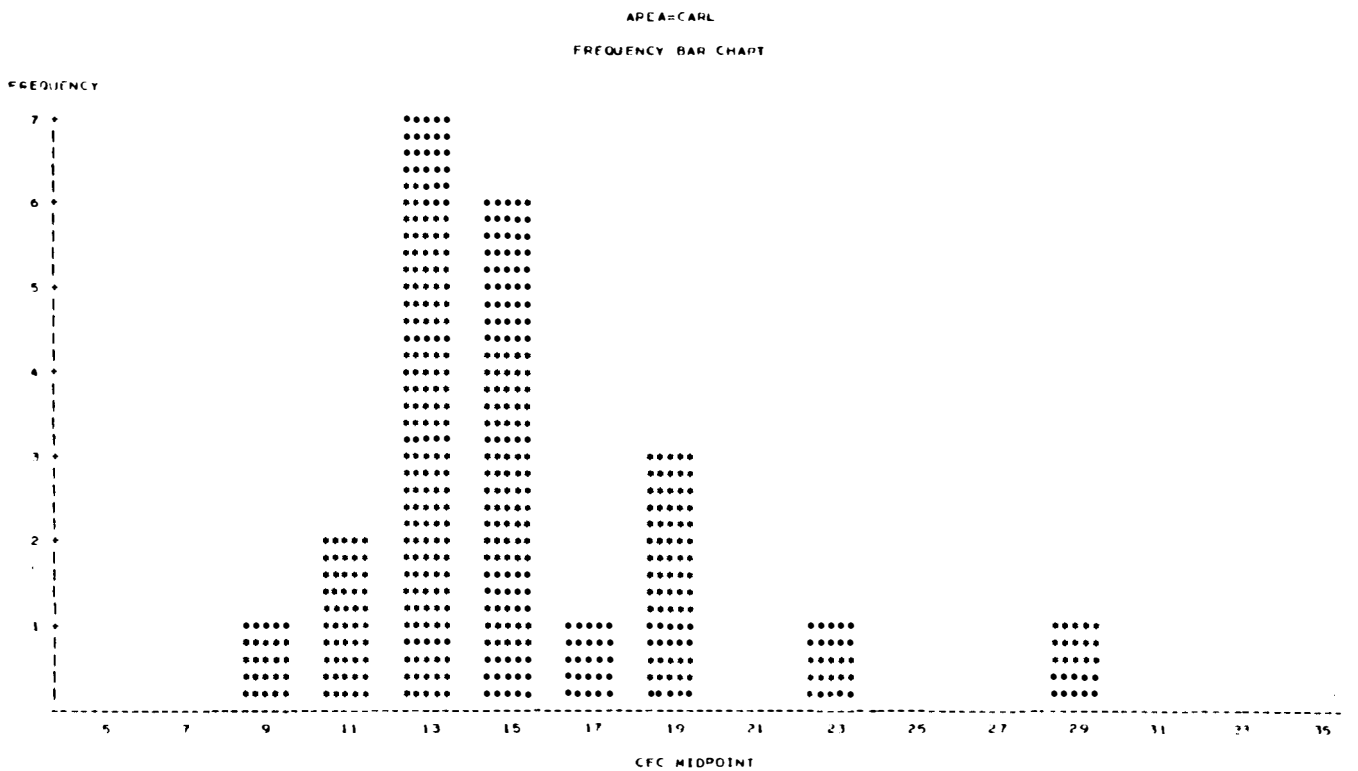

Figure 7. Comparison of frequency distribution of CEC values of the CARL and FR outcrops. Both follow the same basic pattern. Samples of the FR outcrop have a slightly greater range of CEC values.

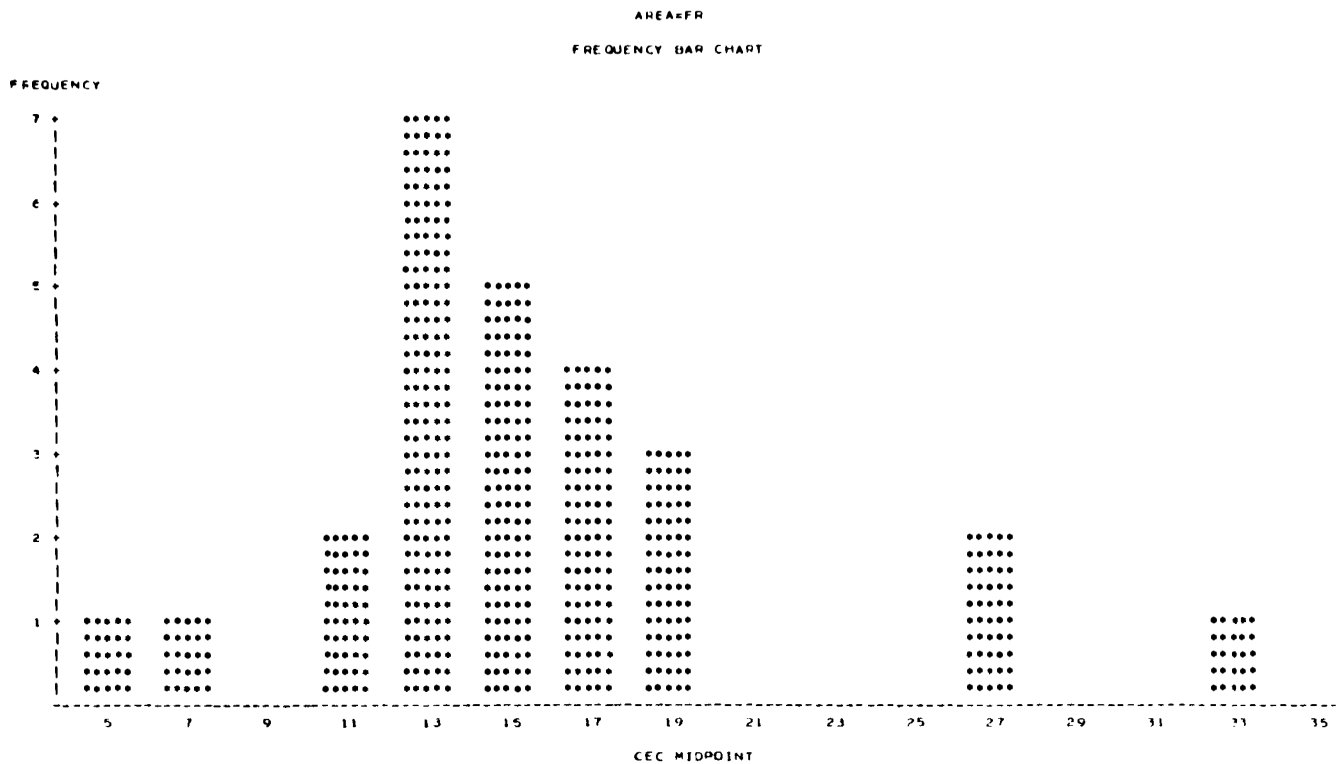

Figure 7 (continued)

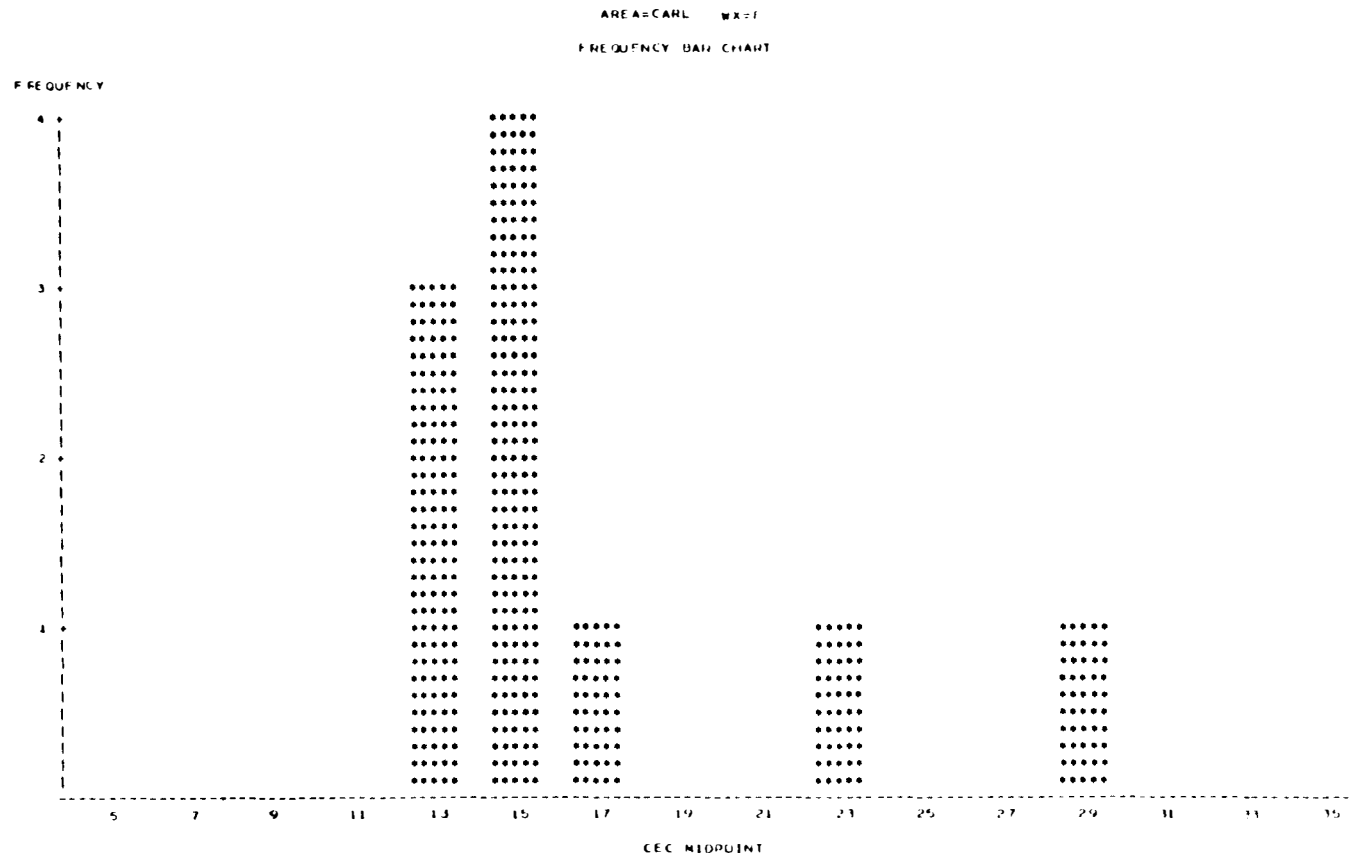

Figure 8. Frequency chart for fresh vs. weathered segments of CARL samples. Fresh segments exhibit a slight skewness towards higher CEC values as opposed to the more normally distributed weathered segments.

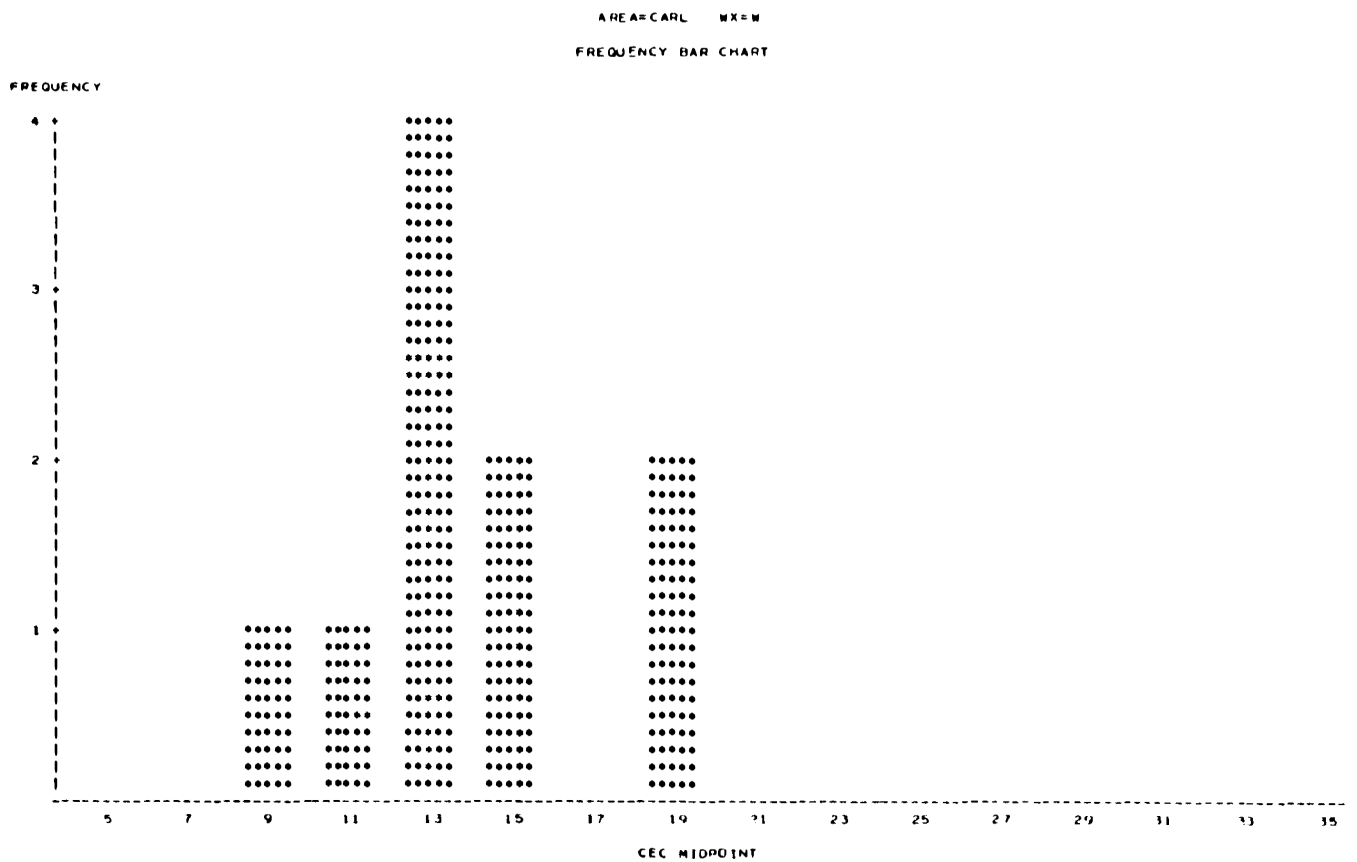

Figure 8 (continued)

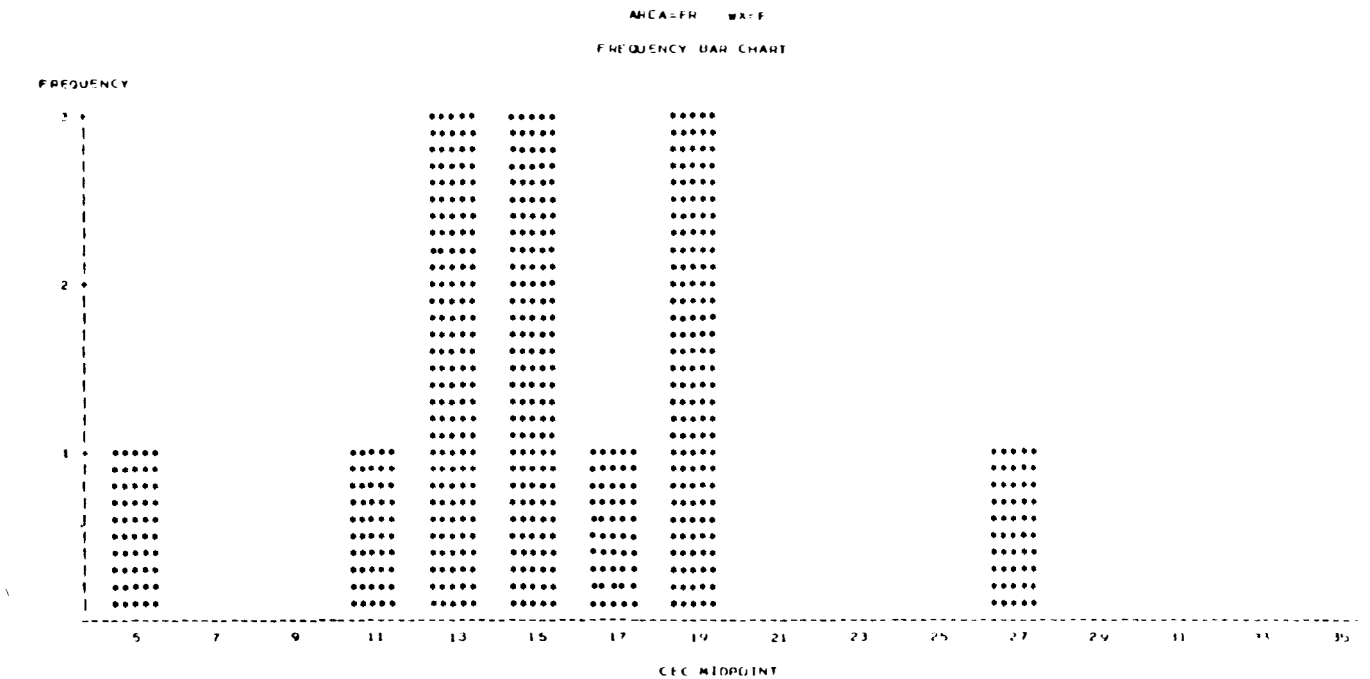

Figure 9. Frequency chart for fresh vs. weathered segments of samples of the FR outcrop. Weathered segments have a slightly higher maximum value and the fresh segments have a slightly lower minimum.

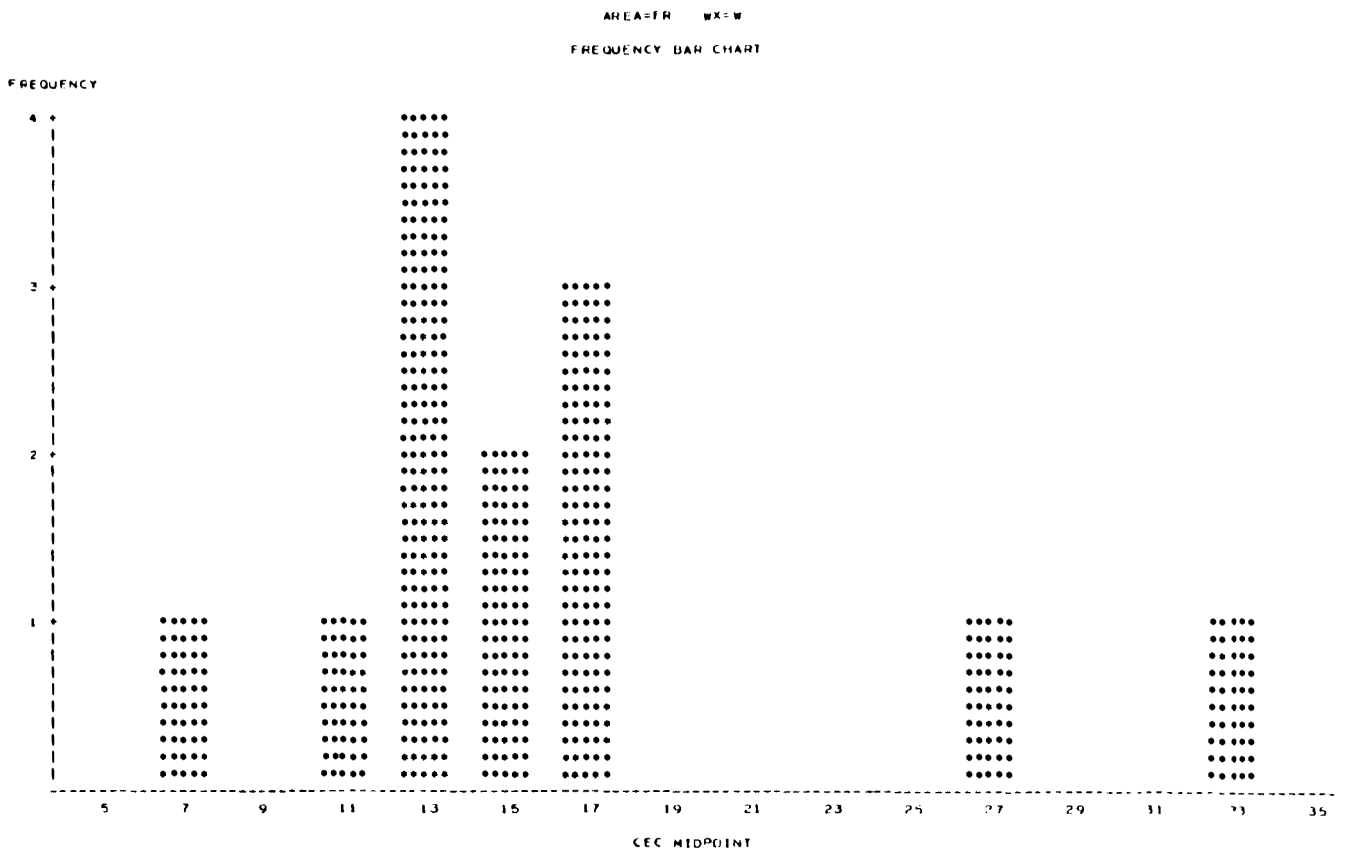

Figure 9 (continued)

Lithology. Unlike the comparisons of the fresh and weathered segments, distinct correlations exist between CEC values and lithology. These are clearly illustrated in Figs. 10 and 11. As a group, claystones possess the highest CEC values due to their comparatively higher clay mineral content. The paucity of clay in the siltstones accounts for their lower overall values.

Rome and Conasauga. It is well established that the Rome and Conasauga exhibit a gradational contact; however, the data gathered in this study were analyzed to reveal any significant differences between them. In the analyses, the data from both outcrops were considered since the FR location has very little of the Conasauga exposed.

The CEC distribution of the Rome and Conasauga are quite similar (see Fig. 12) and the lithologic CEC trends are applicable to both (see Fig. 13). There appears to be a slight increase in the number of siltstones in the Conasauga (taking into consideration the greater number of Rome samples), which is balanced by the fact that there are more sandstones in the Rome. No sharp distinctions can be made between the argillaceous units of the rome and Conasauga. Therefore the contact must be gradational.

Macroscopic Observations of the Argillaceous Samples

The pertinent information observed in the field for both argillaceous and coarser-grained components has been presented and summarized in the stratigraphic columns (Figs. 2 and 3, pages 10 and 15). Some points, such as distinctive coloration and fabric/texture of the argillaceous materials merit further discussion.

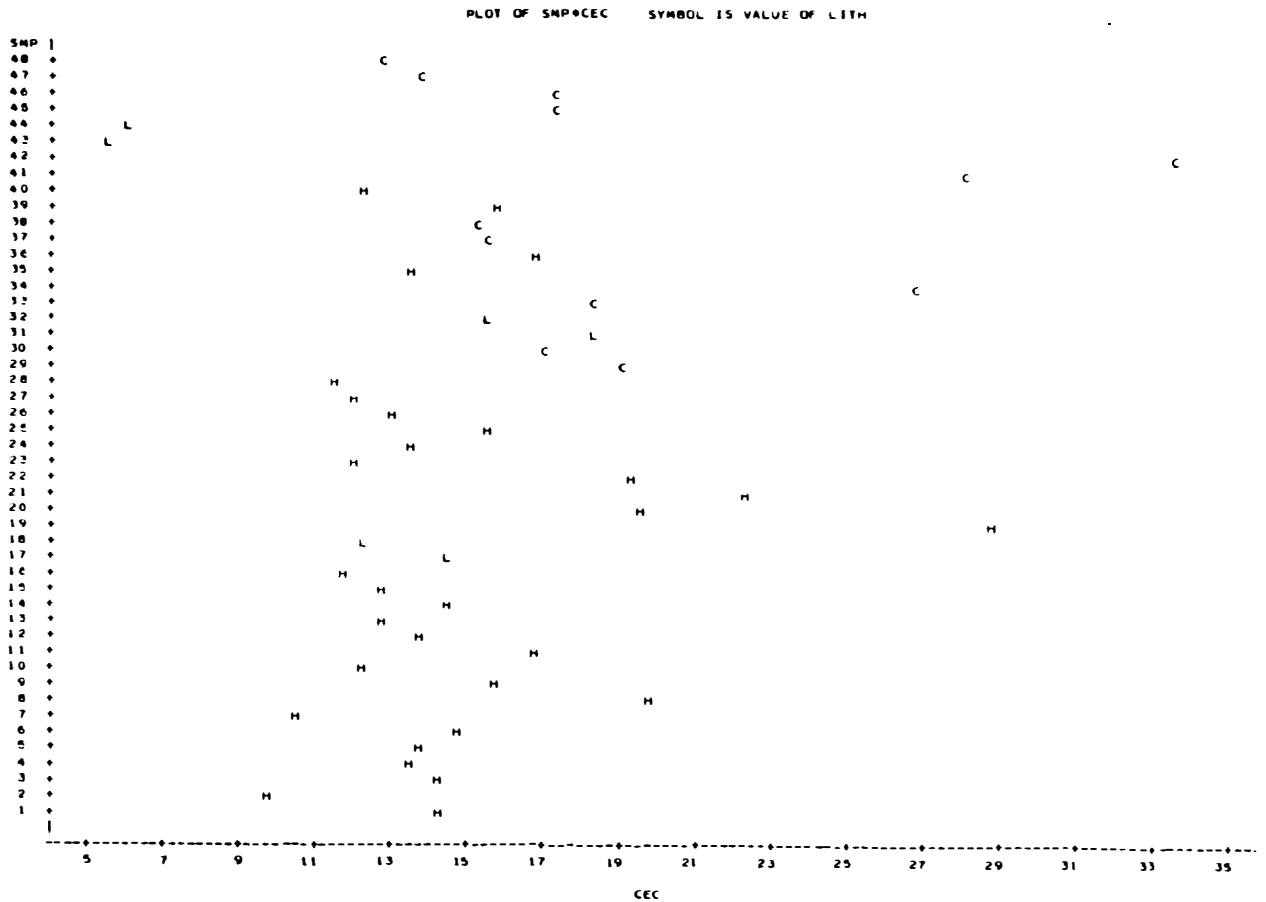

Figure 10. Plot of the CEC values of the CARL and FR outcrops related to the lithology of the individual samples. The general trend of the claystones (C) possessing the highest values and the siltstones (L) concentrated toward lower values is clearly illustrated.

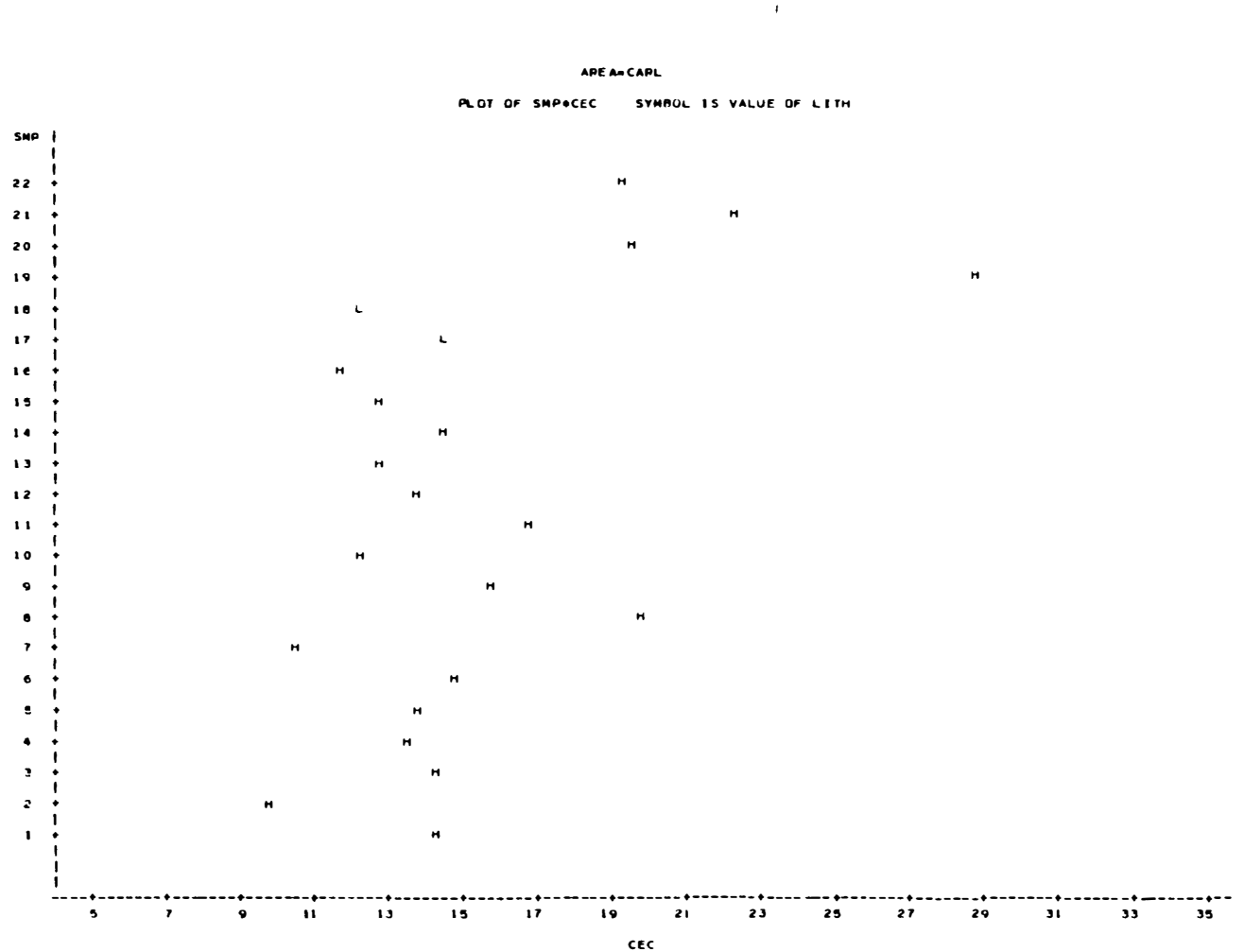

Figure 11. Plot of CEC values and lithologies of the CARL and FR samples. In the CARL samples, the two siltstones are located at the lower end of the scale. The FR data supports the hypothesis of claystones (C) having the greatest CEC values, siltstones (L) considerably lower, and shales (H) with intermediate values.

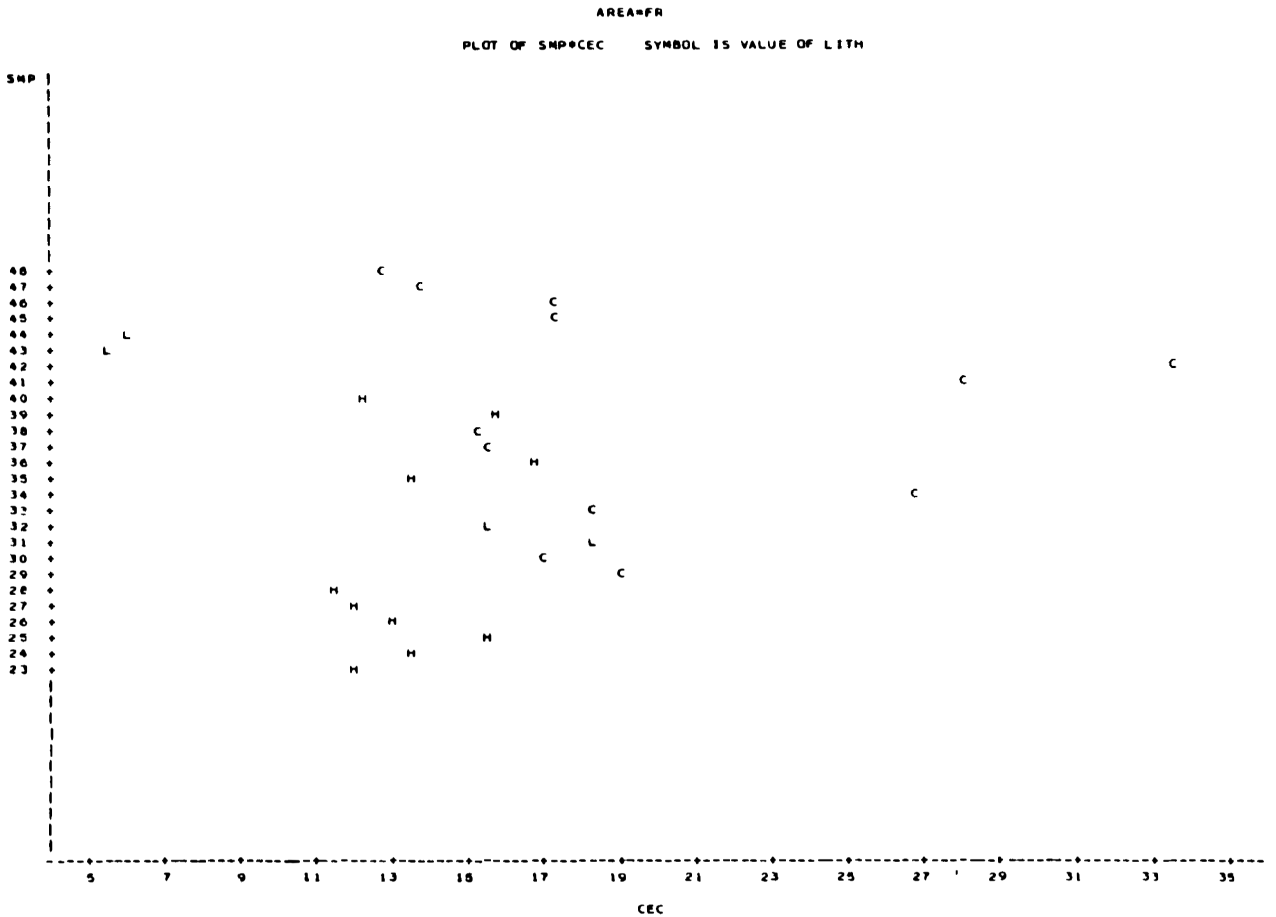

Figure 11 (continued)

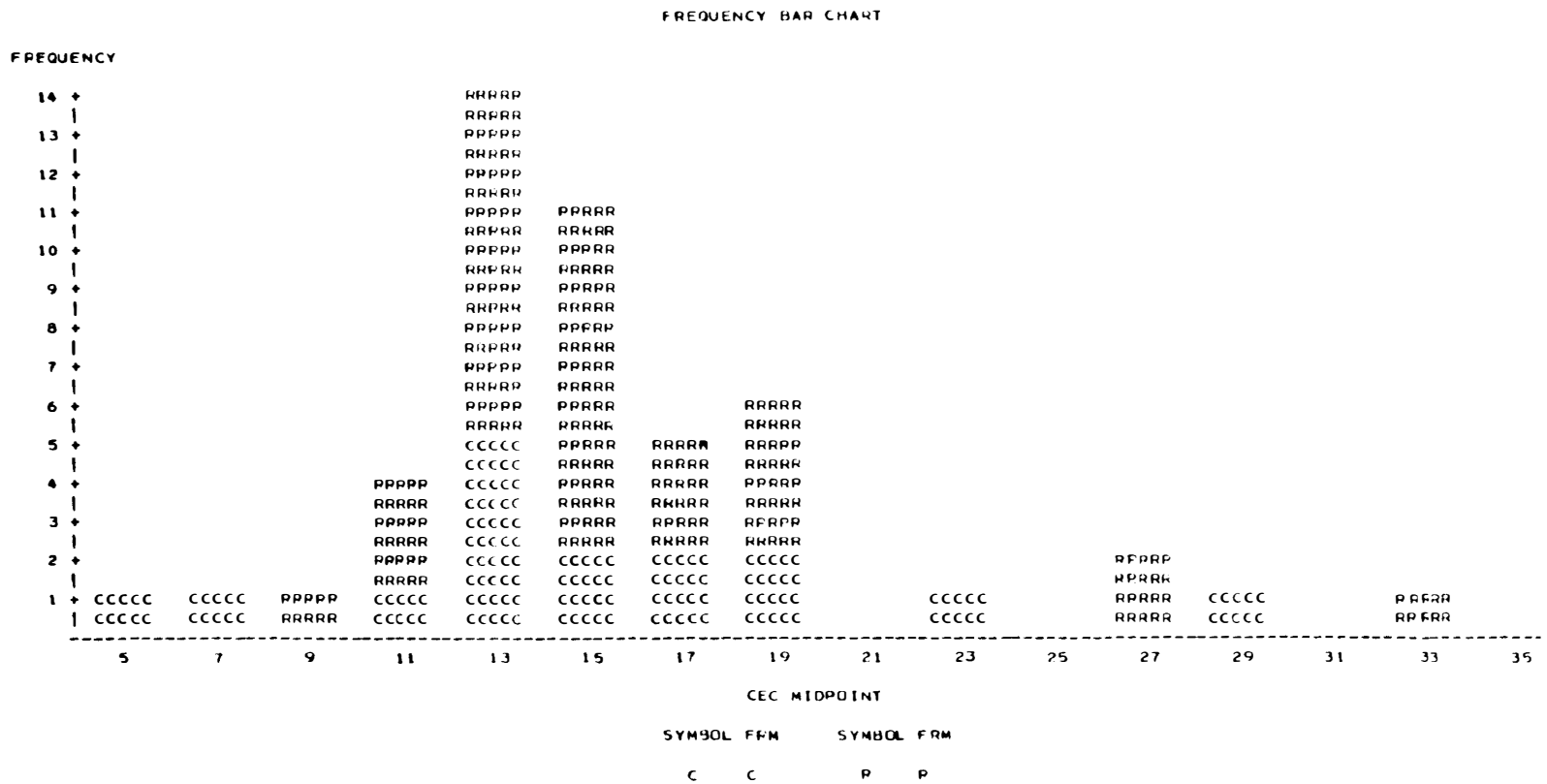

Figure 12. Frequency chart for the CEC values of the Rome Formation and Conasauga Group. There appears to be no differences between the two.

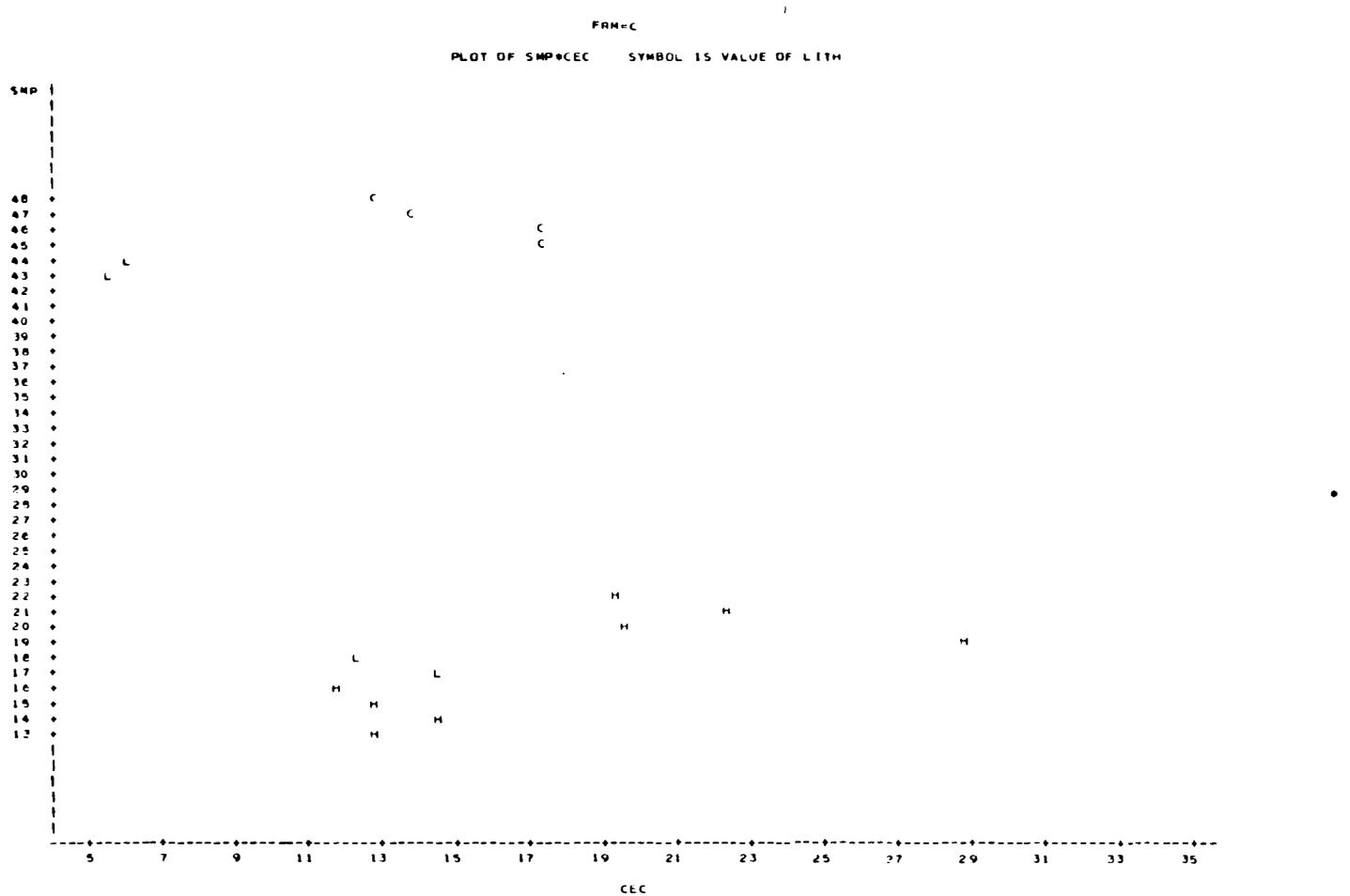

Figure 13. Plot relating the CEC values and lithologies of the Rome and Conasauga. The previously established trends of claystones (C) and siltstones (L) is observed.

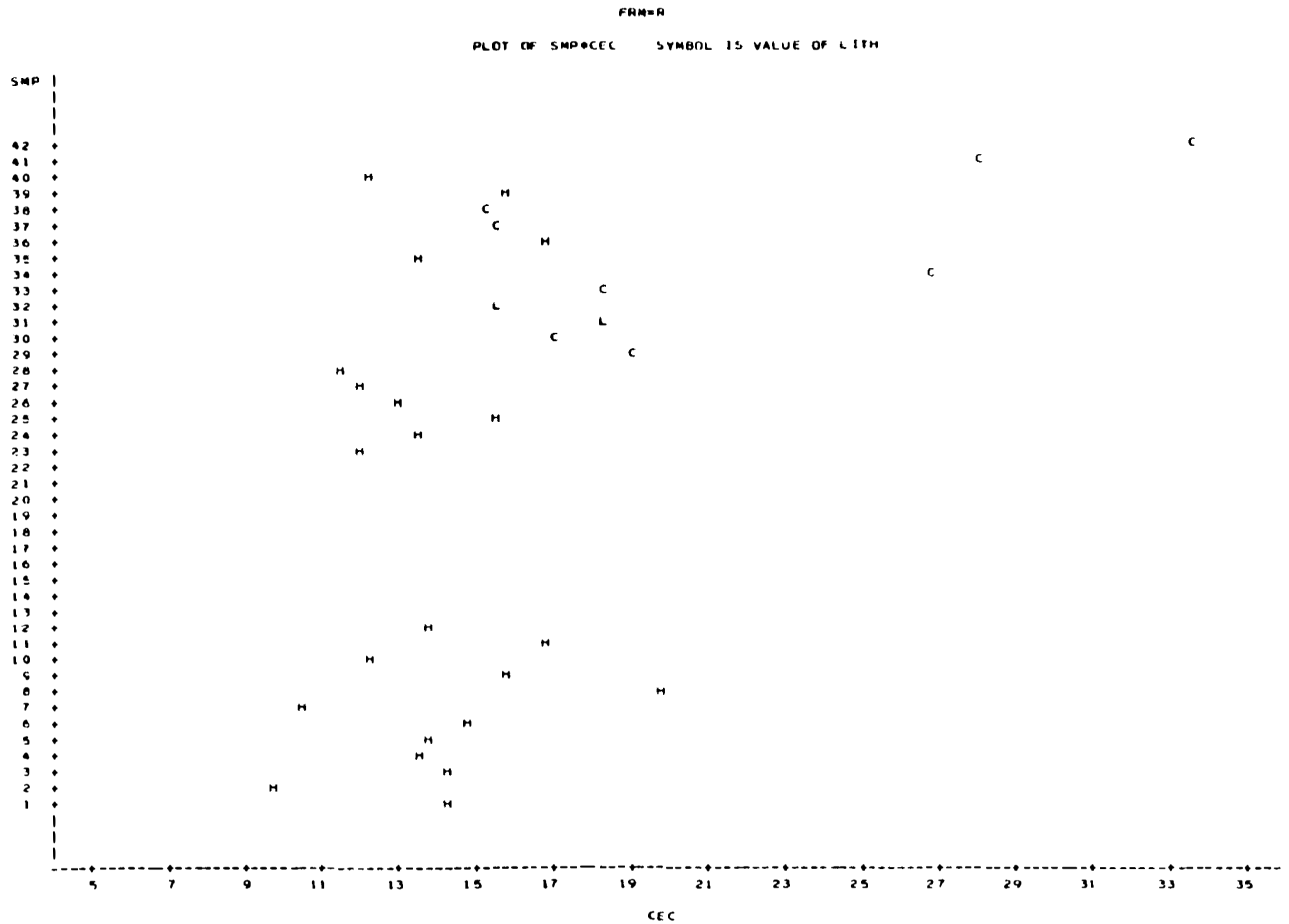

Figure 13 (continued)

The presence of some minerals was suggested in the field by the various colors. Frequently, coloration is due to red and purple hematite; green illite, glauconite, and chlorite (ferrous iron); and black organic matter. Yellow, olive, and grey shales are commonly a result of a mixture of black organic material and green clays (McBride, 1974). Brown and tan shades suggest the presence of limonite/goethite. Similar conclusions were drawn by Samman (1975) in his study of the Rome.

Texture/fabric data on shales, although not intended as a part of this study, might provide valuable insight with respect to the interrelationships between the mineralogy and the physical characteristics of lithologies. Sophisticated equipment such as the SEM, TEM, and EMP (Siever and Kastner, 1972; O'Brien, 1970; Gipson, 1966; Rich and Kunze, 1964) would be required to resolve the minute grain size and provide valuable mineralogical and textural data.

Sandstone CEC

Although it was previously stated that the sandstones were thought to have negligible CEC values, five pairs of sandstones were analyzed to test the validity of this assumption. It is realized that the samples selected do not represent a valid sampling of the sandstone units. Great difficulty was encountered in grinding due to the well-indurated nature of the majority of the sandstones collected. The FQ 1, 2, 3 series (both fresh and weathered) were exceptional cases; they were extremely friable. CEC values of selected sandstones are presented in Table 6. Once again it should be noted no trend in CEC values of fresh and weathered segments exists, for they are not

TABLE 6

CEC VALUES OF SELECTED SANDSTONES

Sample	CEC (meq/100 g)
CE 15 F	6.09
CE 15 W	5.84
CF 19 F	3.13
CF 19 W	3.83
CG 23 F	1.62
CG 23 W	0.70
FQ 2 F	10.40
FQ 2 W	11.84
FQ 3 F	9.29
FQ 3 W	9.29

significantly different. The FQ 2 and 3 series have unusually high values; this is believed to be due to the effects of weathering on this particular type of lithology (petrographic analyses presented in Chapter III). The apparent high clay content (visual estimation) and friability are likely manifestations of this process. Their values are thought to represent a maximum exchange capacity for sandstones, but are not truly representative of the vast majority of the sandstones encountered.

Disregarding the FQ samples, the values appear to be near or below the lowest siltstone value (5.52 meq/100 g). Therefore, it is reasonable to assume that the typical sandstones have very low CEC values. It seems reasonable therefore, to refer only to the argillaceous components when discussing CEC. In the event of seepage of radioactive wastes from the pits, the more argillaceous units would be more effective in removing radioisotopes than the sandier units.

CHAPTER III

PETROGRAPHIC ANALYSIS OF THE SANDSTONES AND SILTSTONES

Introduction

Although there are no sandstones of significance in the Pumpkin Valley Shale (the lowest stratigraphic member of the Conasauga Group) where some waste is buried, there are thick and medium-bedded sandstones at the top of the Rome Formation, directly below. If seepage should reach these underlying sandstones and siltstone units, a potentially hazardous aquifer system could exist. The argillaceous units of the overlying Conasauga and the underlying Rome bound the coarser-grained rocks of the Upper Rome.

In this phase of the investigation, determination of the mineralogy and porosity of the coarser-grained constituents of the Rome and Conasauga were the principal goals. Analyses of thin sections provided important data concerning porosity, mineralogy, and indirectly, permeability. Porosity and permeability are obvious concerns in migration of waste fluids. Determining the mineralogy would reveal the components of the rocks and provide insight into interpreting behavior and interaction of waste material coming into contact with these lithologies.

Porosity and Permeability

Porosity and permeability are the two principal mass properties considered in assessing a potential aquifer. Absolute porosity refers to the total percentage of void space in the rock, whereas effective porosity accounts for only interconnected voids (Pettijohn et al., 1973).

In nearly all cases, effective porosity is less than the absolute porosity value. Permeability is the measure of the ability of a medium to transmit fluids.

The relationship between permeability and effective porosity is primarily dependent on the grain size distribution, pore sizes and their distribution, pore path tortuosity, and the number of pore interconnections and their widths (Chilingarian and Wolf, 1976). While porosity is fairly straightforward, the concept of permeability is not yet fully understood due to the complexities involved with the number of parameters and their interactions. Rock properties significantly affecting permeability are grain size, sorting, orientation, packing of framework grains, cementation, and bedding.

Figure 14 is presented (from Pettijohn et al., 1973) to more clearly illustrate the primary controls on permeability and porosity for coarse siltstones and sandstones. Investigation of these parameters for argillaceous rocks is beyond the scope of this study.

Porosity

The major factors affecting porosity (refer to Fig. 14) were considered when petrographic studies were performed. To maintain proper perspective, all porosity values were obtained from samples taken near the surface: with increasing depth, porosity tends to decrease (Chilingarian and Wolf, 1976).

Determination of Absolute Porosity

There can be serious errors in the estimate of pore space determined by the common procedure of point counting due to two factors:

1) submicroscopic pore space

Porosity

1. Grain size
2. Sorting
3. Sphericity
4. Roundness
5. Packing
6. Cement
7. Clay content

Permeability

1. Bedding facies: bed thickness, types and abundance of sedimentary structures, frequency of shale beds which act as impermeable barriers to flow
2. Texture and Fabric: grain size, sorting, packing, shape orientation of framework grains (defines primary pore system)
3. Sedimentary structures: cross beds, ripples, parting lineations, etc.
4. Composite sand bodies: characteristics of many alluvial and deltaic sandstones

Figure 14. Factors influencing porosity and permeability.

2) edge effects resulting from the thickness of slides (30 microns) which allows for the underestimation the pore volume and overestimation grain and cement volumes (Halley, 1978).

The former factor generally has a significant effect when dealing with carbonate rocks, such as micrite. It is highly doubtful that the sandstones/siltstones of the Rome and Conasauga have any significant submicroscopic porosity (Halley, 1978). However, the clastic nature of these lithologies, with fine sand and coarse silt sizes dominating, may allow edge effects to seriously interfere with accurate porosity determinations. The magnitude of error for edge effects increases with decreasing grain size, tighter packing, increasing grain irregularities, and decreased sorting.

Point counting is a valid procedure, but the assumption that areas of rock elements are proportional to volumes of the elements is not always true; section thickness can create edge errors arising from the curvature within the 30 micron thickness (Halley, 1978). With decreasing grain size, larger portions of grains and pores are within the thin section slice. As the average grain size of the rock approaches the thickness of a section, thin section includes more portions of grains which include their largest diameter (for spherical grains less than 60 microns the section incorporates the largest diameter of each grain). Around each grain is an "error envelope" where the voids are hidden by the grain edge: this error increases for smaller grain sizes and proportionally decreases with increasing grain size. Fewer and fewer interparticle pores extend entirely through the section as grain size decreases. When the maximum pore dimension is less than 30 microns, the pore "vanishes" by enclosure within the section, or is

masked by material below and above. For larger sand size grains, masking is not as great, yet still can be significant. In some cases, artificially high values are not the sole culprits in underestimating porosity. Cements, coating the grains, can also contribute.

Several methods for minimizing edge error are offered by Halley (1978), all of which involve reducing the effective thickness of the thin sections. In this study, ultra-thin (10-12 microns) thin sections were employed for determining porosity.

A blue plastic material was used in the impregnation of all slides to aid in distinguishing voids. The procedure followed in thin-section preparation of the impregnated sample insured that all voids (interconnected or not) would have the blue plastic infilling. Although Halley points out that the use of colored impregnation material can result in an overestimation of pore space if caution is not exercised during the point counting process, its use is believed to have no detrimental effects on the porosity determinations in this study, since ultra-thin slides were used. With conventional thin sections, the color may be considered as pore space, even though it underlies or overlies grains.

Following Chayes' (1956) recommendations for point counting "banded" rocks, the slides (25 X 50 mm, 10 microns thick) were counted at an angle (37° or 57°) to the banded fabric; it is uncertain if concentrations of voids are located in laminations. Low porosities were anticipated in some instances; therefore, 1000 points per slide were counted to insure statistically valid results (Van Der Plas and Tobi, 1965). Porosity values for all 29 of the "fresh" samples are presented in Table 7. Since waste is buried 4-5 m below the surface,

TABLE 7

MINERALOGY AND POROSITY DETERMINATIONS FROM PETROGRAPHIC ANALYSES OF THE SANDSTONES AND SILTSTONES

AREA=CARL

OBS	LOCA	SAM	WX	LITH	Q	KSPAR	PLAG	MUS	BIO	GLAU	MAT	CEM	MISC	PORO	FRM
1	CA	1	F	SS	55	18.0	2.0	3.0	1.0	6.0	12	2.0	1.0	1	R
2	CA	1	W	SS	58	26.0	2.0	2.0	0.5	3.0	6	0.0	3.0	-1	R
3	CA	2	F	L	53	24.0	3.0	2.0	0.5	9.0	5	2.0	2.0	1	R
4	CA	2	W	L	55	3.0	0.0	1.0	0.5	22.0	10	9.0	0.5	-1	R
5	CB	4	F	SS	28	26.0	4.0	1.0	0.0	0.5	32	8.0	0.5	1	R
6	CB	4	W	SS	25	40.0	7.0	2.0	0.0	0.5	10	7.0	1.0	-1	R
7	CB	6	F	SS	-1	-1.0	-1.0	-1.0	-1.0	-1.0	-1	-1.0	-1.0	0	R
8	CB	8	F	SS	61	24.0	4.0	1.0	0.5	0.0	6	1.0	2.0	0	R
9	CB	8	W	SS	60	30.0	5.0	1.0	0.0	0.5	2	0.5	1.0	-1	R
10	CB	9	F	SS	87	1.0	0.0	0.0	0.0	0.0	5	5.0	2.0	2	R
11	CB	9	W	SS	90	0.0	0.5	0.5	0.5	0.0	7	0.5	1.0	-1	R
12	CD	13	F	SS	47	14.0	3.0	6.0	1.0	1.0	25	2.0	0.5	0	R
13	CD	13	W	SS	52	26.0	2.0	4.0	0.0	0.0	14	1.0	0.5	-1	R
14	CE	17	F	SS	60	22.0	1.0	0.5	0.0	0.0	10	4.0	2.0	0	R
15	CE	17	W	SS	64	23.0	3.0	0.5	0.0	0.0	6	2.0	1.0	-1	R
16	CF	19	F	SS	45	19.0	4.0	0.0	0.0	0.0	25	4.0	2.0	0	R
17	CF	19	W	SS	52	19.0	2.0	0.0	0.0	0.0	21	4.0	2.0	-1	R
18	CF	20	F	SS	71	20.0	3.0	0.5	0.0	0.0	3	1.0	1.0	0	R
19	CF	20	W	SS	70	18.0	3.0	0.5	0.0	0.0	3	5.0	0.5	-1	R
20	CF	22	F	L	60	15.0	2.0	0.0	0.0	0.5	20	1.0	2.0	0	R
21	CF	22	W	L	55	16.0	1.0	0.5	0.5	0.5	23	0.5	2.0	-1	R
22	CG	24	F	SS	70	13.0	5.0	2.0	0.0	0.0	5	2.0	3.0	3	R
23	CG	24	W	SS	56	21.0	3.0	1.0	0.5	0.0	15	1.0	2.0	-1	R
24	CH	28	F	SS	50	1.0	2.0	0.5	2.0	24.0	19	0.0	1.0	1	C
25	CH	28	W	SS	52	0.5	2.0	2.0	2.0	18.0	23	1.0	0.5	-1	C
26	CI	32	F	L	-1	-1.0	-1.0	-1.0	-1.0	-1.0	-1	-1.0	-1.0	2	C
27	CI	33	F	SS	26	0.0	1.0	1.0	2.0	21.0	41	8.0	0.5	2	C
28	CI	33	W	SS	36	0.5	1.0	0.5	1.0	29.0	23	9.0	1.0	-1	C
29	CI	35	F	L	-1	-1.0	-1.0	-1.0	-1.0	-1.0	-1	-1.0	-1.0	3	C

AREA=FR

OBS	LOCA	SAM	WX	LITH	Q	KSPAR	PLAG	MUS	BIO	GLAU	MAT	CEM	MISC	PORO	FRM
30	FL	4	F	SS	48	36	1.0	2.0	0.0	0	8	4	1.0	2	R
31	FL	4	W	SS	53	23	2.0	1.0	0.0	0	5	15	0.5	-1	R
32	FM	3	F	L	47	28	1.0	0.5	0.0	0	7	4	12.0	5	R
33	FM	3	W	L	56	35	1.0	0.0	0.0	0	5	2	1.0	-1	R
34	FM	4	F	SS	-1	-1	-1.0	-1.0	-1.0	-1	-1	-1	-1.0	9	R
35	FM	5	F	SS	58	31	1.0	1.0	0.5	0	4	2	3.0	5	R
36	FM	5	W	SS	51	37	0.0	1.0	0.5	0	5	4	1.0	-1	R
37	FM	8	F	SS	58	28	2.0	3.0	1.0	0	4	3	1.0	1	R
38	FM	8	W	SS	61	29	0.5	1.0	0.0	0	3	4	1.0	-1	R
39	FM	9	F	SS	-1	-1	-1.0	-1.0	-1.0	-1	-1	-1	-1.0	3	R
40	FM	2	F	SS	-1	-1	-1.0	-1.0	-1.0	-1	-1	-1	-1.0	2	R
41	FM	7	F	SS	59	10	5.0	1.0	1.0	0	14	3	7.0	2	R
42	FM	7	W	SS	46	38	0.0	1.0	0.0	0	13	2	0.5	-1	R
43	FQ	1	F	SS	-1	-1	-1.0	-1.0	-1.0	-1	-1	-1	-1.0	3	R
44	FQ	1	F	SS	-1	-1	-1.0	-1.0	-1.0	-1	-1	-1	-1.0	3	R
45	FQ	2	F	SS	-1	-1	-1.0	-1.0	-1.0	-1	-1	-1	-1.0	2	R
46	FQ	3	F	SS	67	16	0.5	1.0	0.0	0	12	1	2.0	10	R
47	FQ	3	W	SS	65	23	0.5	0.0	0.0	0	11	0	1.0	-1	R
48	FR	3	F	SS	73	19	0.5	1.0	0.5	0	4	0	2.0	9	C
49	FR	3	W	SS	69	25	1	1	0	0	3	0	0.5	-1	C

-1 denotes no data were obtained. 0.5 denotes a trace (<1%).

"weathered" segments were not included in the porosity study. Unlike certain predictable trends observed in a mineralogical comparison of fresh and weathered segments, there appear to be no definite trends established for porosity between fresh and weathered segments of the same sample.

Permeability

According to Chilingarian and Wolf (1976), the distribution of shale beds is the most important factor in permeability studies (see Fig. 14). Shales can serve as very effective impermeable barriers. In the outcrops studied, the vast majority of the siltstone and sandstone units were fairly thinly bedded, with abundant intercalated shales. There were a few notable exceptions (refer to Figs. 2 and 3, pages 10 and 15) described below.

1) CG 24, FQ 3: These units are of prime concern because they represent the uppermost portion of the Rome Formation. These thick to medium-bedded sandstones are not interrupted by shaley units to any significant degree, but are bounded by fairly extensive argillaceous units.

2) CD 13, CF 20, FM 3, FM 4, FM 9: These units have concentrations of thin sandstones with few shale beds within the units and are of minor importance.

Second in importance are texture and fabric. They illustrate the complex interweaving of porosity and permeability, and define the primary pore system. Petrographic analysis (the principal analytical method employed for the non-argillaceous constituents) supplied abundant data on fabric, textures, and microstructures: a detailed discussion of the petrographic analysis is presented later in this chapter.

Sedimentary structures are believed to play a relatively minor role, as they are not large scale and are often ill-defined; hence they would have limited effect on the direction of fluid flow.

Composite sand bodies (Figure 14) are not applicable in this case, since the environment of the Rome and Conasauga is intertidal to subtidal (Harris and Milici, 1977; Samman, 1975).

Results

Results are presented in Table 7.

Discussion

The porosity of the samples analyzed can be attributed to four major factors:

1) deterioration of the micaceous (i.e., muscovite and biotite) and glauconitic grains
2) microscopic voids
3) microscopic cracks (discontinuous)
4) macroscopic cracks (continuous and discontinuous)

Figures 15 and 16 present photographs illustrating a number of factors affecting porosity.

Continuous cracks extending throughout the entire slide were noted in only one case (CI 35 F SL) and were considered as void spaces in the point count. Only 0.6% of the porosity value (3%) can be attributed to the continuous crack.

It is possible that in the initial cutting and grinding of the slabs prior to impregnation, some of the grains or deteriorating grain portions (factors 1 and 2) were plucked out, thus artificially

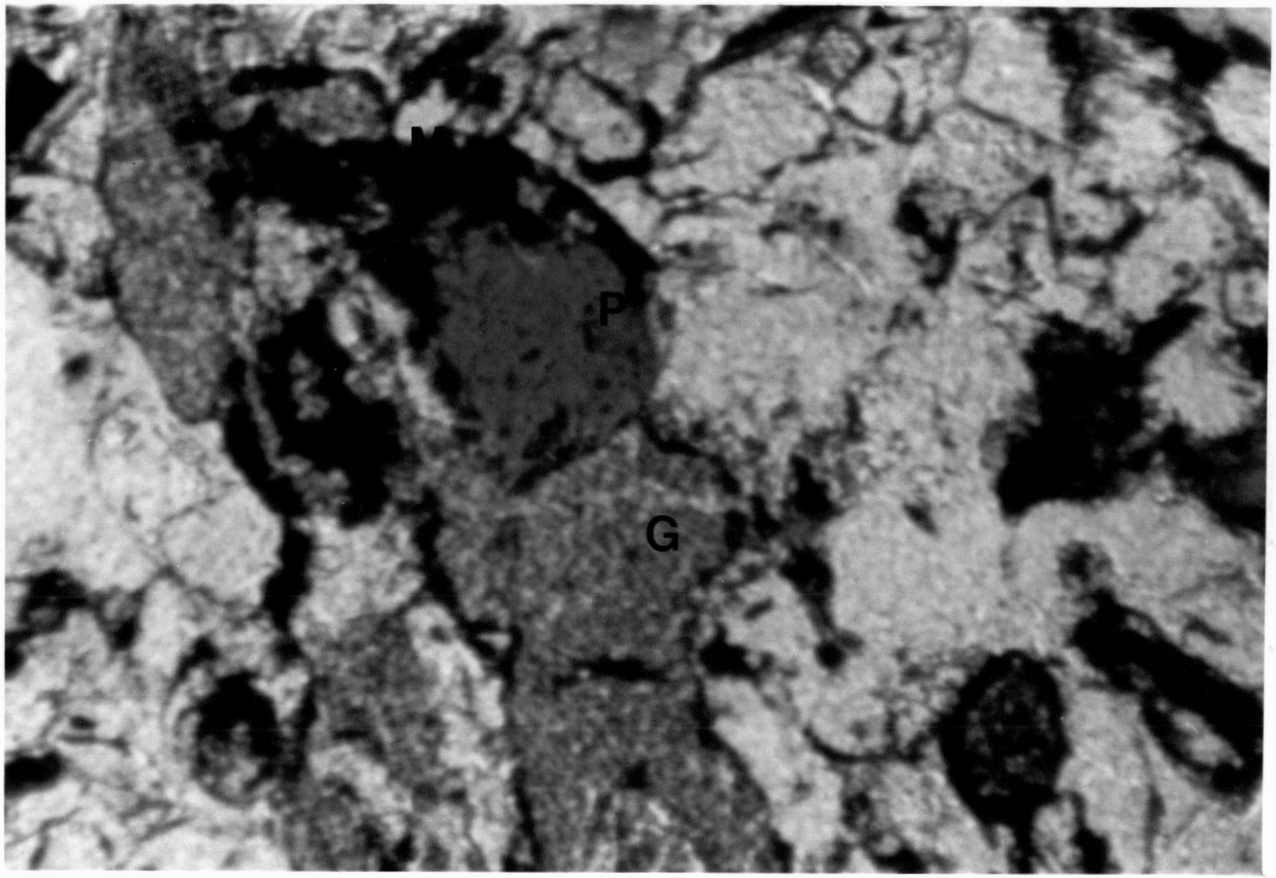

Figure 15. Deterioration of glauconitic (G) and micareous (M) material allowing for the development of pores (P). Length of photo represents 0.45 mm.

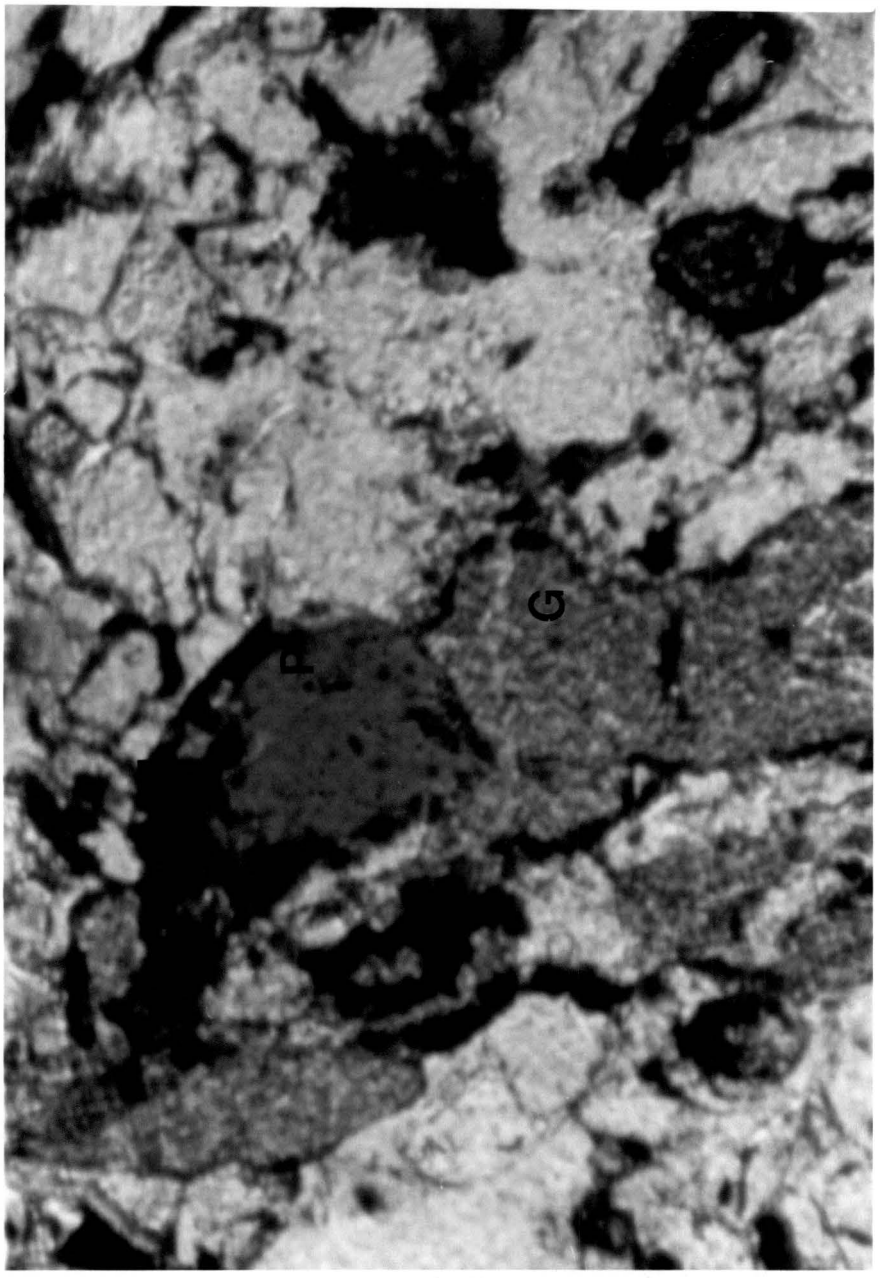

Figure 16. Well developed pore spaces (P). Length of photo represents 0.8 mm.

increasing porosity values. Deteriorating grains observed showed no signs of mechanical abuse, while plucking of sand grains, particularly in friable sandstones, is nearly impossible to discern from "natural" voids.

Porosities of samples FM 3, FQ 1, 2, 3, and FR 3, may have been affected by plucking, but it is believed to have accounted for a maximum of 0.6% of the porosity values (FM 3, 5% and FQ 3, 10.1) and 0.3% of the porosity values (FQ 1, 3% and 2, 2%), which would have little effect on the resultant porosity values.

Due to the fine-grained nature of the sandstones and the numerous minute cracks dispersed throughout, great difficulty was encountered in determining the porosity of FQ 3 hence the 10% value obtained may be in error by as much as 40% (estimated) in excess of true porosity. Similar, though considerably lesser difficulties were involved when analyzing FQ 1, 2, and FR 3. Some skepticism of these porosity values may be warranted, but they could only be in maximum excess of approximately 1% of the porosity values (FQ 1, 3% and 2, 2%) to 2% of the porosity values (FR 3, 9%).

Measured porosity values from the CARL and FR outcrops indicate a pronounced trend. The sandstones and siltstones of the FR outcrop have significantly higher overall porosities, as opposed to the similar CARL lithologies. Table 8 shows porosity trends in the CARL and FR outcrops. This trend is believed to be attributable to CARL being a "fresher" outcrop. Field studies and rock samples from the two locations were compared mineralogically in the following segment to refute or substantiate this conclusion.

TABLE 8

POROSITY TRENDS IN THE CARL AND FR OUTCROPS

Porosity	CARL	FR
≥ 4%	0%	39%
3-4	12	15
2-3	6	23
1-2	19	15
0-1	63	8

Average CARL sample porosity = 0.7%

Average FR sample porosity = 3.7%

Average CARL + FR porosity = 2.5%

Mineralogical Determinations

Procedure

Initially, all 58 slides were analyzed and described. Forty slides (20 fresh and 20 weathered) of standard thickness were selected for mineralogical modal analysis (point count); they represent the typical siltstones and sandstones present in the Rome and Conasauga. All were stained for Kspar (see Appendix 4). Four hundred points per slide were counted (counts based on the study by Van Der Plas and Tobi, 1965) and recorded.

Results

Results are presented in Table 7, page 65.

Discussion

A brief description of the lithologic components (grains, cement, and matrix) is presented below to provide basic information concerning the sandstones and siltstones analyzed. Figure 17 presents the average mineralogical composition of the sandstones/siltstones analyzed, and Figure 18 gives the mineral frequency distribution.

Grains. 1) Quartz: Nearly all the quartz was monocrystalline, well-rounded to subrounded, and subequant to slightly elongate. In most samples (except CI 33 and CB 4), quartz was the principal mineral constituent, composing about 58% of the rock (refer to Table 9).

2) Feldspar: In the samples analyzed, the feldspar grains observed range from subrounded to angular and tend to be sub-elongate in form. Commonly, feldspars exhibit cleavage and twinning. All slides were stained (see Appendix 4), however, to aid in the identification of Kspar.

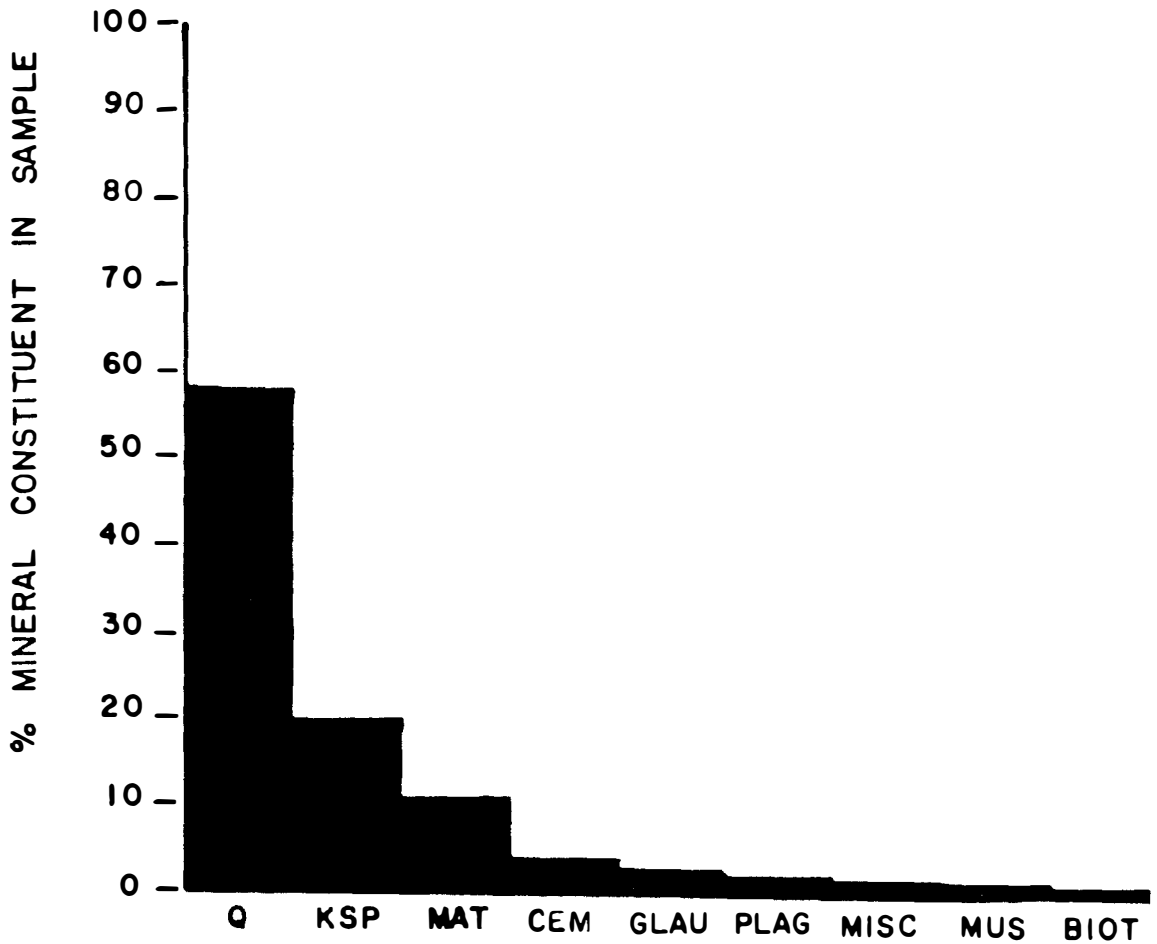

Figure 17. Mineralogical composition of the average Rome and Conasauga sandstone/siltstone.

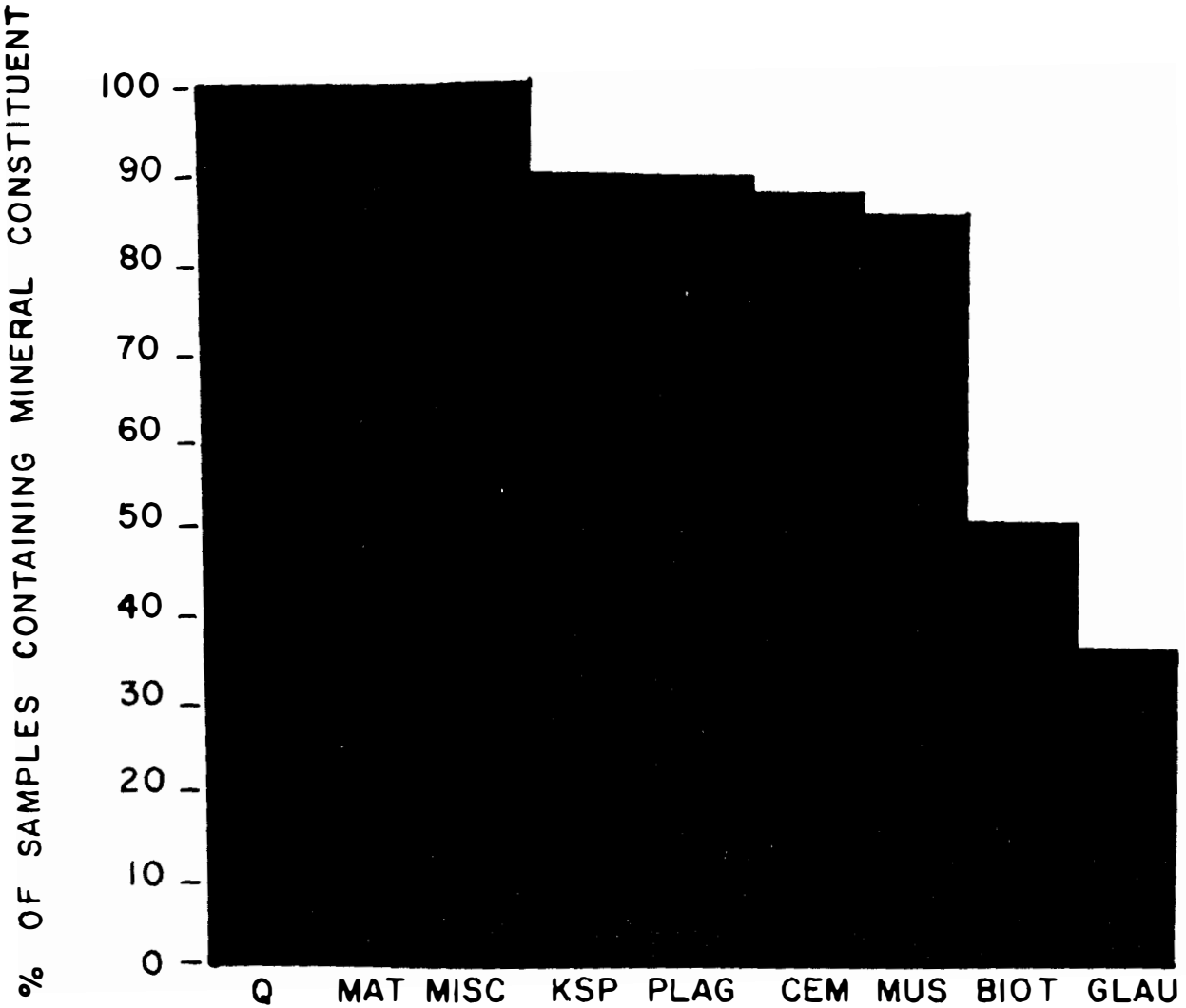

Figure 18. Mineral distribution of the sandstones and siltstones.

TABLE 9

AVERAGE MINERALOGICAL COMPOSITIONS OF THE SANDSTONES AND SILTSTONES ANALYZED WITH RESPECT TO DEGREE OF WEATHERING, OUTCROP LOCATION, AND GEOLOGIC UNIT

	Q	Kspar	Plag	Mus	Bio	Clau	Mat	Cem	Misc
Fresh									
CARL Outcrop									
a. Rome	58%	18%	2%	1%	.5%	2%	13%	3%	2%
b. Cona	38	.5	2	1	.5	23	30	4	.5
c. R + C	55	15	2	1	.5	4	16	3	2
FR Outcrop									
a. R + C	69	24	2	1	.5	0	8	3	4
CARL + FR Outcrops	60	18	2	1	.5	2	13	3	2
Weathered									
CARL Outcrop									
a. Rome	57	19	3	1	.5	2	11	6	1
b. Cona	44	.5	2	1	1	24	23	5	.5
c. R + C	55	16	2	1	.5	4	13	6	1
FR Outcrop									
a. R + C	57	30	.5	1	.5	0	6	4	.5
CARL + FR Outcrops	56	21	2	1	.5	4	10	5	1
AMC*	58	20	2	1	.5	3	10	4	1

*average mineralogical composition overall

Cona - Conasauga

According to Van Der Plas and Tobi (1965), values are 1-5% depending on the percentage calculated.

At times, orthoclase is not easily distinguishable from quartz, and microcline's twinning (when observed) is often difficult to discern from the twinning of some plagioclase. Orthoclase and microcline were the two types of Kspar present, although they were not separately categorized in the modal analysis. Kspar is generally the second most abundant component, about 20%. No attempt was made to discriminate between the possible types of plagioclase present, as they totaled only 2% on the average. The presence of calcic plagioclase was suspected in a few instances, as evidenced by deteriorating plagioclase grains intimately associated with calcite.

3) Muscovite: Muscovite flakes were found in 85% of all samples but only constituted 1% of the total mineralogical composition. It appears that the vast majority of muscovite contributes heavily to the matrix material; it is not surprising that so few of the delicate flakes are preserved as individual grains.

4) Biotite: Biotite was found in approximately 55% of the samples generally as a trace mineral (0.5%). Most biotite flakes observed were fairly deteriorated. On rare occasions, well-preserved, euhedral biotites were noted (samples CG 24 F, CI 32 F, CI 35 F, FM 9 F, FQ 3 F). Euhedral biotite may be evidence for vulcanism (Siribhakdi, 1976).

5) Glauconite: Glauconite was observed in two varieties: pelletal and micaceous. The former accounted for over 95% of the mineral noted in the thin sections. In several cases, minor quantities of glauconite could be discerned as part of the matrix. Quantities of the mineral were normally low (2-4%), with a few notable exceptions (CH 28 and CI 33:23-24%). Terminology associated with glauconite is exceedingly confusing and can be misleading. Frequently it is a general

term for any small, greenish, rounded pellets observed in the field, with no specific mineral composition. There are two major schools of thought regarding the mineralogical nature of true glauconite (and glauconitic pellets):

1) According to Thompson and Hower (1975), glauconite is an iron-rich, mixed-layer illite-smectite, generally composed almost entirely of illite.

2) The once accepted idea of glauconite being a subspecies or variety of illite was refuted by Velde and Odin (1975), with the claim that glauconites are not chemically related to illites. Their analyses of smectite-glauconite and smectite-illite mixed-layers do reveal crystallographic similarities.

Cements. Three types of cements were encountered in the slides analyzed: quartz, hematite, and calcite. Average cement content was approximately 3-5%. The true cement content of many samples may be greater than this range. Due to the fine-grained nature of most samples, quartz overgrowths were probably present, but were not counted as cement because of poor resolution.

1) Quartz: Quartz overgrowths were the most abundant and widely distributed cement type. Detailed resolution was frequently difficult due to the fine grain sizes, but was commonly inferred by the interlocking pattern of the quartz grains.

2) Hematite: Although hematitic cement is fairly ubiquitous, it constitutes a very minor quantity in nearly all samples. One exception, however is the FL 4 sample series (fresh and weathered), where it is the dominant cement. Miniscule amounts of hematite cement often preceeded quartz overgrowths.

3) Calcite: Relatively uncommon in most slides, calcite cement generally occurs in localized patches and is ordinarily associated with calcite veins and veinlets; cathodoluminescence frequently defines and enhances this relationship. Minor quantities of the cement were found only in the following samples: CB 6 f, w; CB 9 f, w; CE 17 f, w; CF 19 f, w; CF 20 f, w. In CB 4, it is the dominant cement. All samples containing carbonate cement are from the CARL outcrop. Perhaps no carbonate cement was noted in the FR samples, either because there was considerably less calcite cementation at that location or the FR outcrop was more weathered, thus allowing for the dissolution of any calcite that might have been present. Samples drawn from core samples could possibly provide an answer.

Matrix. In this study, matrix was defined as any material less than silt size (0.063 mm) which could not be clearly resolved using an ordinary petrographic microscope. The vast majority of the matrix can be categorized as "pseudomatrix," (Dickinson, 1970) where grains are sufficiently deformed to form matrix. The pseudomatrix appears to be composed principally of micaceous materials such as muscovite, biotite, chlorite, and glauconite. Frequently, hematite and limonite are disseminated throughout the matrix, imparting a yellowish to deep reddish hue. Average matrix content is approximately 10-13% (with some exceptions).

Miscellany. This group includes apatite, zircons, dolomite rhombs, rock fragments (extremely uncommon), and any other grains which do not belong in any previously designated category. The principal "miscellaneous" components are zircon and dolomite rhombs. The typically well-rounded variety of zircon predominates, although there are a few

notably angular and euhedral grains. Dolomite rhombs are believed to be of diagenetic origin.

Data Analysis

Procedure

The data were examined from a petrologic and mineralogic viewpoint to establish any trends between the:

1) Rome and Conasauga
2) CARL and FR outcrop locations
3) fresh and weathered segments of the same rock sample

Rome and Conasauga

Rome. The majority of the non-argillaceous units of the Rome consisted of well-sorted, mature, very fine sandstones to silty sandstones. The average sandstone is subarkosic (based on Folk, 1974). Data for all 17 samples is briefly listed in Table 10. Refer to Table 11 for compositional classifications.

Conasauga. Generally, the predominant lithologies of the Conasauga were moderately sorted, immature sandy siltstones to silty sandstones. Refer to Table 7, page 65. Refer to Table 11 for compositional classifications.

Mineralogic. According to Van Der Plas and Tobi (1965), there is a relationship between the number of points counted and the accuracy of the results when performing modal analysis on thin sections. In this investigation, 400 points were counted per thin section, therefore the resultant percentages determined for each mineral had a variation of $\pm$ 1% to $\pm$ 5% (depending on the calculated percentage of that mineral).

TABLE 10

DISTRIBUTION OF GRAIN SIZE, SORTING, AND TEXTURAL MATURITY IN THE ROME SANDSTONES (BASED ON FOLK, 1974)

Grain Size		Sorting		Textural Maturity	
medium sand	4%	very well	31%	supermature	3%
fine sand	8	well	41	mature	57
very fine	46	mod. well	14	submature	9
silty sand	23	moderately	14	immature	31
sandy silt	19				

TABLE 11

COMPOSITIONAL CLASSIFICATION OF THE SANDSTONES/SILTSTONES
(BASED ON FOLK, 1974)

Sample	Quartz	Feldspar	Classification
CA 1 F	74%	26%	arkose
CA 1 W	67	33	arkose
CA 2 F	66	34	arkose
CA 2 W	95	5	orthoquartzite
CB 4 F	48	52	arkose
CB 4 W	34	66	arkose
CB 8 F	69	31	arkose
CB 8 W	63	37	arkose
CB 9 F	99	1	orthoquartzite
CB 9 W	99	1	orthoquartzite
CD 13 F	75	25	subarkose
CD 13 W	65	35	arkose
CE 17 F	73	27	arkose
CE 17 W	71	29	arkose
CF 19 F	66	34	arkose
CF 19 W	71	29	arkose
CF 20 F	76	24	subarkose
CF 20 W	77	23	subarkose
CF 22 F	78	22	subarkose
CF 22 W	76	24	subarkose
CG 24 F	80	20	subarkose
CG 24 W	70	30	arkose
CH 28 F	94	6	subarkose
CH 28 W	96	4	orthoquartzite
CI 33 F	96	4	orthoquartzite
CI 33 W	97	3	orthoquartzite
FL 4 F	56	44	arkose
FL 4 W	68	32	arkose

TABLE 11 (continued)

Sample	Quartz	Feldspar	Classification
FM 3 F	62%	38%	arkose
FM 3 W	61	39	arkose
FM 5 F	64	36	arkose
FM 5 W	58	42	arkose
FM 8 F	66	34	arkose
FM 8 W	68	32	arkose
FN 7 F	80	20	subarkose
FN 7 W	55	45	arkose
FQ 3 F	81	19	subarkose
FQ 3 W	74	26	arkose
FR 3 F	79	21	subarkose
FR 3 W	73	27	arkose

These variations were considered when analyzing the data for any trend in mineralogic compositions between the various groups.

Some differences did arise between the Rome and Conasauga when comparing the non-argillaceous materials. In analyzing the data of Table 12, the following statements concerning these specific mineralogical differences can be made. The principal difference is that the Rome contains a greater percentage Kspar and the Conasauga a greater percentage of matrix and glauconite. This may be a manifestation of the tectonic or environmental changes.

The six remaining components illustrate no significant differences between the Rome and Conasauga.

CARL and FR

Lithologic. There is only one apparent lithologic difference between the CARL and FR outcrops: the FR location appears to be more intensely weathered than CARL. This field-observed characteristic is reflected in several samples, particularly in the uppermost 30 m (Fig. 3, page 15), samples FO 1 through FR 3.

Mineralogic. All the differences noted between the mineral quantities of CARL and FR samples (refer to Table 9, page 75) were no greater than 6%, with the vast majority falling below that maximum. Therefore, no distinctions can be made between the CARL and FR outcrops on a mineralogical basis.

Fresh and Weathered

Mineralogic. The data of all 20 pairs of samples (see Tables 7 and 9, pages 65 and 75) were carefully scrutinized to detect and evaluate any of the following trends: f > w, f = w, f < w (f = fresh,

TABLE 12

SIGNIFICANT MINERALOGICAL DIFFERENCES BETWEEN
THE ROME AND CONASAUGA

	$\bar{X}$	σ*	t**
Kspar:			
Rome	22.3%	10.3	3.6
Conasauga	7.7	11.3	11.3
Glauconite:			
Rome	4.1	1.3	0.5
Conasauga	15.3	12.4	12.4
Matrix:			
Rome	7.6	10.5	3.7
Conasauga	18.8	14.1	14.1

*one standard deviation

**t distribution calculated at a 95% probability (according to Folk, 1974)

w = weathered). No trends were established for the following minerals: quartz, glauconite, biotite, matrix, Kspar, and cement. However, there are a few pertinent observations concerning the fresh and weathered aspects of some of the aforementioned constituents:

1) cement: Higher cement abundances were noted in samples lower in the stratigraphic column (both CARL and FR)

2) glauconite: No glauconite was observed in any sample at the FR outcrop, while anomalously high values were noted in two sampling locations at CARL:

a) all of the Conasauga samples (CH 28 f, w; CI 33 f, w) ranged from 18-29% glauconite content

b) the Rome samples (CA 1 f, w; CA 2 f, w) ranged from 3-22% glauconite content

Since the CARL and FR outcrops are believed to be fairly correlative, the total absence of glauconite at FR is somewhat unusual. Glauconite pellet formation is thought to require specific conditions to form. There are numerous proposed modes of origin (summarized by Burst, 1958), however, formation by small-scale phenomena involving chemical transfer in a microenvironment is presently the accepted process (Velde and Odin, 1975). Normally, glauconite pellets are formed in localized zones. Quite possibly, optimum conditions did not exist in the FR vicinity. Perhaps weathering might have eliminated the glauconite. Note the significantly lower matrix levels (a material expected to behave similarly) between the two locations (CARL 15%, FR 7%, see Table 9, page 75). Further support for this hypothesis is found in an earlier phase of this investigation; determinations suggested four factors for the development of porosity, one of which was the deterioration of micaceous and glauconite grains.

For the remaining constituents, it is difficult to ascertain the existence of a trend. Their low overall content can yield a 100% difference between fresh and weathered values (i.e., if f = 1% and w = 2%). Significant difference, in such cases, is questionable. Components sharing this dubious status on fresh/weathered trends are plagioclase, muscovite, and miscellaneous materials. There is very little mineralogical difference between the fresh and weathered segments as illustrated in 70% of all samples. The noteworthy exceptions are FN 7, FM 3, FL 4, CI 33, CB 4, and CA 2.

CHAPTER IV

SUMMATION AND CONCLUSIONS

Purpose

This investigation was intended to provide fundamental information concerning the petrologic, mineralogic, and ion exchange characteristics of the Rome Formation and Conasauga Shale. Low-level radioactive waste is presently being buried in the Conasauga Group, which directly overlies the sandstones of the Rome Formation.

The information supplied by this study will aid in assessing potential hazards associated with waste burial and hydrofracture operations in the Pumpkin Valley Shale, and the potential risk of an aquifer, with the Upper Rome sandstones being the porous unit, sandwiched between impermeable shales.

Summation

Argillaceous Units. The two methods employed in the analysis of the argillaceous units were XRD and CEC determinations. X-ray diffraction analyses indicate the presence of the following minerals: illite, glauconite, kaolinite, chlorite, biotite, muscovite, quartz, hematite, calcite, dolomite, Kspar, and plagioclase. Data gathered were treated essentially on a qualitative basis, as quantification of shales is greatly complicated by the diffraction characteristics of clay minerals. The occurrence of a few broad peaks in the patterns (thought to include peaks of illite, muscovite, biotite, and/or glauconite), suggests the occurrence of either randomly mixed-layer clays, discrete crystallites, or a combination. No exact cause for the broad peaks could be cited from the work done in this investigation.

CEC values for the argillaceous samples ranged from 5.52 to 33.61 meq/100 g. A trend, believed to be directly linked to the overall clay content (since clays are the major contributors to CEC), exists between CEC values and lithologic group: (presented in order of average decreasing CEC values) claystones, shales, siltstones, and sandstones. The sandstones analyzed generally had CEC values at or below the lowest value for siltstones.

Non-Argillaceous Units. Petrographic slides were utilized in the study of the sandstones and coarse siltstones: determinations of the mineralogy and porosity were the primary goals. Quartz, Kspar, matrix, cement (quartz overgrowths, hematite, calcite), glauconite, plagioclase, miscellany, muscovite, and biotite were the constituents. Quantification of data (point counting) permits the determination of an "average" composition for all samples analyzed: quartz = 58%, Kspar = 20%, matrix = 10%, cement = 4%, glauconite = 3%, plagioclase = 2%, muscovite = 1%, miscellaneous = 1%, biotite = trace.

The "typical" Rome sandstone is a mature, well-sorted, subarkosic, very fine sandstone to silty sandstone. Sandy siltstones to silty sandstones, which are moderately sorted and immature, dominate the Conasauga's non-argillaceous segment.

There are a few distinctive differences between the Rome and Conasauga sandstones/siltstones. Slightly higher percentages of glauconite (11% higher) and matrix (11% higher) were found in the average Conasauga sample, whereas slightly greater percentages of Kspar (14%) were noted in the average Rome samples. These variations are believed to be a reflection of the gradual tectonic or environmental changes experienced in the area.

In comparing fresh and weathered segments of the same sample, approximately 70% had the same constituents in very similar proportions.

Porosity of the samples examined were attributed to

1) deterioration of the glauconitic and micaceous grains
2) microscopic voids
3) discontinuous microscopic cracks
4) macroscopic cracks (continuous and discontinuous)

Porosity values ranged from 0% to 10%, with the average being only 2.5%. There is a distinctive difference between the overall porosity values of the CARL and FR outcrops; average porosity of CARL units = 0.7%, FR units = 3.7%. This significant difference is believed due to the fact that the FR outcrop is more weathered as compared to CARL. Weathering tends to destroy cementing agents and facilitates the deterioration of particularly susceptible grains such as micaceous and glauconitic materials (incipient pore space).

Conclusions

The mineralogic, petrologic, and ion exchange data gathered in this study was intended to provide information on the sandstones, siltstones, and shales of the Rome and Conasauga. The components of the lithologic units must be known in order to understand and accurately predict any reactions or interactions, should any seepage of waste material occur, especially into the Rome sandstones.

CEC values are important in the event of waste fluid coming into contact with a lithologic unit. Generally, CEC values are directly proportional to the clay mineral content. Studies indicate the claystones have the highest CEC's, followed by shales, siltstones, and sandstones.

Porosity and permeability are the two major factors involved in the assessment of a potential aquifer. Although no direct measurements of permeability were made in this study, valuable insight into this factor was provided by the data gathered on porosity of the sandstones and siltstones. While permeability is a complex concept, it is highly dependent upon the level of effective porosity. Absolute porosities were determined in this investigation; effective porosity is nearly always lower than absolute porosity.

The uppermost sandstone units of the Rome are composed principally of quartz and feldspar, with less than 5% cement and matrix, and no glauconite. Since the largest number of pores observed were attributable to deteriorating micaceous material, there is little threat of a sizeable porosity increase in that manner. Unless there is a dramatic increase in the extent of fracturing (generated by man-made or natural means), there appears to be little need for concern for a porosity increase above the current 3%. The uppermost sandstone unit of the Rome is bounded by shale layers. In the event of seepage of waste material, it should be realized that shales are several times more effective in removing cations, as well as being fairly impervious. If any waste fluid does reach the sandstones of the Rome, it is highly unlikely that an aquifer system could develop, since the sandstones have very low porosities (suggesting low permeabilities). In addition, their primary mineral constituents are quartz and Kspar, not unstable minerals nor components easily alterable by migrating fluids.

Suggestions for Further Studies

This investigation was designed to provide information on bulk rock samples. In the case of the argillaceous components, a more detailed study would be desirable. Separation into various size fractions, with special emphasis on the clay size fraction, would allow for more thorough characterization of the clay mineral components and for a more quantitative approach. Due primarily to clay minerals, claystones and shales have the most effective exchange capabilities of all lithologies studied. A more precise understanding of clay interstratification (if any), textures, fabrics, and assorted physical and chemical properties of the argillaceous units would be beneficial in understanding their interactions with waste fluids.

During the course of this investigation, it was not possible to make direct measurements of permeability. Such data would help to refute or confirm the petrographically established conclusion that most Rome sandstones are likely to have low permeabilities (samples of these rocks are still available and could possibly be used in permeability determinations).

Actual position of the Rome sandstones with respect to established as well as future burial sites should be determined. Although it is believed that these sandstones have low porosities/permeabilities, they also have fairly low CEC values. If for any reason (increased fracturing, etc.), waste fluids should enter these sandstones, they would be the least capable lithology to remove hazardous cations.

SELECTED REFERENCES

SELECTED REFERENCES

Almon, W. R., Fullerton, L. B. and Davies, D. K., 1976, Pore space reduction in Cretaceous sandstones through chemical precipitation of clay minerals: Jour. Sed. Pet., v. 46, p. 89-96.

Austin, G. S. and Leininger, R. K., 1976, The effect of heat treating sedimented mixed-layer illite-smectite as related to quantitative clay mineral determinations: Jour. Sed. Pet., v. 46, p. 206-215.

Bailey, S. W., 1980, Summary of recommendations of AIPEA nomenclature committee on clay minerals: Am. Mineralogist, v. 65, p. 1-8.

Bardossy, G., Bottyan, L., Gado, P., Griger, A., and Sasvari, J., 1980, Automated quantitative phase analyses of bauxites: Am. Mineralogist, v. 65, p. 135-141.

Barr, A. J., Goodnight, J. H., Sall, J. P., Blair, W. H. and Chilko, D. M., 1979, SAS User's Guide: SAS Institute Inc., 494 p.

Brown, G. (ed.), 1961, The X-ray Identification and Crystal Structures of Clay Minerals: Mineralogical Society of London, Jarrold and Sons, London, 544 p.

Brown, G. and Newman, A. C., 1970, Cation exchange properties of micas: Clay Minerals, v. 8, p. 277-279.

Burst, J. F., 1958, "Glauconite pellets": their mineral nature and applications to stratigraphic interpretations: Amer. Assoc. Petroleum Geologists Bull., v. 42, p. 310-327.

Busenberg, E. and Clemency, C. V., 1973, Determination of cation exchange capacity in clays and soils using an ammonia electrode: Clays and Clay Minerals, v. 21, p. 213-217.

Byers, C. W., 1974, Shale fissility: relation to bioturbation: Sedimentology, v. 21, p. 479-484.

Carroll, D., 1959, Ion exchange in clays and other minerals: Geol. Soc. Amer. Bull., v. 70, p. 749-780.

Chayes, F., 1956, Petrographic Modal Analysis: Wiley and Sons, New York, 113 p.

Chilingarian, G. V. and Wolf, K. H. (eds.), 1975, Developments in Sedimentology: Compaction of Coarse-Grained Sediments, I: Elsevier Pub. Co., Amsterdam, 550 p.

Chilingarian, G. V. and Wolf, K. H. (eds.), 1976, Developments in Sedimentology: Compaction of Coarse-grained Sediments, II: Elsevier Pub. Co., Amsterdam, 808 p.

Cowser, K. E. and Parker, F. L., 1957, Soil disposal of radioactive wastes at ORNL: criteria and techniques of site selection and monitoring: Health Physics, v. 1, p. 152-163.

Cubitt, J. M. and Wilkinson, J. G., 1974, A novel method for the study and classification of shales: Chemical Geology, v. 13, p. 57-63.

Cubitt, J. M., 1975, A regressive technique for the analysis of shales by x-ray diffractometry: Jour. Sed. Pet., v. 45, p. 546-553.

Davis, C. E. and Holdridge, D. A., 1969, Quantitative estimation of clay minerals by D.T.A.: Clay Minerals, v. 8, p. 193-199.

Davis, J. C., 1973, Statistics and Data Analysis in Geology: Wiley and Sons, New York, 550 p.

deLaguna, W., Tamura, T., Weeren, H., Struxness, E. G., McClain, J. and Sexton, R., 1968, Engineering development of hydraulic fracturing as a method for permanent disposal of radioactive wastes: ORNL Report 4259, 259 p.

De Vore, G. W., 1957, The surface chemistry of feldspars as an influence on their decomposition products: Clays and Clay Mineral Proc., 6th Conf., p. 26-41.

Dickinson, W. R., 1970, Interpreting detrital modes of grey wackes and arkose: Jour. Sed. Pet., v. 40, p. 695-707.

Eberl, D., 1978, The reaction of montmorillonite to mixed-layer clay: the effect of interlayer alkalai and alkaline earth cations: Geochim. et Cosmochim. Acta, v. 42, p. 1-9.

Evans, L. J. and Adams, W. A., 1975, Chlorite and illite in some lower Paleozoic mudstones of mid-Wales: Clay Minerals, v. 10, p. 387-397.

Folk, R. J., 1974, Petrology of Sedimentary Rocks: Hemphill Pub. Co., Austin, Texas, 182 p.

Foth, H. D. and Turk, L. M., 1972, Fundamentals of Soil Science: Wiley and Sons, New York, 454 p.

Gaudette, H. E., Eades, J. L. and Grim, R., 1964, The nature of illite: Clays and Clay Mineral Proc., 13th Conf., p. 33-49.

Gibbs, R. J., 1965, Error due to segregation in quantitative clay mineral x-ray diffraction mounting techniques: Am. Mineralogist, v. 50, p. 741-751.

Gipson, M., 1966, A study of the relations of depth, porosity, and clay mineral orientation in Pennsylvania shales: Jour. Sed. Pet., v. 36, p. 888-903.

Greensmith, J. T., 1958, Preliminary observations on chemical data from some British upper Carboniferous shales: Jour. Sed. Pet., v. 28, p. 209-210.

Grim, R. E., Bradley, W. F. and White, W. A., 1957, Petrology of the Paleozoic shales of Illinois: Ill. State Geol. Survey Report 203, 35 p.

Grim, R. E., 1968, Clay Mineralogy: McGraw-Hill, Inc., New York, 596 p.

Halley, R. B., 1978, Estimating pore and cement volumes in thin section: Jour. Sed. Pet., v. 48, p. 642-650.

Hardcastle, J. H. and Mitchell, J., 1974, Electrolyte concentration-permeability relationships in sodium illite-silt mixtures: Clays and Clay Minerals, v. 22, p. 143-154.

Harris, L., 1964, Facies relations of the exposed Rome Formation and Conasauga Group of northeast Tennessee: Geol. Soc. Amer. Prof. paper 501-B, 25 p.

Harris, L., and Milici, R. C., 1977, Characteristics of thin-skinned tectonics in the southern Appalachians and potential hydrocarbon traps: U.S. Geol. Survey Prof. Paper 1018, 40 p.

Harrison, J. L. and Haydn, M., 1957, Clay mineral stabilization and formation during weathering: Clays and Clay Mineral Proc., 6th Conf., p. 144-153.

Heald, M. T. and Larese, R. E., 1974, Influence of coatings on quartz cementation: Jour. Sed. Pet., v. 44, p. 1269-1274.

Hein, J. R., Allevardt, A. O. and Griggs, G. B., 1974, The occurrence of glauconite in Monterey Bay, California; diversity, origin, and sedimentary environmental significance: Jour. Sed. Pet., v. 44, p. 562-572.

Heller-Kallai, L. and Kalman, Z. H., 1972, Some naturally occurring illite-smectite interstratifications: Clays and Clay Minerals, v. 20, p. 165-168.

Hiscott, R. N. and Keller, F. B., 1980, Personal communications: Univ. Tenn., Knoxville.

Keller, W. D., 1953, Illite and montmorillonite in green sedimentary rocks: Jour. Sed. Pet., v. 23, p. 3-9.

Keller, W. D., 1956, Clay minerals as influenced by environments of their formation: Amer. Assoc. Petroleum Geologists Bull., v. 40, p. 2689-2710.

Kidder, G. and Reed, L., 1972, Swelling characteristics of hydroxy-aluminum interlayered clays: Clays and Clay Minerals, v. 20, p. 13-20.

Kossovskaya, A. G. and Drits, V. A., 1970, The variability of micaceous minerals in sedimentary rocks: Sedimentology, v. 15, p. 83-101.

Kotel'nikov, D. D. and Solodkova, N. A., 1977, Authigenous clay minerals in late Precambrian deposits of the Enisei Range: Lithology and Mineral Resources, v. 12, p. 670-684.

Krumhansl, J. L., 1979, Final report: Conasauga near-surface heater experiment: Sandia Lab Report 79-1855, 98 p.

Lomenick, T., Jacobs, D. G. and Struxness, E. G., 1967, The behavior of strontium-90 and cesium-137 in seepage pits at ORNL: Health Physics, v. 13, p. 897-905.

Low, P. F., 1960, Influence of adsorbed water on exchangeable ion movement: Clays and Clay Mineral Proc., 9th Conf., p. 219-228.

McBride, E. F., 1974, Significance of color in red, green, purple, olive, brown, and grey beds of the Difunta Group, northeastern Mexico: Jour. Sed. Pet., v. 44, p. 760-783.

McMaster, W. M., 1963, Geologic map of the Oak Ridge Reservation, Tennessee: Health Physics Report, ORNL-TM-713, 23 p.

Mesri, G., 1971, Mechanisms controlling the permeability of clays: Clays and Clay Minerals, v. 19, p. 151-158.

Millot, G., 1970, Geology of Clays: Springer-Verlag, New York, 429 p.

Mills, J. G. and Zwarich, M. A., 1972, Recognition of interstratified clays: Clays and Clay Minerals, v. 20, p. 169-174.

Murav'ev, V. I. and Voronin, B. I., 1975, nonuniformity of the composition of glauconite grains: Lithology and Mineral Resources, v. 10, p. 324-333.

Muravyov, V. S., 1970, Formation of carbonate cement in clastic rocks: Sedimentology, v. 15, p. 139-145.

Nelson, B., 1955, The illites from some northern Ohio shales: Clays and Clay Minerals, v. 4, p. 116-125.

O'Brien, N. R., 1970, The fabric of shale - an electron microscope study: Sedimentology, v. 15, p. 229-247.

Palmer, A. R., 1971, The Cambrian of the Appalachians; in Holland, C. H. (eds.), Cambrian of the New World: Wiley and Sons, v. 1, p. 169-217.

Pearson, M. J., 1978, Quantitative clay mineralogical analyses from the bulk chemistry of sedimentary rocks: Clays and Clay Minerals, v. 26, p. 423-433.

Pettijohn, F. J., 1970, Introduction, in Studies of Appalachian Geology, central and southern (Fisher, et al., eds.) p. 1-3.

Pettijohn, F. J., Potter, P., and Siever, R., 1973, Sand and Sandstones: Springer-Verlag, New York, 618 p.

Pierce, J. W. and Siegel, F. R., 1969, Quantification in clay mineral studies of sediments and sedimentary rocks: Jour. Sed. Pet., v. 39, p. 187-193.

Purton, M. J. and Youell, R. F., 1969, An x-ray investigation of some argillaceous rocks from the Skipton Anticline, Yorkshire: Clay Minerals, v. 8, p. 29-37.

Resser, C. E., 1938, Cambrian system (restricted) of the southern Appalachians: Geol. Survey Amer. Sp. Paper 15, 140 p.

Reynolds, R. C. and Hower, J., 1970, The nature of illite interlayering in mixed-layer illite-montmorillonites: Clays and Clay Minerals, v. 18, p. 25-36.

Rich, C. I. and Kunze, G. W. (eds.), 1964, Soil Clay Mineralogy: A Symposium: Univ. No. Carolina Press, Chapel Hill, 330 p.

Rodgers, J., 1953, Geologic map of East Tennessee with explanatory text: Tenn. Div. Geol. Bull. 58, part 2, 168 p.

Rodgers, J., 1956, The known Cambrian deposits of the southern and central Appalachian Mountains: Intl. Geol. Congress, XX Session, Mexico City, v. 2, p. 353-384.

Safford, J., 1869, Geology of Tennessee, State of Tennessee, Nashville, 550 p.

Samman, N. F., 1975, Sedimentation and Stratigraphy of the Rome Formation in East Tennessee: unp. Ph.D. dissertation, Univ. Tenn., Knoxville, 336 p.

Sawhney, B. L., 1970, Potassium and cesium ion selectivity in relation to clay mineral structure: Clays and Clay Minerals, v. 18, p. 47-52.

Schultz, L. G., 1958, Quantitative x-ray determinations of some aluminous clay minerals in rocks: Clays and Clay Mineral Proc., 7th Conf., p. 216-225.

Schultz, L. G., 1964, Quantitative interpretation of mineralogical composition from x-ray and chemical data for the Pierre Shale: U.S. Geol. Survey Prof. Paper 391-C, 30 p.

Shaw, D. B. and Weaver, C. E., 1965, The mineralogical composition of shales: Jour. Sed. Pet., v. 35, p. 213-222.

Sibley, D. F. and Blatt, H., 1976, Intergranular pressure solution and cementation of the Tuscarora orthoquartzite: Jour. Sed. Pet., v. 46, p. 881-886.

Siever, R. and Kastner, M., 1972, Shale petrology by electron microprobe; pyrite-chlorite relations: Jour. Sed. Pet., v. 42, p. 350-355.

Siribhakdi, K., 1976, Evidence for Cambrian pyroclastic vulcanism preserved in the Rome Formation near Oak Ridge, Tennessee: unp. M.S. thesis, Univ. Tenn., Knoxville, 50 p.

Spigai, J. J., 1963, A study of the Rome Formation in the Valley and Ridge of East Tennessee: unp. M.S. thesis, Univ. Tenn., Knoxville, 179 p.

Stokke, P. R. and Carson, B., 1973, Variation in clay mineral x-ray diffraction results with the quantity of sample mounted: Jour. Sed. Pet., v. 43, p. 957-964.

Suchecki, R. K., Perry, E. and Hubert, J., 1977, Clay petrology of Cambro-Ordovician continental margin, Cow Head Klippe, western Newfoundland: Clays and Clay Minerals, v. 25, p. 163-170.

Tammemagi, H. Y., Gale, J. E. and Sanford, B. V., 1977, Underground disposal of Canada's nuclear waste: Geoscience Canada, v. 4, p. 71-77.

Tamura, T. and Jacobs, D. G., 1960, Structural implications in cesium sorption: Health Physics, v. 2, p. 391-398.

Tank, R. W. and McNeeley, L., 1970, Clay minerals associated with the Precambrian Gowganda Formation of Ontario: Clay Minerals, v. 8, p. 471-477.

Tettenhorst, R. and Grim, R. E., 1975, Interstratified clays: Am. Mineralogist, v. 60, p. 49-60.

Thompson, G. R. and Hower, J., 1975, The mineralogy of glauconite: Clays and Clay Minerals, v. 23, p. 289-300.

Tien, P. L., 1974, A simple device for smearing clay on glass slides for quantitative x-ray diffraction studies: Clays and Clay Minerals, v. 22, p. 367-368.

Towe, K. M., 1974, Quantitative clay petrology: The trees but not the forest?: Clays and Clay Minerals, v. 22, p. 375-378.

Van Der Plas, L. and Tobi, A. C., 1965, A chart for judging the reliability of point counting results: Am. Jour. Science, v. 263, p. 87-90.

van Olphen, H. and Fripiat, J. J. (eds.), 1979, Data Handbook for Clay Minerals and Other Non-metallic Minerals: Pergamon Press, Oxford, 346 p.

Velde, B. and Hower, J., 1963, Petrological significance of illite polymorphism in Paleozoic sedimentary rocks: Am. Mineralogist, v. 48, p. 1239-1254.

Velde, B. and Odin, G. S., 1975, Further information related to the origin of glauconite: Clays and Clay Minerals, v. 23, p. 376-381.

Velde, B., 1976, The chemical evolution of glauconite pellets as seen by microprobe determinations: Mineralogical Magazine, v. 40, p. 753-760.

Velde, B., 1977, Clays and Clay Minerals in Natural and Synthetic Systems: Elsevier Pub. Co., Amsterdam, 218 p.

Warshaw, C. M., 1958, Experimental studies of illite: Clays and Clay Mineral Proc., 7th Conf., p. 303-317.

Weaver, C. E., 1957, The distribution and identification of mixed-layer clays in sedimentary rocks: Am. Mineralogist, v. 41, p. 202-221.

Wilson, M. D. and Pittman, E. D., 1977, Authigenic clays in sandstones: recognition and influence on reservoir properties and paleoenvironmental analysis: Jour. Sed. Pet., v. 47, p. 3-31.

Young, A., Low, P. and McLatchie, A. S., 1964, Permeability studies of argillaceous rocks: Jour. Geophysical Research, v. 69, p. 4237-4245.

APPENDICES

APPENDIX 1

GRINDING STUDY

In order to determine the optimum grinding time, a "typical" sample (CH 29 W SH) was selected and ground mechanically for 0.5*, 1.0, 2.0, 4.0, and 8.0 hours. *(One half hour of mechanical grinding was the minimum time required for obtaining suitable particle size for preparation of the smear mount and/or sedimented slide for x-ray diffraction.) Each sample was analyzed by x-ray diffractometry (conditions: CuKα, 35 kv, 17 ma, 10 cps, TC 2, 1/2°/min.). The results obtained indicate the following:

1) Eight hours of mechanical grinding did not adversely affect the crystalline structures of any of the mineral components present.

2) Although there were no significant measurable differences in the intensity and sharpness, the peaks generated from the samples ground for 1 and 2 hours appeared to be very slightly superior. It should be noted that identical results may not be obtained when using a grinder other than the one employed in this study (Fisher 10 v/60 cycle).

APPENDIX 2

SMEAR MOUNT PREPARATION

A small quantity of the mechanically ground portion of the sample was mixed with deionized water until a "pasty" consistency evolved. To achieve relatively constant consistencies throughout preparation of all samples, there was no further addition of water when the paste attained the ability to form stiff peaks. A dollop of "paste" was placed on a frosted slide and smeared over the slide's entire surface. To insure uniform thickness of the smear over the slide, as well as maintaining the same thickness in all slides, a special slide holder was prepared. At each end of a large (2 X 3) petrographic slide was mounted a small (1 X 2) slide, leaving just enough space for a smear mount slide. Atop the two small slides were glued cover slides. Thus, with a slide in place, between the two smaller slides, the paste can be easily and evenly distributed over the entire slide in a few motions with another slide, plastic ruler, or any other rigid, smooth, flat object. A metal device of similar design is described by Tien (1974).

APPENDIX 3

DETERMINATION OF CEC VALUES

In the procedure outlined by Busenberg and Clemency (1973), the following equation was used to determine the CEC values:

$$CEC = \frac{(c)\ (v)}{(w)\ (f)}$$

CEC = cation exchange capacity in meq/100 g.

c = concentration of ammonia in moles/l.

This value was obtained graphically, from reading the calibration curve which was prepared using known solutions of ammonium chloride. The ammonia concentrations (in moles/l) were plotted against the ammonia electrode potential (in mv).

v = volume of water (100 mls added in each case of this study).

w = weight of sample in mg.

f = conversion factor (enables final result to be expressed in meq/100 g). In this study, this factor was 10^{-5}.

APPENDIX 4

STAINING FOR KSPAR

The original procedure of R. N. Hiscott and F. B. Keller (pers. comm., 1980) was modified slightly for this particular suite of samples. Important: Etching and immersion times may vary with the reagents used and the type of rock.

Caution: When working with HF use an adequate hood, exercise caution when handling, and dispose of properly.

1) Fill a few compartments (to match area of surface to be etched) of a large cube ice tray, or other suitable container, 3/4 full with HF (52-55%). Be certain acid is fairly fresh. Place slide (rock side down) over fumes, shifting periodically with tongs to assure total exposure, for 2-2 1/2 minutes.

2) Using tongs, transfer the slide to saturated Na-cobaltinitrite solution, and immerse for 5 minutes. The solution should be freshly prepared (not more than 2 days old). Since large quantities of Na-cobaltinitrite powder are required, it is advantageous to minimize the amount of solution for staining. A petri dish (100 X 15 mm size) holds approximately 25 mls of solution and comfortably accomodates a 2 X 3 slide. Of course, other containers may be employed.

3) Lift slide from solution with tongs, and swish several times in a beaker of clean, cool water. The slide can now be safely handled without tongs.

4) Rinse slide in cool tap water for 20-30 seconds to eliminate any excess stain.

5) Set on clean paper or cloth toweling (rock side up) to dry.

VITA

In 1956, Janine Gajda Sledz was born on Friday, January 13th, in Chicago, Illinois. Upon graduating from Chicago's Lourdes High School in August 1972, she attended Western Illinois University, Macomb. After receiving a BS degree in Geology in February 1976, she worked for two years as an assistant technical researcher at Nalco Chemical Company. In September 1978, she accepted a teaching assistantship in the Geology Department at The University of Tennessee, Knoxville, enrolling in the Master of Science program. The following year, she was placed on the ORNL/UT research program, which sponsored her graduate studies. In December 1980, she received the MS degree in Geology.

Since September 1976, she has been happily married to Jim Sledz, in spite of the "professional handicap" of being married to a fellow geologist.